Functional characterization of the mitotic kinesin-like protein Mklp2

Dissertation
zur Erlangung des Doktorgrades der Naturwissenschaften
(Dr. rer. nat.)
der Fakultät für Biologie der Ludwig-Maximilians-Universität
München

vorgelegt von

Stefan Hümmer

Martinsried / München 2009

Erstgutachter: Prof. Dr. Erich A. Nigg

Zweitgutachter: Prof. Dr. Heinrich Leonhardt

Tag der mündlichen Prüfung: 14.12.2009

Ehrenwörtliche Erklärung über frühere Promotionsversuche

Hiermit erkläre ich, dass ich, Stefan Hümmer, die vorliegende Dissertation selbständig und ohne unerlaubte Hilfe angefertigt habe. Sämtliche Experimente sind von mir selbst durchgeführt, ausser wenn explizit auf Dritte verwiesen wird. Ich habe weder anderweitig versucht, eine Dissertation einzureichen oder eine Doktorprüfung durchzuführen, noch habe ich diese Dissertation oder Teile derselben einer anderen Prüfungskommission vorgelegt.

München, den 13.12.2009

Table of Contents

Acknowledgements

I would like to thank Prof. Erich Nigg for giving me the opportunity to work in his lab, to be part of a wonderful international scientific department and especially for his continuous interest and support of my work.

I am thankful to Prof. Heinrich Leonhardt for reviewing my thesis.

I am deeply grateful to Prof. Thomas Mayer for the supervision of my thesis, for his support and the guidance of my work over all the years. I thank him for his continuous help in the form of discussions, brainstorming and teaching me in an excellent way how to approach scientific problems. His scientific enthusiasm and the great atmosphere in his lab were of immense help for me to carry out my PhD.

I am especially thankful to Prof. Stefan Jentsch and Prof. Olaf Stemmann for hosting me in their lab and for their generous support of my work.

I would like to thank my colleagues and friends from the Mayer lab: Jenny Bormann, for her countless technical help but also for being "Jenny" – the god soul in the lab. Monika Mayr, for the good neighbourship on the bench (there was always something to laugh about) and the endless travels from Munich to Konstanz. Stefan Florian, for listening always to me and having nice discussions. Mario Catarinella, for the long evenings in the lab, for sharing the Kabuff, for the soccer discussions and for lending me a couch to sleep on. Eva Hörmanseder, for her continous support and for the great scientific discussions with her. Nadine Rauh, who shared with me the first time of my PhD. Johanna Kastl, thanks for overtaking my projects and Martina Baak and Wiebke Bauernfeind, for their help in the lab in Konstanz.

I would also like to thank my colleagues and friends in the Nigg department: Tom and Louise Gaitanos, for their friendship and specially for helping to correct this manuscript. Sabine Elowe and Michael Schwab, for their friendship and support; Sabine for taking always care of me and Michael for sharing the interest in 2nd league with me. Alex Haas, for his friendship and countless discussions ("fish antibodies"). Rüdiger Neef, for giving me advice from an "old wise man". And finally to all the people who made work enjoyable at the MPI: Jens Westendorf (for teaching me "Platt"), Ravi Chalamalasetty (now I also understand the cricket rules), Herman Sillje, Roman Körner, Anja Hanisch, Mikael LeClech, Stefan Lamla, Robert

Kopajtich, Julia Kleylein-Sohn. To the old ones: Arno Alpi, Martina Casenghi and Ingvar Ferby, and to the new generations.

My thanks go also to all the people in the lab in Munich and Konstanz who provided a permanent warm atmosphere and perfect setup of the lab. Klaus Weber (for always having a ear open for me), Marianne Siebert, Elena Nigg, Alison Dalfovo, Lidia Pinto, Albert Ries, Alicja Baskaja, Anja Wehner, Claudia Szalma and Marianne Kirn-Reuther and Diana Hoffmann.

My special thanks go to my best friends in the lab – Andreas (Andy, Anderl) Schmidt, Christoph (Baumi) Baumann and Ulf (Ulla) Klein. Thanks guys for all this years together in the lab - for endless discussions, for long evenings, for helping me continuously and supporting me inside and outside the lab, for having a breath of fresh air and for putting me on the right track: just for making life enjoyable in the best way. There will always be a Fanpark or an Oktorberfest in the future for us.

Big thanks to my "non lab friends", the "Feuchtfarmers": Markus Haindl, Christoph Seitz, Markus Neumeier, Peter Jäckel and Werner Reitberger and all the "Bercher und Gorschter" for supporting me all the way through my life.

My biggest thanks go to Anna. Thank you "tesoro" for sharing your life with me and being always there. Thank you my shunshine.

Mein großer Dank geht an meine Eltern Lothar und Rosalinde Hümmer und an meinen Bruder Johannes und meine Schwester Andrea die an mich geglaubt haben und mich über all die Jahre unterstützt haben.

Zusammenfassung

Während der Zellteilung bedarf es einer genauen Koordinierung zwischen Mitose und Zytokinese, um zu gewährleisten, dass nach der exakte Teilung der duplizierten Chromosomen in der Mitose die physikalische Trennung der entstehenden Tochterzellen erfolgt. Der chromosomal passenger complex (CPC), bestehend aus Aurora B, INCENP, Survivn und Borealin, spielt eine Schlüsselrolle bei der Koordination beider Prozesse (Adams et al., 2001a; D'Avino et al., 2005; Eggert et al., 2006; Glotzer, 2005; Straight and Field, 2000). Der Transfer des CPC von den Zentromeren zur Zentralspindel, einer Struktur aus gegenläufigen Mikrotubuli, zu Beginn der Anaphase ist entscheidend für die erfolgreiche Beendigung der Zytokinese (Ainsztein et al., 1998; McCollum, 2004; Ruchaud et al., 2007; Schumacher et al., 1998; Tatsuka et al., 1998; Terada et al., 1998; Wheatley and Wang, 1996). Das mitotische Kinesin Mklp2 (mitotic kinesin like protein) ist für die Rekrutierung des CPC an die Zentralspindel essentiel (Gruneberg et al., 2004).

Im ersten Teil der Arbeit haben wir den Mechanismus untersucht, der die Bindung von Mklp2 und dem CPC an Mikrotubuli der Zentralspindel reguliert. Wir konnten zeigen, dass Mklp2 und der CPC sich gegenseitig für die Lokalisierung an der Zentralspindel brauchen. Diese Abhängigkeit beruht auf der Interaktion zwischen Mklp2 und dem CPC, die wiederum negativ von Cdk1 reguliert ist. Darüber hinaus ist die Anwesenheit von stabilen Mikrotubuli Grundvoraussetzung für die Lokalisierung des Mklp2/CPC Komplexes an die Enden von Mikrotubuli. Zusammenfassend implizieren unsere Daten, dass die Inaktivierung von Cdk1 zu Beginn der Anaphase die Assoziation zwischen Mklp2 und dem CPC ermöglicht und diese Assoziierung wiederum versetzt den Mklp2/CPC Komplex in die Lage, an die Enden der stabilen Mikrotubuli in der Zentralspindel zu binden.

Im zweiten Teil der Arbeit haben wir die Mklp2 abhängigen Funktionen des CPC in der späten Zytokinese untersucht. Wir konnten zeigen, dass die phosphorylierungsabhängige Disassemblierung des intermediär Filamentes Vimentin an der Zentralspindel in der späten Zytokinese durch Aurora B von Mklp2 abängig ist. Interssanterweise korreliert die Anwesenheit von Vimentin in Hela und MCF-7 Zellen mit dem Bedarf an Mklp2 für eine erfolgreiche späte Zytokinese, was wiederum impliziert, dass Vimentin eines der wichtigsten Zielproteine ist, dass über die Mklp2 abhängige Funktion des CPC in der späten Zytokinese reguliert wird.

Im dritten Teil der Arbeit haben wir versucht, kleine chemische Inhibitoren für mitotische Kinesine, unter anderem Mklp2, zu identifizieren. Mit der Entdeckung von VS-83, einem potenten Inhibitor von Eg5, konnten wir unsere Stratgie bestätigen, kleine chemische Inhibitoren für mitotische Kinesine mittels eines sogenannten „reverse chemical genetics" Ansatzes zu idendifizieren. Mit Hilfe dieses Ansatzes konnten wir auch neue Inhibitoren für

Kinesine mit einer Funktion in der Zytokinese identifizieren, die wir SH Substanzen genannt haben. SH Substanzen inhibieren die ATPase Aktivität von Mklp2 und MPP1 *in vitro*. Darüber hinaus verursachen diese Substanzen einen zweikernigen Phänotyp *in vivo* und erste Hinweise deuten darauf hin, dass Mklp2 das relevante Zielprotein von SH2 in Zellen ist.

Summary

Cell division involves the accurate coordination of mitosis and cytokinesis to ensure that faithful segregation of the duplicated chromosomes during mitosis is followed by the physical separation of the nascent daughter cells during cytokinesis. The chromosomal passenger complex (CPC) comprising Aurora B, INCENP, survivin, and borealin, is a key component for the coordination of both processes (Adams et al., 2001a; D'Avino et al., 2005; Eggert et al., 2006; Glotzer, 2005; Straight and Field, 2000). The transfer of the CPC from centromeres to the spindle midzone, a structure composed of antiparallel microtubules (MTs), at anaphase onset is critical for the completion of cytokinesis (Ainsztein et al., 1998; McCollum, 2004; Ruchaud et al., 2007; Schumacher et al., 1998; Tatsuka et al., 1998; Terada et al., 1998; Wheatley and Wang, 1996). The mitotic kinesin-like protein Mklp2 in turn is essential for recruitment of the CPC to the spindle midzone (Gruneberg et al., 2004). In this first part of this work, we investigated the mechanism, regulating the timed transfer of the CPC and Mklp2 to the spindle midzone in anaphase. We could demonstrate that Mklp2 and the CPC are mutually depended on each other for midzone localization. This interdependency is based on the interaction between Mklp2 and the CPC which in turn is negatively regulated by Cdk1. Furthermore, stable MTs are required to localize the CPC and Mklp2 to the tips of MTs. Collectively, our data suggest that inactivation of Cdk1 at anaphase onset triggers the association between the CPC and Mklp2 and that this association targets the Mklp2/CPC complex to the ends of stable MTs in the spindle midzone.

In the second part of this work, we analyzed the Mklp2-mediated functions of the CPC in late cytokinesis. We could show that the phosphorylation-induced disassembly of vimentin at the central spindle by Aurora B in late cytokinesis is dependent on Mklp2. Interestingly, the requirement for Mklp2 in late cytokinesis correlates with the presence of vimentin in HeLa and MCF-7 cells, implying that vimentin is a major downstream target of the Mklp2-mediated function of the CPC in late cytokinesis.

In the third part of this work, we aimed to identify small molecule inhibitors for mitotic kinesins, including Mklp2. The discovery of VS-83, a potent inhibitor of Eg5, validated our strategy to identify small molecule inhibitors of mitotic kinesins via a reverse chemical genetics approach. Using this approach, we could identify novel inhibitors of cytokinetic kinesins, which we called SH compounds. SH compounds inhibit the ATPase activity of the kinesins Mklp2 and MPP1 *in vitro.* Moreover, SH compounds induce a binucleated phenotype *in vivo* and first evidences indicate that Mklp2 is the relevant target of SH2 in cells.

Introduction

1 The cell cycle and cell division

Every living cell today has its origin in a single ancestral cell that lived around three to four billion years ago. This fundamental principle of life was originally formulated by Rudolf Virchow in 1858 in his doctrine "*omnis cellula e cellula*": every cell originates from another cell.

The highly regulated series of events in which a cell first duplicates its contents and then divides into two is called the cell cycle, and is typically defined by the basic processes of duplication and segregation of the genomic material, the chromosomes, which carry the information for the synthesis of all other cellular components. The chromosomes are duplicated only once per cell cycle, in the S phase (synthesis phase) and are segregated into newly forming daughters during M phase (mitosis and cytokinesis). The phases in between S and M phase are called gap phases (G1 and G2). The phases G1, S and G2 are collectively called interphase. Non proliferative cells exit the cell cycle in G1 and stay in a metabolically active state, called G0 until they are reactivated by extra-cellular signals. To ensure fidelity of cell reproduction, the precise order of these events is controlled by a cell-cycle control system. This system is based on the oscillating activities of cyclin-dependent kinases (Cdk), the master regulators of the cell cycle. The activity of these regulators define the cell cycle state and is coupled to a system of three independent checkpoints, which integrate signals concerning the current state of the cell and block transition into to the next cell cycle state until error free progression can be ensured. The discovery of the key molecular determinants coordinating the cell cycle by Tim Hunt, Paul Nurse and Lee Hartwell was rewarded by the Nobel prize in Medicine in 2001.
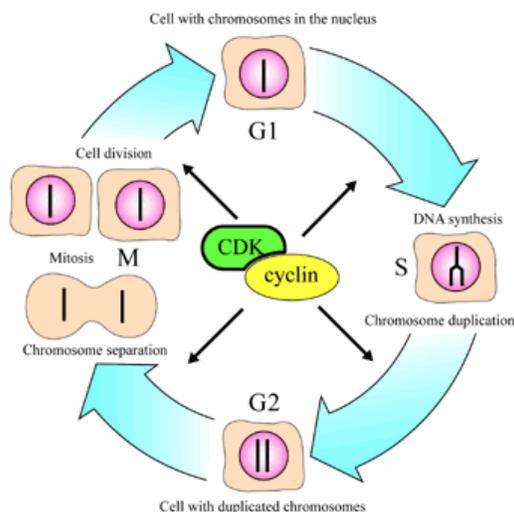
Figure 1. Overview of different cell cycle stages in eukaryotic cells.
Interphase is divided into G1, S and G2 phase. In M-phase, mitosis (nuclear division) is followed by cytokinesis (cytoplasmic division). Image adapted from the Nobel prize release in medicine for Tim Hunt, Paul Nurse and Lee Hartwell, 2001.

2 M-phase

In order to ensure genomic integrity during cell division, the duplicated chromatids must be assembled in such a way to allow their equal separation into nascent daughter cells. In 1882 Walther Flemming was the first cytologist to describe in details how chromosomes reposition during cell division, without knowing that this is the fundamental process required for the equal segregation of genomic information into newly formed daughter cells. Due to the thread-like structures he observed under the microscope, he termed this process mitosis (Greek for thread), and designated the individual phases as prophase, metaphase, anaphase and telophase; terms which are still used to describe the steps of cell division today.
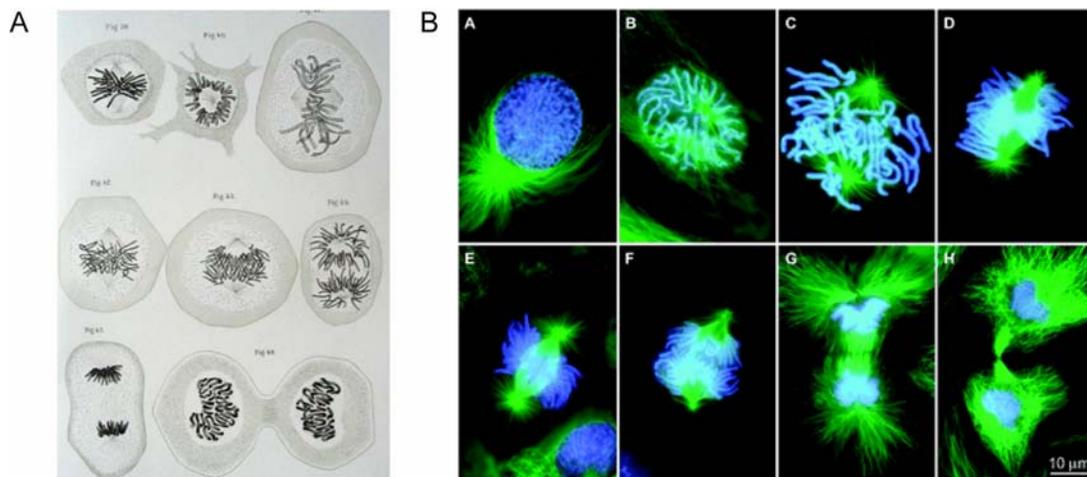
Figure 2. The stages of M-phase.

(A) Illustration from the German discoverer of chromatin and chromosomes, Walther Flemming from the book "Zellsubstanz, Kern und Zellteilung", F.C.W Vogel Verlag, Leipzig 1882. **(B)** The classical stages of M-phase in a newt lung cells, visualized by immunofluorescence microscopy. A, prophase. B, nuclear-envelope breakdown and the onset of prometaphase. C, mid-prometaphase. D, late prometaphase. E, metaphase. F, early anaphase. G, early telophase; H, cytokinesis. MTs are shown in green and DNA is shown in blue. Adapted from (Rieder and Khodjakov, 2003).

2.1 The mitotic spindle

The process of mitosis ensures that the duplicated genetic material, a set of 46 chromosomes in humans, is equally separated into the dividing daughter cells. This complex mechanism follows one basic principle: bi-orientation of the sister chromatids using a bipolar array of MTs – the mitotic spindle. This structure based on MTs, a polar polymer of α/β-tubulin, starts to be assembled at the beginning of mitosis and contains three different types of MTs: astral-, kinetochore (KT)- and interpolar MTs. In this bipolar array, the minus ends of the MTs are anchored at the centrosome, the MT organizing center (MTOC). Depending on the type of MTs, the plus-ends are either connected to KTs (KT-MTs), proteinaceous structures that are assembled at the centromeres of the chromosomes or are attached to the

cortex (astral MTs) or overlap along the spindle equator (interpolar MTs). The assembly, maintenance and function of this structure are based on two basic mechanisms: the dynamic instability of MTs and the organization of a bipolar structure by MT-dependent motor proteins (Gadde and Heald, 2004). The dynamic instability of MTs is a stochastic event, characterized by rapid transitions between growth and shrinkage of MTs that allows the cell to rapidly reorganize the MT network (Desai and Mitchison, 1997; Mitchison and Kirschner, 1984). In addition to the dynamic instability of MTs, the bipolar array is formed by a balance of opposing forces generated by motor proteins, which lead to the focusing of MT minus-ends at the poles, separation of the two half spindles by the cross linking activity of the plus end directed motor protein Eg5 and the attachment of the spindle to the cell cortex (Heald, 2000). Although these basic functions are conserved in all eukaryotes, the complexity of the mitotic spindle and the number of proteins, which are required for its functionality, increases not only with the number of chromosomes that have to be separated, but also with the geometry of the cell, e.g. small somatic cells versus large oocytes. Thus the individual requirement for certain proteins varies between different organisms and even different cell types.
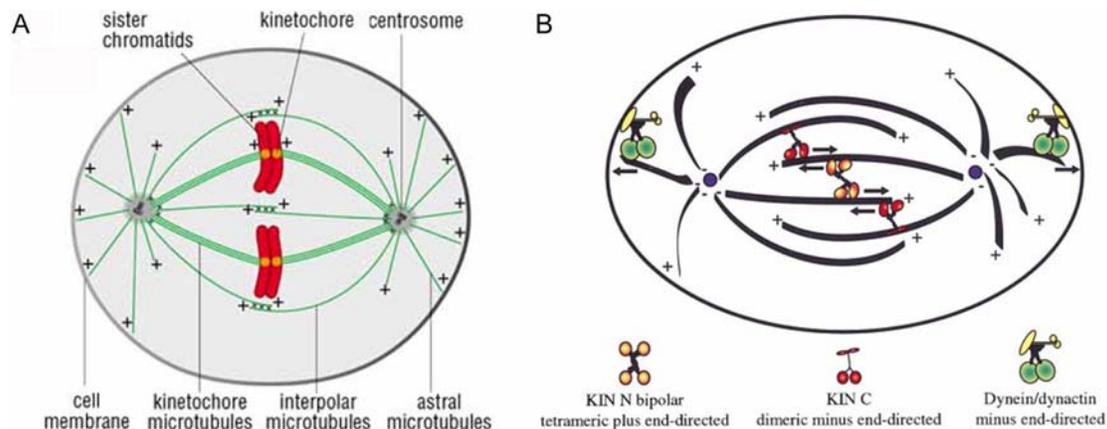
Figure 3. The mitotic spindle – composition and organization by motor proteins.
(A) Features of the metaphase mitotic spindle. With their minus ends tethered at the spindle poles, MT plus ends (+) extend either to the KTs of paired chromatids (KT fibers), to the central spindle where they form an overlapping antiparallel array (interpolar MTs), or away from the spindle towards the cell cortex (astral MTs). Adapted from (Gadde and Heald, 2004) **(B)** Cross-linking motors that increase (KIN C) or decrease (KIN N) the overlap of antiparallel MTs determine spindle pole separation. Cytoplasmic dynein at the cell cortex can contribute to spindle positioning and expansion. Forces are indicated by arrows. Adapted from (Heald, 2000).

2.2 Regulation of mitotic progression by Cdk1

The different phases of the cell cycle are globally defined by the activity of cyclin dependent kinases. Mitosis in particular is defined by the activity of its master regulator Cdk1. Cdk1, like all other Cdks, is a heterodimeric serine/threonine kinase, consisting of a catalytic Cdk subunit and an activating Cyclin subunit (Cyclin A or B) (Morgan, 1997). In order to enable

mitotic entry, Cdk1 needs to be activated, which occurs at different layers of regulation. The most critical and conserved ones during evolution are: i) the association with the A-/B-type Cyclins, ii) the removal of inhibitory phosphorylation on tyrosine 15 and threonine 14 by the dual specific phosphatase cdc25, and iii) activation of the kinase by the Cdk1 activating kinase (CAK) on threonine 161 (Nigg, 2001). Once activated, Cdk1 in complex with either Cyclin A or B phosphorylates numerous substrates in order to allow mitotic entry (Andersen et al., 1997; Blangy et al., 1995; Jackman and Pines, 1997; Lowe et al., 1998; Peter et al., 1990). In addition to Cdk1, additional kinases are required for the ordered progression through mitosis. The most important ones are the polo-like kinase (Plk) and kinases from the Aurora family. (Aurora B is described below in detail. For reviews see also (Barr et al., 2004; Nigg, 2001; Ruchaud et al., 2007)). However, Cdk1 activity not only triggers the entry into mitosis, but also prepares the exit of mitosis by activating the anaphase promoting complex (APC/C), a multisubunit E3 ubiquitin ligase (Peters, 2006). In association with its co-activator cdc20, the APC/C is required to target Cyclin A at the beginning of mitosis and, more importantly, Cyclin B at mitotic exit for degradation (Pines, 2006). In order to avoid that this occurs before all chromosomes are properly aligned at the metaphase plate a surveillance mechanism, called the spindle assembly checkpoint (SAC), is active and prevents full activation of the APC/C by impeding the association with cdc20 (Musacchio and Salmon, 2007; Rieder et al., 1995). The SAC can only be silenced, when all chromosomes are properly aligned, i.e. the two sister chromatids of a chromosome are attached to MTs from the opposite pole and forces from the mitotic spindle induce a tension status between the sister KTs. To what extent a complete lack of MT attachment, or absent tension between KTs, contribute to checkpoint activation in metazoan cells remains to be elucidated (Pinsky and Biggins, 2005). Once the checkpoint is satisfied, the APC/C mediates the ubiquitylation of two key substrates, Cyclin B and securin, and, thereby, triggers their degradation by the proteasome and initiates anaphase onset. Upon degradation of securin and Cyclin B, separase, a large and essential protease, is activated and cleaves the cohesion complex that holds sister chromatids together at the centromeres (Stemmann et al., 2001). The drop in Cdk1 activity caused by the degradation of its regulatory subunit Cyclin B, enables the release of inhibitory phosphorylations on proteins, with specific post-mitotic functions (Sullivan and Morgan, 2007). In addition to cyclin destruction, active dephosphorylation is required in order to relieve the negative regulation by phosphorylation at mitotic exit. In budding yeast, the essential phosphatase cdc14 has long been recognized as a key regulator of mitotic exit (Stegmeier and Amon, 2004). Although negative regulation of post-mitotic events by Cdk1 is evolutionarily conserved (Queralt and Uhlmann, 2008), the executing phosphatase(s) in higher eukaryotes remain elusive so far.
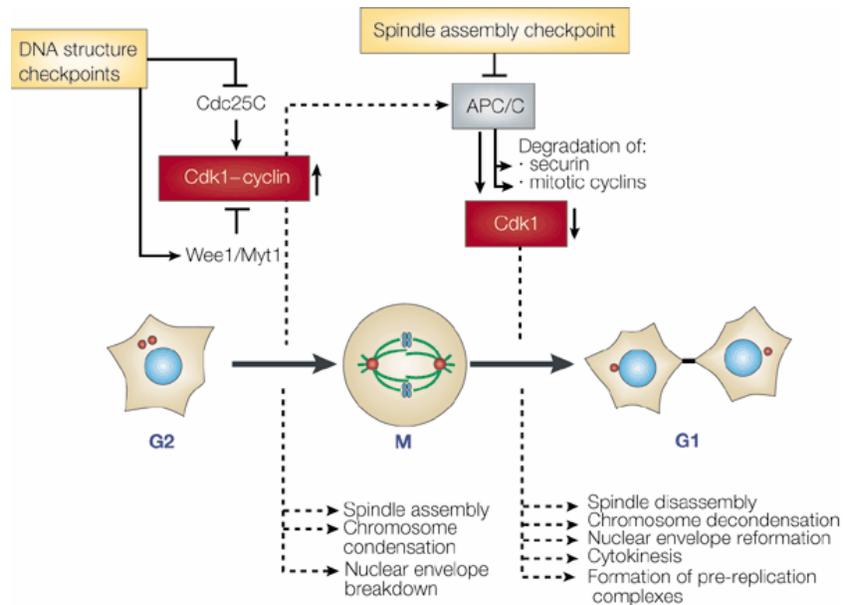
Figure 4. Regulation of mitotic progression by Cdk1.

The entry into mitosis depends on the activation of Cdk1–Cyclin complexes. In mammalian cells, the activation is primarily achieved by dephosphorylation of Cdk1, which occurs when the activity of the phosphatase cdc25C exceeds that of the kinases Wee1 and Myt1. Exit from mitosis depends on the inactivation of Cdk1–Cyclin complexes. This occurs as a consequence of Cyclin destruction, which in turn results from the activation of the APC/C ubiquitin ligase. Adapted from (Nigg, 2001).

3 Cytokinesis

In mitosis, duplicated chromosomes are separated into sister chromatids, which are then moved to opposite poles of a dividing cell. In cytokinesis, the final step of M-phase, two daughter cells are created that contain an identical set of chromosomes and evenly distributed cytoplasmic organelles. This conceptually simple event, carried out in less than 1% of the time required for the remaining cell cycle, is mediated by a complex and dynamic interplay between the MTs of the mitotic spindle, the actomyosin cytoskeleton, and membrane fusion events. Although the basic concepts of cell division are conserved among eukaryotes, the exact processes involved in cytokinesis vary in different organisms like animals, plants and yeast (Balasubramanian et al., 2004). In higher eukaryotes, the position of the cleavage plane is specified in anaphase A and the chromosomes are moved towards the poles. In the subsequent state, anaphase B, the cell elongates MTs form the spindle midzone in between the separating chromosomes and an actomyosin ring is assembled at the cleavage furrow. During telophase, the cleavage furrow constricts the components of the spindle midzone into a focused structure, called the midbody. Finally, two daughter cells are generated during abscission, when the furrow is sealed by membrane fusion events.
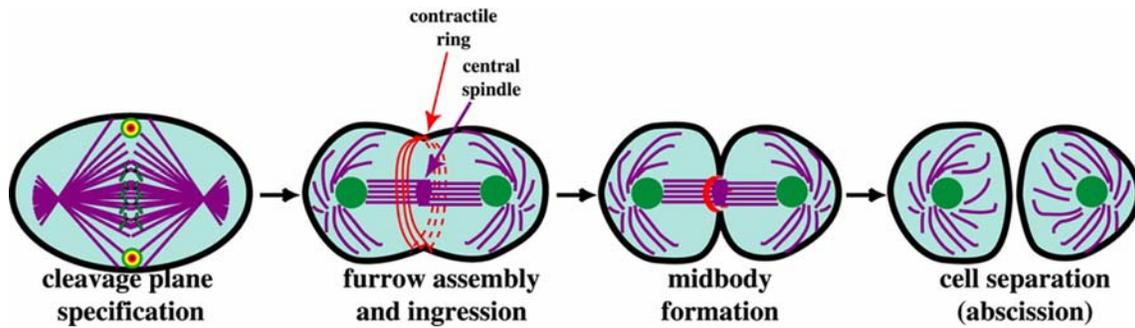
Figure 5. The sub-processes and structures that mediate cytokinesis.
Schematic diagrams of the distribution of MTs (purple), actin (red) and the DNA (green) during the final stages of cell division. Following the segregation of the chromosomes and the specification of the cleavage plane, the central spindle assembles and contractile ring assembly starts. After cleavage furrow ingression, the midbody is formed and the daughter cells are separated from each other during abscission. Adapted from (Glotzer, 2001).

3.1 Assembly and ingression of the contractile ring

The key mechanism of cytokinesis is the separation of the two daughter cells by constriction of the mother cell. The driving force of this process is the contractile ring, which is composed of actin and myosin. Assembled in anaphase at the side of the cleavage furrow, it is a sliding mechanism composed of opposing actin filaments driven by the enzymatic activity of myosin II, which produces a mechano-chemical force that drives ingression of the membranes. A key regulator of this process is the small GTPase RhoA, which is in its active state, bound to GTP. Active RhoA promotes the assembly and function of the contractile ring in two parallel branches. Activation of myosin II is mediated by the RhoA downstream target Rock (Rho-associated coiled coil kinase) and the formation of filamentous actin structures is driven by the inactivation of formin-homology proteins (Figure 6) (Glotzer, 2005). The activity of RhoA itself is regulated by the guanine nucleotide exchange factor (GEF) Ect2/Pebble and the GTPase activating protein (GAP) MgcRacGAP/Cyk-4 (Glotzer, 2005; Piekny et al., 2005). While it was long thought that only active RhoA is able to position and drive furrow ingression, recent evidence indicates instead, that permanent cycling through the GTPase cycle is necessary for this function (Miller and Bement, 2009). This in turn would also uncover the paradox, that a complex formation of the GEF and the GAP is a prerequisite for the function of RhoA at the cortex. Furthermore, binding of Mklp1 to MgcRacGAP (centralspindlin complex, see below) provides a physical link between the spindle midzone MTs and the cell cortex and thus, spatially restricts functional RhoA to the side between the separating chromosomes.
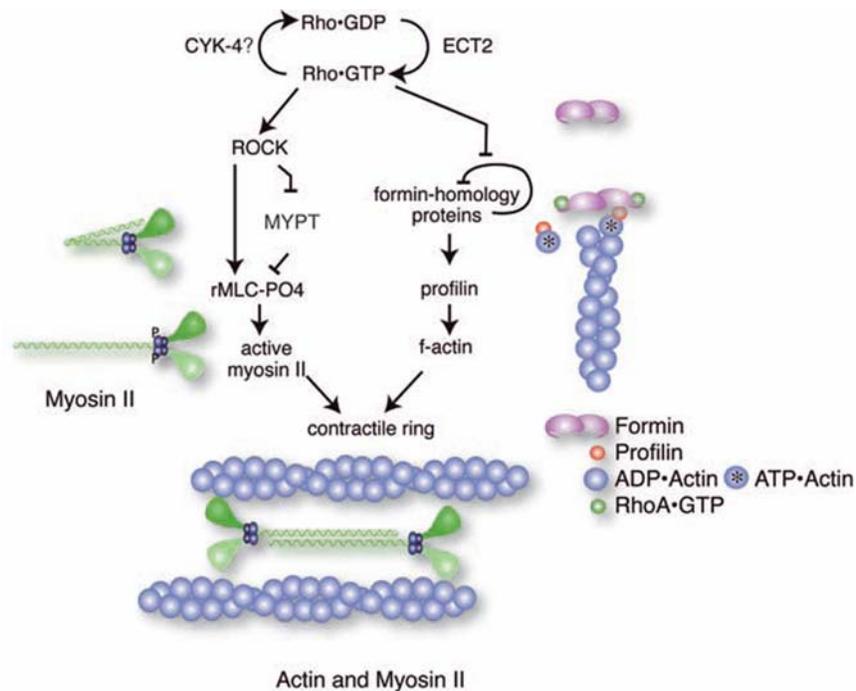
Figure 6. RhoA dependent pathways in cytokinesis.

The RhoA GTPase activates myosin and actin filament assembly. RhoA induces phosphorylation and thus activation of the regulatory light chain of myosin (blue). The auto inhibition of Formin is relieved by RhoA-GTP and allows the processive elongation of the barbed end of actin filaments, a reaction that is profilin dependent. Adapted form (Glotzer, 2005).

3.2 Assembly of the spindle midzone

The mitotic spindle serves as the structural backbone for the accurate alignment of the sister chromatids during mitosis. At the onset of anaphase, the aligned sister chromatids move to the opposite poles of the dividing cell. Since these fundamentally distinct processes are carried out by the same basic structure, an array of MTs, a dramatic change in its structure and organization is required. The KT-MTs, which are attached to the chromosomes, shorten, while astral MTs elongate, and MTs of the cytoplasm form the spindle midzone between the separating chromosomes. This newly formed structure is called the spindle midzone and is composed of an antiparallel, bundled array of MTs with interdigitating plus ends facing the center of the cell (Glotzer, 2009).
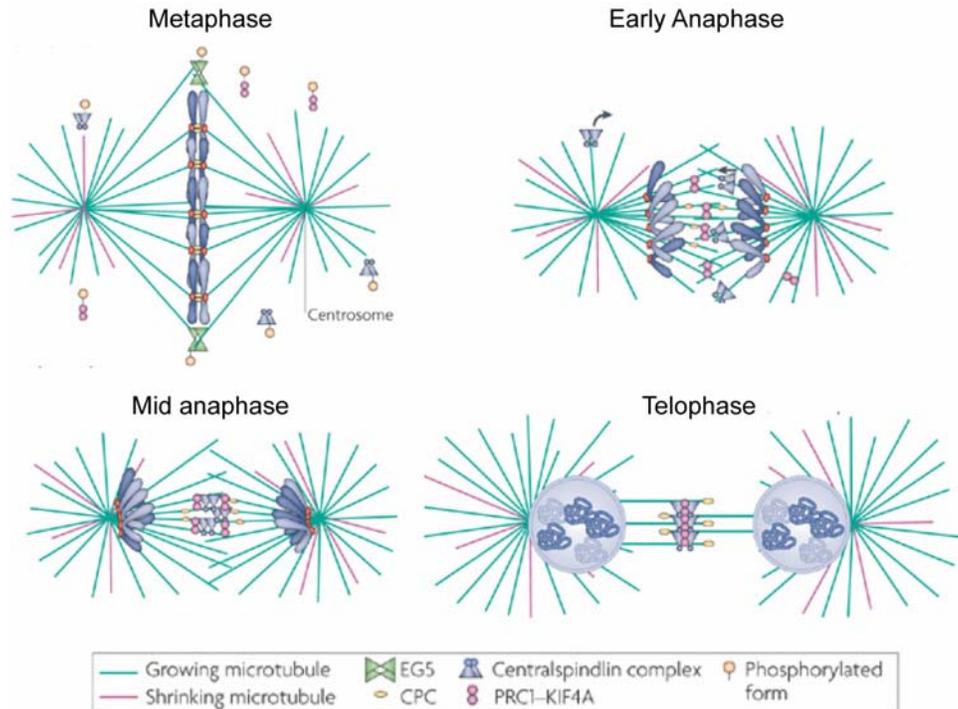
Figure 7. Working model for the assembly of the spindle midzone.
Metaphase: Mitotic spindle assembly factors active, central spindle assembly factors inactivated by phosphorylation. **Early anaphase:** MTs become less dynamic, CPC released from chromosomes, activation of PRC1 and centralspindlin. **Mid anaphase:** CPC stabilizes centralspindlin, PRC1 and centralspindlin become highly concentrated, stabilization of midzone MTs. **Telophase:** Chromosomes de-condense and nuclei reform, central spindle factors become highly ordered. Adapted and modified from (Glotzer, 2009).

The global reorganization of the spindle structure in a timeframe of minutes requires profound changes in MT dynamics, as well as in the localization and/or activation of molecular players involved. Mitotic and spindle midzones differ greatly in the stability of MTs contained therein. The turn over of MTs slows down dramatically from a half life of 10-20 seconds in metaphase, to more than 2 minutes in anaphase (Salmon et al., 1984; Saxton and McIntosh, 1987; Saxton et al., 1984). This increase in stability is furthermore characterized by a higher resistance of anaphase MTs of the spindle midzone to low doses of MT depolymerizing agents (Murthy and Wadsworth, 2008). Following metaphase to anaphase transition, the spindle midzone is formed between the separating chromosomes and it has been thus assumed, that the mitotic spindle acts as a template for the newly formed spindle midzone structure. While this could be an assisting mechanism, enabling a rapid and accurate formation of the spindle midzone, the structure itself can also be formed *de novo*, as indicated by the existence of structural equivalents that are formed in the absence of chromosomes or centrosomes (Alsop and Zhang, 2003). Consistent with this, spindle midzone formation is mainly mediated by a specific subset of MT associated proteins

(MAPs) and kinesins, which are geared towards this process in their function and activity. The most prominent players required for spindle midzone formation are the MT bundling protein PRC1 (protein required for cytokinesis) (Jiang et al., 1998) and centralspindlin, a complex of the kinesin motor Mklp1 and the GTPase activating protein MgcRacGAP (Male germ cell specific RAC GTPase activating protein) (Mishima et al., 2002). The requirement of PRC1 for cell division is conserved from yeast to human (Glotzer, 2009). Its ability to bundle antiparallel MTs as shown by *in vitro* studies seems to be essential for its function in cytokinesis (Mollinari et al., 2002). In contrast to yeast, the human homolog requires the kinesin motor protein KIF4A for the accurate binding to the spindle midzone (Juang et al., 1997; Kurasawa et al., 2004). In higher eukaryotes, the centralspindlin complex exerts the same function as PRC1 in the formation of the spindle midzone by its ability to bundle antiparallel MTs (Mishima et al., 2002).

3.3 Regulation of cytokinesis in space and time

The position of the cleavage furrow and its activation must be tightly coupled to chromosome segregation in space and time in order to ensure genomic integrity of the forming daughter cells. More than 40 years ago, experiments performed by Rappaport already indicated that the position of the mitotic spindle determines the position of the future cleavage furrow. While this idea is still valid, and the essential role of MTs for furrow positioning is established, it remains under debate as to which part of the spindle transmits the signal – the spindle midzone or the spindle poles. In animal cells, three modes of division site positioning have been demonstrated (Figure 8). The astral relaxation hypothesis of furrow ingression suggests, that the influence of astral MTs results in a relaxation of cortical contraction near the poles and therefore furrows form at the equator (Wolpert, 1960). Meanwhile, the astral stimulation hypothesis proposes that the overlapping influence from both asters at the equator results in a maximum of stimulatory signals in this region (Rappaport, 1961). In addition to the proposed signals from the spindle poles, a stimulatory signal at the cell equator can be also transmitted from the spindle midzone (Alsop and Zhang, 2003; Giansanti et al., 2001). Compelling evidence for signals from both, the spindle poles and the spindle midzone, implies their co-existence and the importance of either factor may also depend on the studied organism or even the size of the cell. This is currently best illustrated by studies in *C. elegans*, describing that temporally distinct signals from both the aster and the spindle midzone are required for the positioning of the furrow (Bringmann and Hyman, 2005).
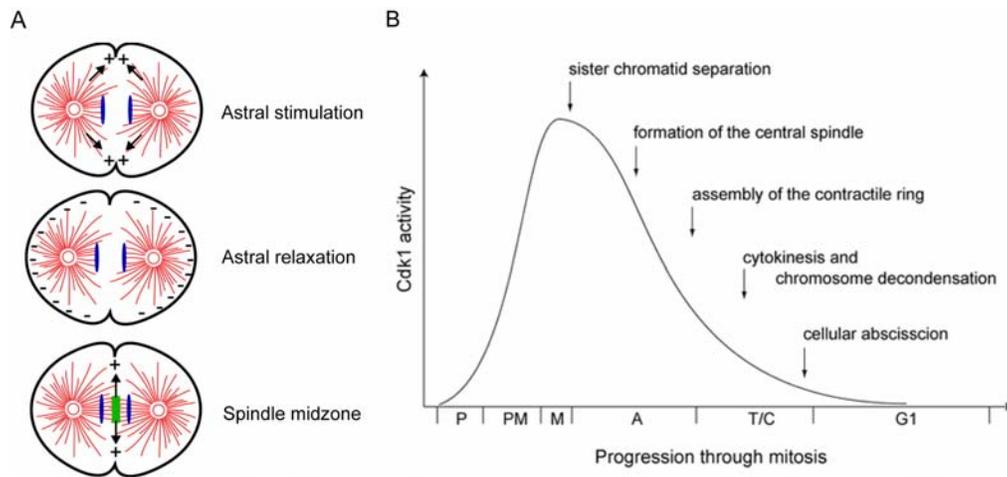
Figure 8. Regulation of cytokinesis in space and time.
(A) Three models for cleavage plane positioning in animal cells. Astral MTs stimulate cleavage furrow formation at the division site (Astral stimulation). Astral MTs inhibit cortical contractility at the cell ends to promote cleavage furrow formation at the division site (Astral relaxation). The overlapping MT bundles at the cell spindle midzone specify the cleavage plane (spindle midzone). Adapted form (Glotzer, 2004). **(B)** Control of exit from mitosis by timed dephosphorylation of Cdk substrates. Dephosphorylation of key regulators of late mitotic events, such as formation of the central spindle, cytokinesis and cellular abscission might control the exit from mitosis. P, prophase; PM, prometaphase; M, metaphase; A, anaphase; T/C, telophase/cytokinesis; G1, G1 phase. Adapted from (Wolf et al., 2007).

As well as local control, it is equally important to ensure that the initiation of cleave furrow formation and cytokinesis do not occur before anaphase onset. This temporal control is subdivided in different layers of regulation, dominated by one basic principle – the inhibition of post-metaphase events by Cdk1/Cyclin B. After the last chromosome has aligned at the metaphase plate, the inactivation of the spindle assembly checkpoint triggers the inhibition of Cdk1 activity by APC/C mediated degradation of its co-activator Cyclin B. Subsequent removal of the inhibitory phosphorylations of certain Cdk1 substrates finally activates their specific post-mitotic functions. One of the first examples underlying this basic principle was shown for the homolog of INCENP in budding yeast, sli-15, member of the evolutionary conserved CPC. The dephosphorylation of sli-15 by cdc14 after mitotic exit is prerequisite for the binding of sli-15 to the post-mitotic spindle (Pereira and Schiebel, 2003). The activation of cdc14 itself is mediated by its release from the nucleolus in a separase dependent manner, a yeast specific mechanism that has yet to be identified in humans. But despite this, and the fact that spindle midzone transfer of the CPC in higher eukaryotes requires the kinesin-6 family member Mklp2 (Gruneberg et al., 2004), which is not present in yeast, the negative regulation of post-mitotic events by Cdk1 seems to be conserved in humans, since sustained Cdk1 activity prevents spindle transfer of the CPC member Aurora B (Murata-Hori et al., 2002). Until now, an increasing number of proteins, including Plk1, PRC1, centralspindlin and

Ect2, have been shown to be negatively regulated in their late mitotic localization, and/or function, by Cdk1 phosphorylation (Mishima et al., 2004; Neef et al., 2007; Yuce et al., 2005). In contrast to the negative regulation of cytokinesis by Cdk1, Aurora B and Plk1 promote cytokinesis (Carmena, 2008; Petronczki et al., 2008). Since both kinases are known to be active during entire M-phase, their cytokinesis-specific functions have to be timely regulated in order to avoid interference with mitotic progression. This in turn seems to be coupled to the negative regulatory circuit by Cdk1. As described above, the localization of Aurora B to the spindle midzone, which is thought to be prerequisite for its function in cytokinesis, is negatively regulated by Cdk1 (Murata-Hori et al., 2002; Pereira and Schiebel, 2003). The localization of Plk1 to the spindle midzone, mainly mediated by PRC1, is regulated in a similar manner. Specifically, binding of Plk1 to PRC1 requires a priming phosphorylation which is carried out by Plk1 itself (self-docking). This priming phosphorylation is prevented during early mitosis by Cdk1 phosphorylation of PRC1 (Neef et al., 2007). But not only the localization of the kinases Aurora B and Plk1, also their downstream effectors are kept inactive by Cdk1 during mitosis. Among an increasing number of examples, the function of Ect2 in cytokinesis is regulated by both, Cdk1 and Plk1 in a reciprocal manner. While Cdk1 phosphorylation of Ect2 inhibits its association with the centralspindlin complex (Yuce et al., 2005), phosphorylation of Ect2 by Plk1 is essential for its localization at the spindle midzone (Burkard et al., 2007). Thus, the dual control of proteins with a specific function in cytokinesis ensures their specific activation at anaphase onset which can be maintained until the end of cytokinesis.

4 The chromosomal passenger complex (CPC)

The CPC in higher eukaryotes is composed of the serine-threonine kinase Aurora B and the non-enzymatic subunits INCENP, survivin and borealin (Ruchaud et al., 2007). Initially, INCENP was discovered over 20 years ago in a screen for new components of the chicken chromosome scaffold (Cooke et al., 1987). Further studies revealed that the inner centromere protein (INCENP) was found to be localized at centromeres during metaphase but subsequently transferred to the spindle midzone upon anaphase onset (Earnshaw and Cooke, 1991). Based on this dynamic localization the INCENP-containing complex was termed "chromosomal passenger complex". Already at this time, it was proposed, that the different localization of the CPC reflects the different functions of the CPC during cell division (Earnshaw and Cooke, 1991; Eckley et al., 1997). This theory is still valid, and the pivotal roles of the CPC throughout M-phase, comprises functions in chromatin modification, assembly of the centromere/KT region, correction of KT-MT attachment, aspects of the SAC, assembly of a stable bipolar spindle as well as the spindle midzone, and completion of

cytokinesis (Adams et al., 2001a; Ruchaud et al., 2007; Vader et al., 2006). The known downstream targets of the CPC in these distinct stages of M-phase are depicted in Figure 9.
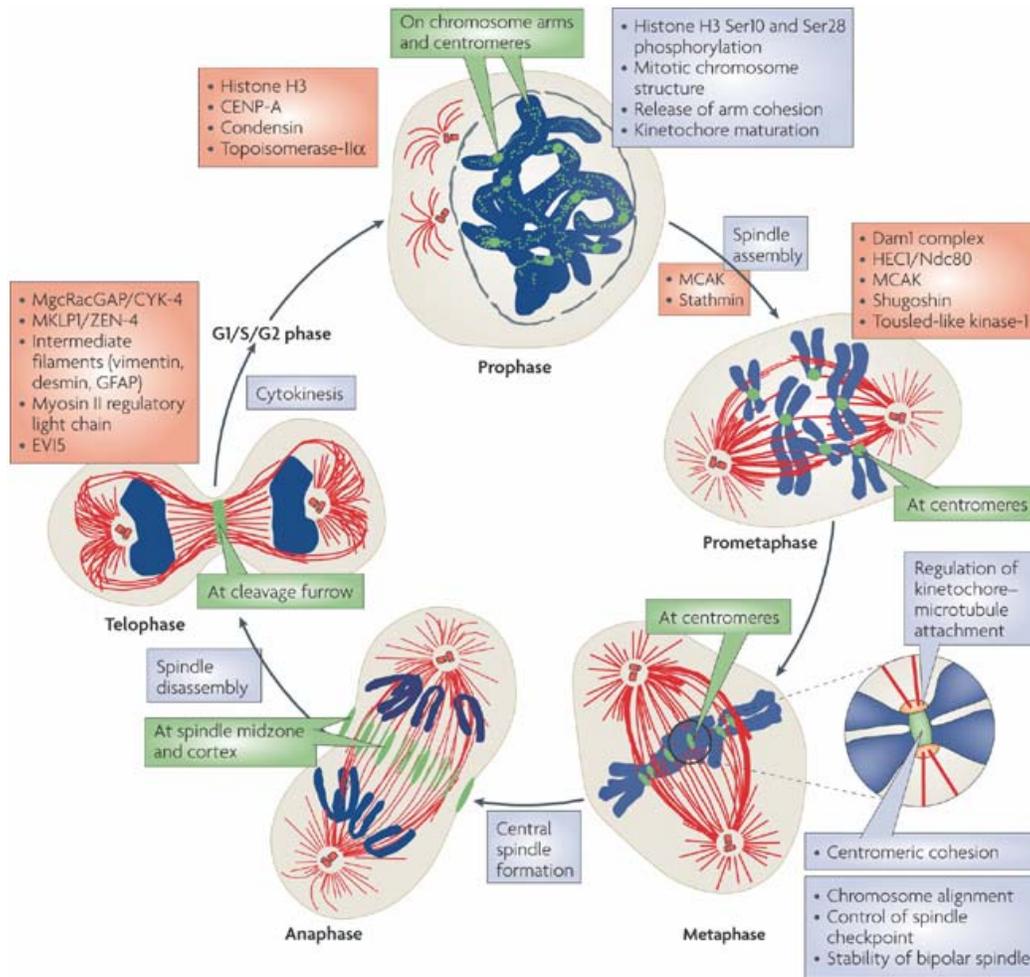
Figure 9: The chromosomal passenger complex (CPC).
Illustration of the CPC localization (green) correlated with its multiple functions (blue boxes) and principal targets of the kinase Aurora B (red boxes) during the different phases of mitosis. In prophase, the CPC is found on chromosome arms and is involved in the release of arm cohesion and mitotic chromosome structure. During this phase the CPC starts to accumulate at centromeres. From prophase/prometaphase to anaphase, the CPC is required for the formation of a bipolar spindle. In metaphase, the CPC has a central role in centromeric cohesion and the regulation of KT–MT attachments, and controls the correct alignment of chromosomes on the spindle equator and the SAC. Upon the onset of anaphase the CPC translocates to the spindle midzone where it is involved in the formation of the spindle midzone. In telophase the CPC concentrates at the cleavage furrow and subsequently at the midbody, where it is required for the completion of cytokinesis. Chromosomes are shown in blue; tubulin in red; nuclear envelope in grey. Adapted from (Ruchaud et al., 2007).

While the function of the CPC is mainly carried out by Aurora B, the other members control the stability, activity and subcelluar localization of the complex. INCENP acts as the scaffold of the CPC by integrating the three other members in the complex (Klein et al., 2006; Lens et al., 2006). This is achieved by the formation of a ternary complex with survivin and borealin at the N-terminus and an interaction with Aurora B via the so called IN-Box at the C-terminus of INCENP (Jeyaprakash et al., 2007; Klein et al., 2006). In addition, the latter is required for regulation of kinase activity (Honda et al., 2003). Underlining the existence of the CPC as a functional unit, knockdown by RNA interference (RNAi) of any member of the complex, affects the stability of the other subunits, delocalizes the other members and results in the disruption of mitotic progression (Klein et al., 2006).

As suggested by its name the localization of the CPC is highly dynamic during mitosis. While being localized to chromosome arms during prophase, the CPC is concentrated at the centromere during prometaphase. The structural element required for this localization is composed of the N-terminus of INCENP (aa 1-58), which is capable of assembling the ternary complex with survivin and borealin (Klein et al., 2006). Furthermore, an interplay between the ubiquitylation and deubiquitylation, carried out by UFD1 and hFam, respectively keeps this localization highly dynamic (Vong et al., 2005).

At the metaphase-anaphase transition, the CPC leaves the inner centromere and transfers to the spindle midzone MTs. While INCENP itself is capable of binding MTs *in vitro* (Wheatley et al., 2001), additional components seem to be required for the timed transfer of the CPC to the spindle midzone *in vivo*. On one hand, the kinesin-6 motor protein Mklp2 has been shown to be essential for the localization of the CPC at the spindle midzone (Gruneberg et al., 2004). On the other hand, the transfer to the spindle midzone appears to be subjected to different layers of regulation. Ubiquitylation of Aurora B by the Cul3 E3 ubiquitin ligase complex is required for the removal of the Aurora B from the mitotic chromosomes (Sumara et al., 2007). In budding yeast dephosphorylation of sli-15, the homolog of INCENP, by the phosphatase cdc14 is required for the binding of the CPC to the spindle midzone after anaphase onset (Pereira and Schiebel, 2003). However, it remains to be clarified, how these different components are integrated in order to ensure proper localization of the CPC to the spindle midzone upon anaphase onset.

While the essential role of the CPC for cytokinesis is undisputable (Ainsztein et al., 1998; Carmena, 2008; Eckley et al., 1997; Ruchaud et al., 2007; Schumacher et al., 1998; Tatsuka et al., 1998; Terada et al., 1998; Wheatley and Wang, 1996), the precise function of the complex is less well understood. Since it is experimentally difficult to dissect the late function of the CPC during cytokinesis from the early one in mitosis, the interpretation of mutant analyses is complicated. Furthermore, it seems that the mechanism of cytokinesis varies depending on the studied organism which has furthermore hampered the understanding of the exact function of the CPC in this process. In line with this, it has been proven in all

studied organisms that the function of the centralspindlin complex is regulated by the CPC, but dependent on the applied methods and the studied organism different regulatory mechanisms have been proposed (Carmena, 2008). Thus future research effort will be clearly required to delineate the exact underlying mechanisms. Beyond that, it has been shown that ipl-1 (homolog of Aurora B in budding yeast) is also involved in the negative regulation of cytokinesis. This function is integrated in the so called "NoCut pathway", which ensures that abscission only takes place after successful segregation of the chromosomes (Norden et al., 2006). A similar pathway has been also proposed in human, but the underlying mechanism remains elusive thus far (Steigemann et al., 2009).

5 Kinesins and the kinesin-6 family

Molecular motors convert energy dependent conformational changes in mechano-chemical forces. Among these molecular motors three classes are known, which depend on cytoskeletal fibers for their activity: myosin, which interacts with actin filaments, and two types of MT motors, dynein and kinesin. All these motors contain a catalytic motor domain that harbors two binding sites: one for ATP and one for the cytoskeleton (Woehlke and Schliwa, 2000).
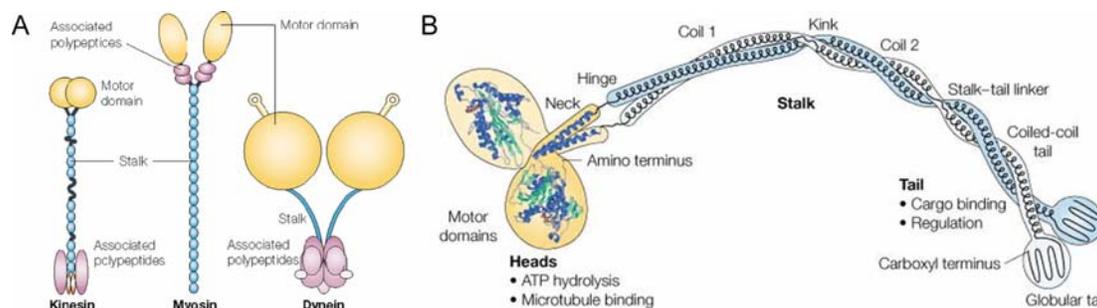
Figure 10. Kinesins.

(A) Overview of the three molecular motor 'prototypes'. The MT motors conventional kinesin (left) and cytoplasmic dynein (right) as well as the actin-based motor skeletal muscle myosin (middle) are shown. Catalytic domains are depicted in yellow, the stalks in blue and the associated polypeptides in purple. **(B)** Domain organization of the conventional kinesin heavy-chain dimer. Structure of the catalytic domains and neck are drawn according to the crystal structure, the stalk and tail are obtained from electron microscopic images and the coiled-coil regions as well as the flexible regions are inferred from predictions. Adapted from (Woehlke and Schliwa, 2000).

Kinesins have been identified more than 20 years ago (Brady, 1985; Scholey et al., 1985; Vale et al., 1985). Conventional kinesin, founding member of this class of motor proteins and most extensively studied, is composed of four major elements: head, neck, stalk and tail (Figure 10). Based on the sequence conservation of the catalytic core (head), up to date

more than 40 kinesins have been described and are, dependent on the homology of this region, subcategorized into 14 different families (Lawrence et al., 2004). The domains outside the catalytic core are highly divergent in their molecular architecture among different kinesins and also greatly differ even in members of the same family. This diversity is further transmitted into the different biological functions, which include not only the transport of associated cargo proteins such as membrane-bound organelles and messenger RNA, but also cell division, chemosensory and signal transduction functions, MT dynamics, neuronal plasticity and embryonic development (Woehlke and Schliwa, 2000).

The head domain of kinesins mediates both the hydrolysis of ATP and the binding to MTs. Dependent on the type of kinesin, the energy released by ATP-hydrolysis is either converted in the movement along - and/or depolymerization of MTs (Gennerich and Vale, 2009; Mayr et al., 2007; Wordeman, 2005). For the movement along MTs, the conformational change in the head domain is further transmitted into the neck region, whose orientation defines the directionality of the movement (Case et al., 1997; Henningsen and Schliwa, 1997). By formation of homodimers and the coordination of the two head domains, the kinesin can 'walk' along MTs by having one head attached to MTs while the other one moves forward (hand over hand model) (Yildiz et al., 2004).

While the biophysical properties of kinesins are quite well understood, the regulation of these molecular machines is still an emerging field. Clearly, posttranslational modifications, e.g. phosphorylation and the regulated association with interaction partners are important mechanisms to control the activity of kinesins (Woehlke and Schliwa, 2000).

The kinesins Mklp1, Mklp2 and MPP1 (KIF23, KIF20A and KIF20B, respectively) are subcategorized into the kinesin-6 family (Lawrence et al., 2004). This kinesin family differs in two characteristic features from other kinesins: a long extension in the conserved motor domain adjacent to the P-loop (part of the ATP binding domain), and a neck linker region that is five times longer than those in other kinesins (Hizlan et al., 2006; Miki et al., 2005; Mishima et al., 2002). The C-terminal tail region is highly diverse among the three kinesin-6 members. The founding member of the kinesin family Mklp1 is present in all higher eukaryotes. In contrast, Mklp2 and MPP1 are not widely found in sequenced genomes. While both are present in mammals, *Drosophila melanogaster* has only an Mklp2 orthologue, subito, in addition to the Mklp1 orthologue Pavarotti (Pav) and *Caenorhabditis elegans* has only an orthologue of Mklp1 (Zen4) (Glotzer, 2009). The meaning of these evolutionary different requirements for more than one kinesin-6 family member in higher eukaryotes remains unaddressed thus far. Interestingly, the common structural principles of this class of kinesins seem to also be continued in their biological function, since all three members are thought to have a function in cytokinesis (Abaza et al., 2003; Adams et al., 1998; Hill et al., 2000), even while having different binding partners (Gruneberg et al., 2004; Mishima et al., 2002; Neef et al., 2003).
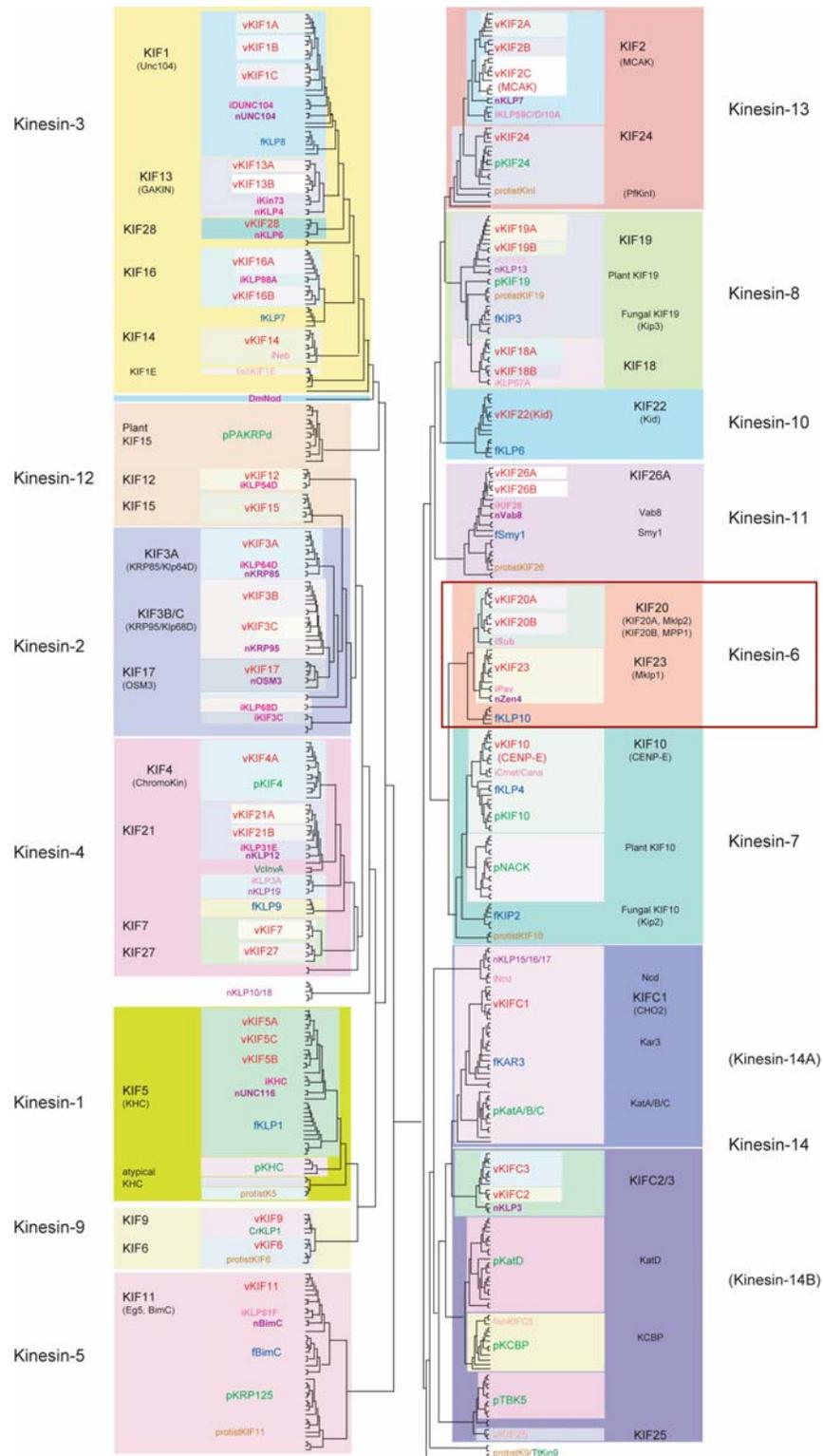
Figure 11. Phylogenetic tree of the kinesin superfamily.
The kinesin-6 family is highlighted with a red square. Adapted from (Miki et al., 2005).

6 The intermediate filament (IF) vimentin

IFs, together with MTs and actin filaments, form the cytoskeletal framework in the cytoplasm of eukaryotic cells and are also present in nuclei as the major component of the nuclear lamina. In contrast to the major components of the cytoskeleton, actin and tubulin, IFs are molecularly highly diverse, resulting in six different classes (I-VI) (Fuchs and Weber, 1994). The domain structure of all types of IFs is conserved and consists of globular domain flanking the central coiled coil domain (rod) (Herrmann and Aebi, 1998; Parry and Steinert, 1992). In order to from filaments, the monomers dimerize via the coiled coil domain and tetramers are formed by the association of these dimers. Filaments are finally formed by the association of individual tetramers (Figure 12.A). In addition to other regulatory mechanisms, protein kinases and phosphatases are known to control dynamic aspects of IF organization and structure (Eriksson et al., 1992; Inagaki et al., 1987; Nigg, 1992; Sihag et al., 2007) (Figure 12.B).
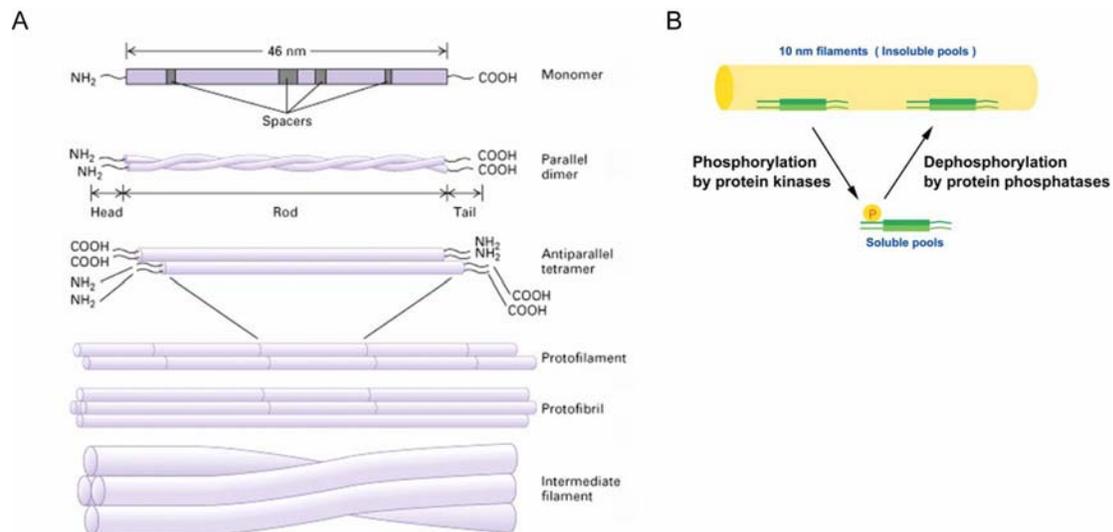
Figure 12. The IF vimentin.

(A) Organization and assembly of IFs. IFs have a central α-helical domain capped on each end by non-helical amino (head) and carboxy (tail) end domains. The α-helical domain is interspersed with non-helical domains (Spacer). Two monomers twist around each other to form a coiled-coil dimer. Two dimers then form an antiparallel tetramer, which, in turn is assembled into a protofilament by interacting with other tetramers. Two protofilaments form a protofibril and four protofibrils form a 10 nm filament. Adapted from Lodish et al., Molecular Cell Biology, 4th edition. **(B)** Regulation of IF organization by phosphorylation. Phosphorylation in the head domain of IFs causes their disassembly. The balance between phosphorylation by protein kinases and dephosphorylation by protein phosphatases controls the continuous exchange between soluble pool and polymerized filaments. Adapted from (Izawa and Inagaki, 2006).

Vimentin belongs to the class III of IFs. Like all other IFs, except lamins, vimentin expression is tissue specific and is most abundant in mesenchymal cells, and transiently in many cells

during the early stages of development (Franke et al., 1982; Franke et al., 1987; Fuchs and Weber, 1994). The expression pattern of vimentin serves as a reliable marker for tumor progression, particularly of invasiveness (Fuchs and Cleveland, 1998). Expression of vimentin in non mesenchymal cells, such as epithelial cells, is one of the hallmarks of epithelial–mesenchymal transition (EMT), which in turn is implicated in tumor progression (Kokkinos et al., 2007). In accordance with its non uniform expression profile, vimentin is not essential for basic cellular functions as shown by the viability of the knock-out mouse (Colucci-Guyon et al., 1994). In line with this, vimentin as a cytoskeletal component is implicated in the support of MT dependent functions in organelle positioning and maintenance of cell integrity particularly under mechanical stress (Eckes et al., 1998; Galou et al., 1997).

Disassembly of IFs during mitosis is a prerequisite for normal cell division (Izawa and Inagaki, 2006; Nigg, 1992). This in turn is mediated by phosphorylation of the filaments by mitotic kinases. Disassembly of the nuclear lamins, required for the break down of the nuclear envelope, is mediated by Cdk1 (Peter et al., 1990). Vimentin and other class III IFs appear to be regulated by a concerted effort between Cdk1, Plk1, Aurora B and Rho kinase (Goto et al., 1998; Goto et al., 2003; Inada et al., 1999; Izawa and Inagaki, 2006; Yamaguchi et al., 2005; Yokoyama et al., 2005). Phosphorylation of vimentin by Aurora B has been shown to be required for efficient disassembly of the filament *in vitro* and *in vivo* (Goto et al., 2003; Yokoyama et al., 2005). This regulation appears to be specifically important for the late stages of M-phase, since a non phosphorylatable mutant of vimentin induces IF bridges between the separating cells and a multinucleation phenotype (Goto et al., 2003; Yasui et al., 2004).

7 Chemical genetics

The use of small molecule inhibitors in the study of cell biology has a long history and has led to many profound discoveries. Focusing on the study of mitosis, the roots of research employing small molecule inhibitors can be followed back to the 18th century, when it was described for the first time that a substance called "colcemid" blocks cell growth. Without knowing its mode of action, this substance was used for many years to study the process of mitosis, to generate agricultural important polyploid strains, and to determine that 46 is the correct number of chromosomes in a diploid human cell. The discovery of tubulin as the target protein of colcemid in 1960 by Ed Taylor and colleagues was thus intimately linked with the discovery of the mitotic spindle and its essential functions in chromosome segregation. Beyond this, many aspects of our current understanding of cell division are based on MT toxins. For example, the discovery of the checkpoint system was based on a

loss-of-function screen for proteins that were not able to sustain the mitotic arrest in the presence of MT poisons (Hoyt et al., 1991; Li and Murray, 1991).

The systematic approach that aims to identify novel small molecules in order to unravel the mechanistic details of complex cellular processes is called "chemical genetics" (Mitchison, 1994; Schreiber, 1998). In accordance with classical genetic approaches, we can distinguish between forward and reverse chemical genetics (Figure 13).
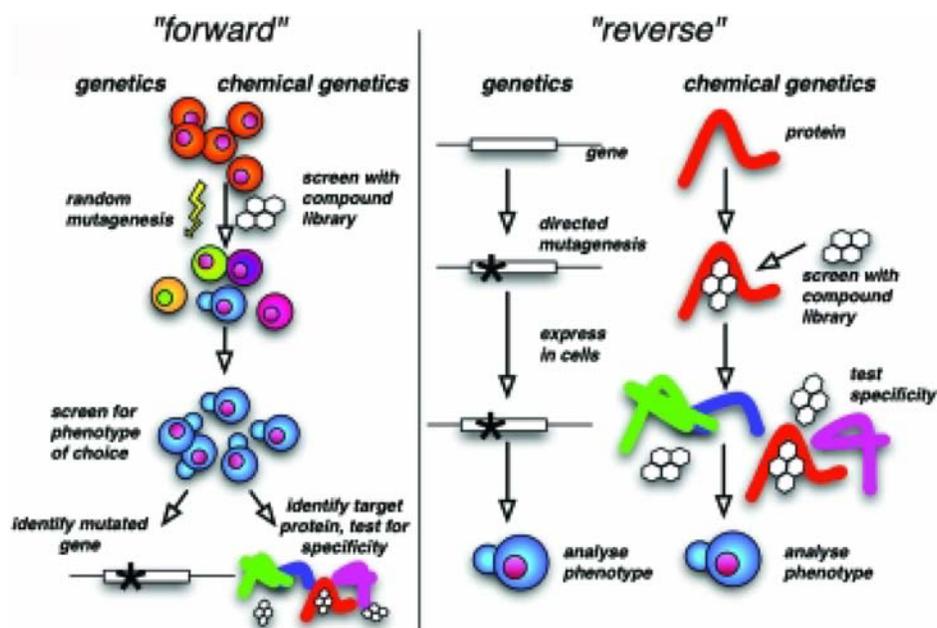
Figure 13. Comparison of forward and reverse genetics and chemical genetics approaches.
Forward screening starts with creating a phenotype by inhibiting or inactivating a target, followed by target identification. In the reverse screening approach a selective target is inhibited / inactivated before the effect is assayed in a biological assay. Adapted from (Florian et al., 2007).

In the forward chemical genetics approach, small molecules are identified in a screen for a desired phenotype, followed by the identification of the target. An example in the context of cell division is the identification of monastrol, a small molecule that inhibits the motor activity of the kinesin Eg5 (Mayer et al., 1999). Monastrol was discovered in a screen for small molecules that arrest cells in mitosis without directly affecting the MT cytoskeleton. The correlation between the characteristic monopolar spindle observed after treatment with monastrol and interference with the function of Eg5, finally led to the identification of the molecular target.

The reverse chemical genetics approach starts from the target of interest. Following this strategy, the small molecule inhibitor blebbistatin was found in a screen for inhibitors of the

ATPase activity of myosin II and consequently was able to block myosin II driven furrow ingression during cytokinesis (Straight et al., 2003).

Since both methods have been successfully applied to the identification of novel small molecule inhibitors, compelling arguments for each approach exist. On one hand, the ability of the substance to induce a certain phenotype in the physiological context ensures that the small molecule is biologically active and that the affected target, even without knowing it, has the expected physiological relevance. On the other hand, starting from a protein of interest ensures that the target of a substance is known. Thus, dependent on the goal of a screen, one or the other approach may offer a higher possibility of success.

Once identified, small molecule inhibitors can often not replace but supplement and improve classical genetic approaches in certain aspects. The potential to use the same compound to study the process of interest in different organisms for example, enables the use of MT poisons across different species and overcomes the necessity of classical genetic approaches to newly engineer a defined genetic background in each organism. Furthermore, the instantaneous activity of small molecules and their (in many cases) reversibility, often helps to overcome the biggest challenge in all classical approaches – the temporal resolution for the study of highly dynamic processes. Due to the reversibility of colcemid for example, the role of the MT-organizing center (MTOC) in nucleating MTs was initially recognized (Brinkley et al., 1975; Osborn and Weber, 1976). Further underlying this advantage of small molecules, only the development of inhibitors for the kinase activity of Plk1 enabled the study of its function in cytokinesis and helped to overcome the problem of classical approaches, in which irreversible interference with the function of Plk1 resulted in a checkpoint dependent arrest, due to its function in early stages of mitosis (Brennan et al., 2007; Burkard et al., 2007; Petronczki et al., 2007; Santamaria et al., 2007).

Aim of this work

The CPC plays pivotal roles throughout all stages of M-phase and its various functions are often reflected by the different localization during cell division (Earnshaw and Cooke, 1991; Eckley et al., 1997; Ruchaud et al., 2007). At anaphase onset, the CPC transfers from centromeres to the spindle midzone, a structure composed of antiparallel MTs (Ainsztein et al., 1998; McCollum, 2004; Schumacher et al., 1998; Tatsuka et al., 1998; Terada et al., 1998; Wheatley et al., 2001). Previous studies revealed that the mitotic kinesin Mklp2 is essential for the recruitment of the CPC to the spindle midzone (Gruneberg et al., 2004). However, the mechanism regulating the binding of Mklp2 to MTs remained unknown.

Mklp2 is required for the localization of the CPC to the central spindle in all studied organisms (Gruneberg et al., 2004; Jang et al., 2005). Furthermore, the CPC has a universal and essential role in cytokinesis (Ruchaud et al., 2007; Schumacher et al., 1998; Tatsuka et al., 1998; Terada et al., 1998; Wheatley and Wang, 1996). However, cytokinesis can be achieved in the absence of Mklp2 in *D. melanogaster* (Cesario et al., 2006). Hence it remains to be addressed, which CPC-mediated functions in cytokinesis require its Mklp2-dependent localization to the central spindle.

Cytokinesis is a highly dynamic process that is intimately linked to mitosis. Thus the study of cytokinesis requires molecular tools with a high temporal resolution. This in turn is one of the key features of small molecules, who act instantaneously and quite often reversible. The identification of small molecule inhibitors for kinesins with a function in cytokinesis, like Mklp2, could thus provide new tools for the study of this highly dynamic process.

Results

Results 1: Regulation of the Mklp2

The CPC is a key component for the coordination of mitosis with cytokinesis (Adams et al., 2001a; D'Avino et al., 2005; Eggert et al., 2006; Glotzer, 2005; Straight and Field, 2000). The translocation of the CPC from centromeres to the spindle midzone, a structure composed of antiparallel MTs at anaphase onset is critical for the completion of cytokinesis (Ainsztein et al., 1998; McCollum, 2004; Schumacher et al., 1998; Tatsuka et al., 1998; Terada et al., 1998; Wheatley et al., 2001). In mammalian cells, the mitotic kinesin Mklp2 is essential for the recruitment of the CPC to the spindle midzone (Gruneberg et al., 2004). However, the mechanism regulating the binding of Mklp2 to MTs remains unknown.

1.1 Binding of Mklp2 to MTs after anaphase onset depends on its active motor domain

To study in detail the mechanism regulating the binding of Mklp2 to MTs in cells, we first analyzed its sub-cellular localization during M-phase by indirect immunofluorescence. As reported previously (Hill et al., 2000), we found Mklp2 diffusely localized in the cytoplasm during early mitosis, but accumulated at the midzone between segregating chromosomes in anaphase and, finally, concentrated at the midbody during cytokinesis (Figure 14.A). These results imply that binding of Mklp2 to MTs is highly regulated during mitotic progression. We next wanted to explore if such regulation is mediated by the affinity of the kinesin motor for MTs. To test this, we created two types of ATP-binding mutants: full-length Mklp2 impaired in its ability to bind ATP (Mklp2^{ATPm}) and, thus, to interact with MTs (Matuliene et al., 1999) and a rigor-type Mklp2 mutant (switch II mutant, Mklp2^{SIIm}) unable to hydrolyze ATP and, therefore, constitutively bound to MTs (Rice et al., 1999). In order to analyze the localization of the different ATP-binding mutants of Mklp2, we performed RNAi-rescue experiments using RNAi duplexes targeting the 3'-untranslated region of Mklp2 (Figure 14.B). In Mklp2 depleted cells transfected with the GFP-vector control, endogenous Mklp2 could not be detected (Figure 14.D), whereas wildtype, full-length GFP-Mklp2 was found to localize correctly to the spindle midzone (Figure 14.E), validating the setup of the RNAi-complementation experiments. GFP-Mklp2^{ATPm} instead, localized diffusely in early mitosis, like the wildtype protein, but it accumulated on chromatin upon entry into anaphase (Figure 14.E), in contrast to GFP-Mklp2^{WT}, indicating that the interaction of Mklp2 with MTs is mainly mediated by the motordomain and not by an additional MT binding site. In contrast, GFP-Mklp2^{SIIm} bound MTs prematurely, decorating the entire metaphase spindle, before it concentrated in anaphase on MTs in the vicinity of the spindle poles (Figure 14.E). These results indicate that the affinity of

the motor domain for MTs might control the localization of Mklp2 during mitotic progression and suggests that the transition from metaphase to anaphase is a critical time point for this regulation.
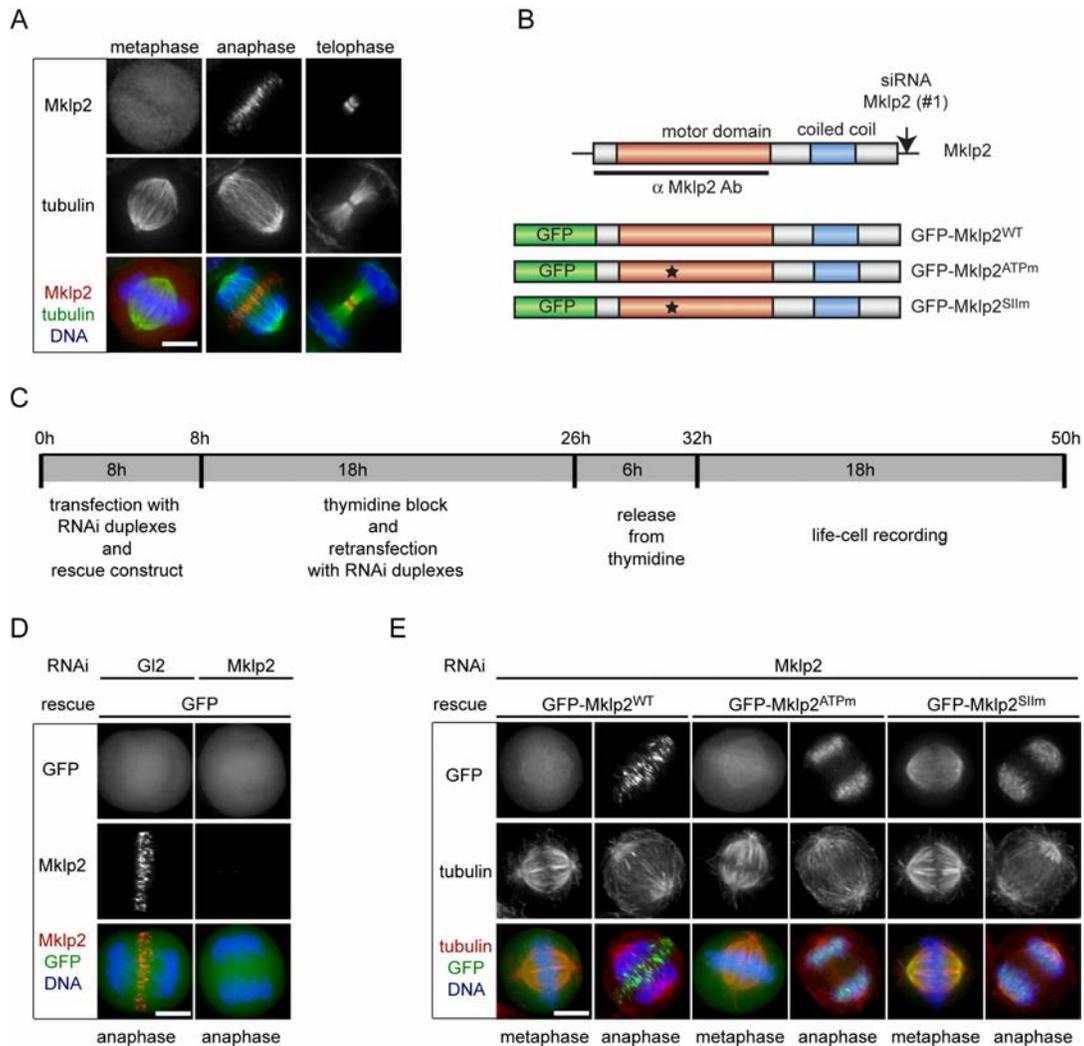
Figure 14. Mklp2 depends on its functional motordomain for midzone localization.

(A) HeLa cells were fixed and stained with antibodies targeting Mklp2 (red) and α-tubulin (green) and Hoechst for DNA (blue). Bar, 10 µm. **(B)** Structure domain of Mklp2. GFP-tagged constructs used in this study are shown below. The targeting region of the applied RNAi duplexes is indicated by an arrow. **(C)** Experimental outline of the RNAi rescue experiments. **(D)** Mklp2- or control depleted (Gl2) HeLa cells transfected with the GFP-vector control were fixed and stained for Mklp2 (red), α-tubulin (green), and DNA (blue). Bar, 10 µm. **(E)** Immunofluorescence images of Mklp2 RNAi HeLa cells transfected with the indicated GFP-Mklp2 variants. α-tubulin is shown in red, GFP in green, and DNA in blue. Bar, 10 µm.

1.2 Mklp2 and the CPC are mutually dependent on each other for midzone localization

The localization of the CPC to the spindle midzone upon anaphase onset depends on Mklp2 (Gruneberg et al., 2004). To investigate the underlying mechanism, we analyzed if the CPC

and Mklp2 are interdependent for their localization. Interestingly, we observed that not only INCENP failed to localize to the midzone in Mklp2-depleted cells, but also Mklp2 was not detectable at the midzone in INCENP-depleted cells (Figure 15.A). As previously shown (Klein et al., 2006), depletion of INCENP resulted in the simultaneous destabilization of Aurora B, whereas Mklp2 protein levels were not affected in INCENP-depleted cells (Figure 15.B), excluding the possibility that an off-target effect of the INCENP RNAi duplexes accounts for the lack of Mklp2 at the midzone. Thus, the CPC and Mklp2 are interdependent for proper midzone localization in anaphase arguing against the idea that the CPC and Mklp2 act just as a cargo and motor-protein, respectively.
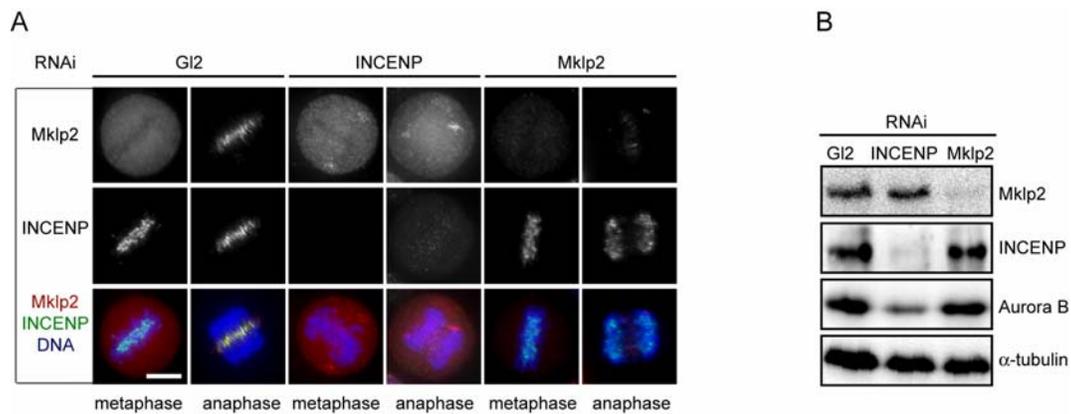
Figure 15. Mklp2 and the CPC mutually depend on each other for midzone localization.
(A) HeLa cells transfected with the indicated RNAi duplexes were fixed and stained for Mklp2 (red), INCENP (green), and DNA (blue). Bar, 10 µm. **(B)** HeLa cells treated as described (A), were processed for Western blot analyses. The α-tubulin Western blot served as a loading control.

1.3 The phospho-mimic mutant of INCENP (T59E) does not complement the function of the CPC in cytokinesis

To rule out that the mislocalization of Mklp2 is an indirect consequence of defects occurring during early mitosis in INCENP depleted cells, we sought for an approach to dissect the late mitotic function of the CPC from the early one. INCENP is phosphorylated at T59 by Cdk1 until the onset of anaphase, but the function of T59 phosphorylation remain unknown (Goto et al., 2006). We speculated that the phosphorylation state of T59 regulates the translocation of the CPC to the spindle midzone.
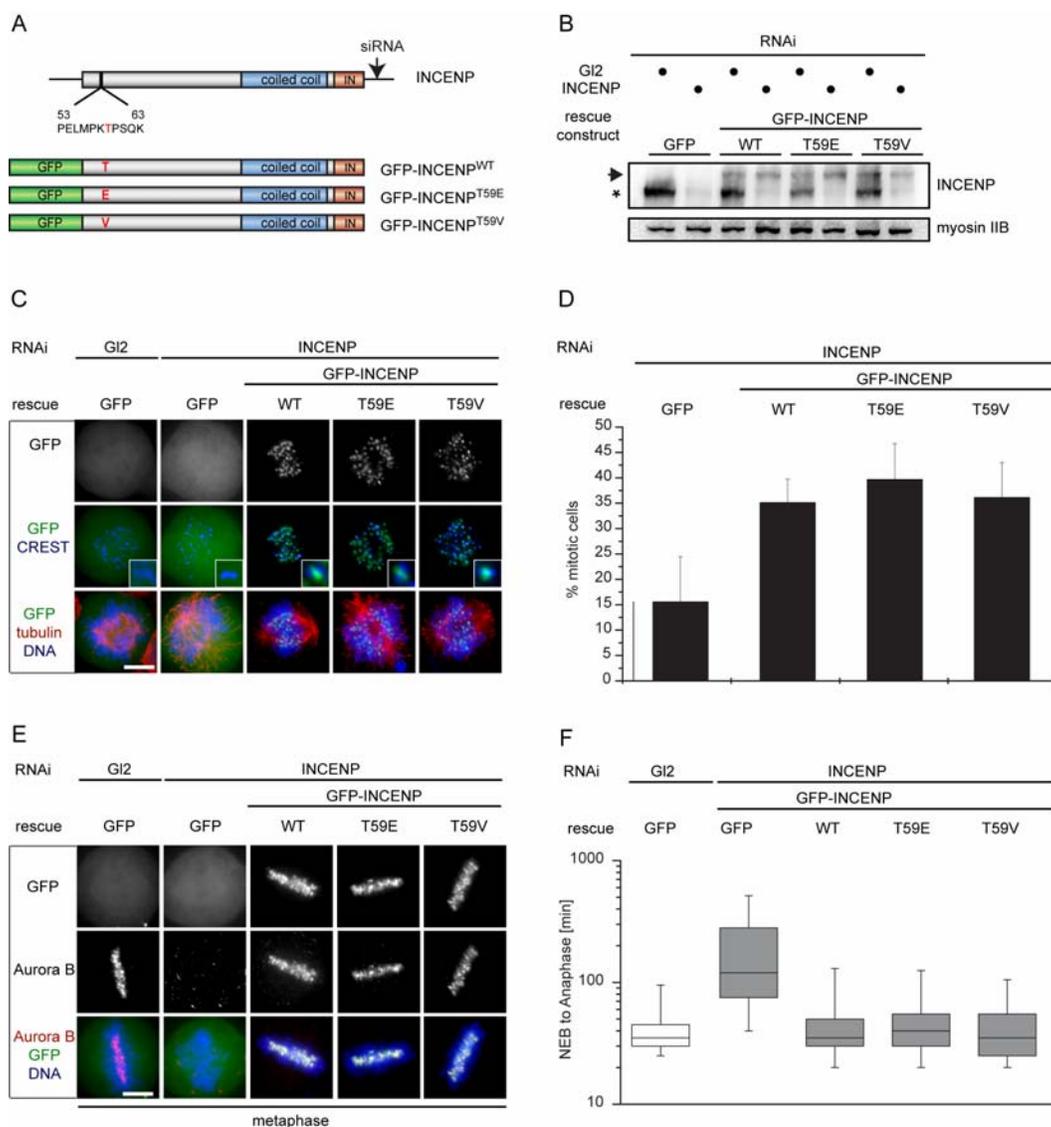
Figure 16. Phosphorylation of INCENP at T59 is not required for the function of the CPC in early mitosis.
(A) Domain structure of INCENP and GFP-tagged constructs used in this study (targeting region of the applied RNAi duplexes indicated by an arrow). **(B)** Western blots of INCENP- or Gl2-depleted HeLa cells transfected with the indicated GFP-INCENP constructs. Asterisk and arrow indicate ectopically expressed GFP-INCENP variants and endogenous INCENP, respectively. The α-myosin IIB Western blot served as a loading control. **(C)** HeLa cells were transfected with the indicated RNAi duplexes and rescue constructs. Merge of the GFP-signal (green) and CREST (blue), a marker for centromeres (middle panel). Merge of GFP (green), tubulin (red), and DNA (blue) (lower panel). Insets show a sevenfold magnification of the centromere region. Bar, 10 µm. **(D)** Quantification of the mitotic index of INCENP-depleted HeLa cells transfected with indicated constructs and treated with 100 nM taxol for 14 hours after releasing the cells from a thymidine-arrest (n=3 experiments, at least 100 cells per experiment were counted, error bars represent standard deviations (SD)). **(E)** Immunofluorescence images of metaphase HeLa cells treated like in (C). DNA, GFP-constructs and Aurora B are shown in blue, green, and red, respectively. Bar, 10 µm. **(F)** Quantification of live-cell recordings of Gl2- or INCENP-RNAi HeLa cells transfected with the indicated constructs (n=4 experiments, analyzing a minimum of 120 cells per experiment). The time from nuclear envelope breakdown (NEB) to anaphase onset was analyzed and the data are presented in a box blot, showing the median (line), the percentile 25/75 (box) and the percentile 10/90 (bars).

To test this, we analyzed the localization of GFP-tagged wildtype (WT), a non-phosphorylatable (T59V), and a phospho-mimic mutant (T59E) of INCENP in INCENP-depleted cells (Figure 16.A). Immunoblot analyses confirmed that endogenous INCENP was efficiently depleted and that the rescue constructs were expressed at similar levels (Figure 16.B).

In line with previous reports (Goto et al., 2006), we observed that T59 was not critical for the early mitotic function of INCENP. This statement is based on the fact that all three variants of INCENP, unlike the empty GFP-vector, restored the localization of the CPC to centromeres in INCENP depleted cells (Figure 16.C and Figure 16.E). Furthermore, we could also show that not only the localization, but also the function of the CPC during early mitosis seems to be independent on the phosphorylation status of T59, since all three variants rescued the timed onset of anaphase and were able to induce a mitotic delay upon treatment of INCENP-depleted cells with the MT toxin taxol (Figure 16.D and Figure 16.F).

A strikingly different result was obtained when cells in anaphase were analyzed. GFP-INCENP^{WT} and the non-phosphorylatable T59V mutant localized correctly to the midzone in INCENP depleted cells, whereas the phospho-mimic T59E variant remained on segregating chromosomes (Figure 17.A). Likewise, Aurora B and survivin were detected at the midzone in INCENP depleted cells expressing WT or T59V, but on chromatin in the case of GFP-INCENP^{T59E} (Figure 17.B and Figure 17.C). Consistent with their ability to rescue CPC localization in anaphase, live-cell recording demonstrated that wildtype and T59V, but not T59E or the GFP-vector control, efficiently complemented cytokinesis (Figure 17.D). Thus, INCENP^{T59E} cannot support the post-metaphase function of the CPC, which enables us to study the role of the CPC in Mklp2 localization uncoupled from its function in early mitosis.
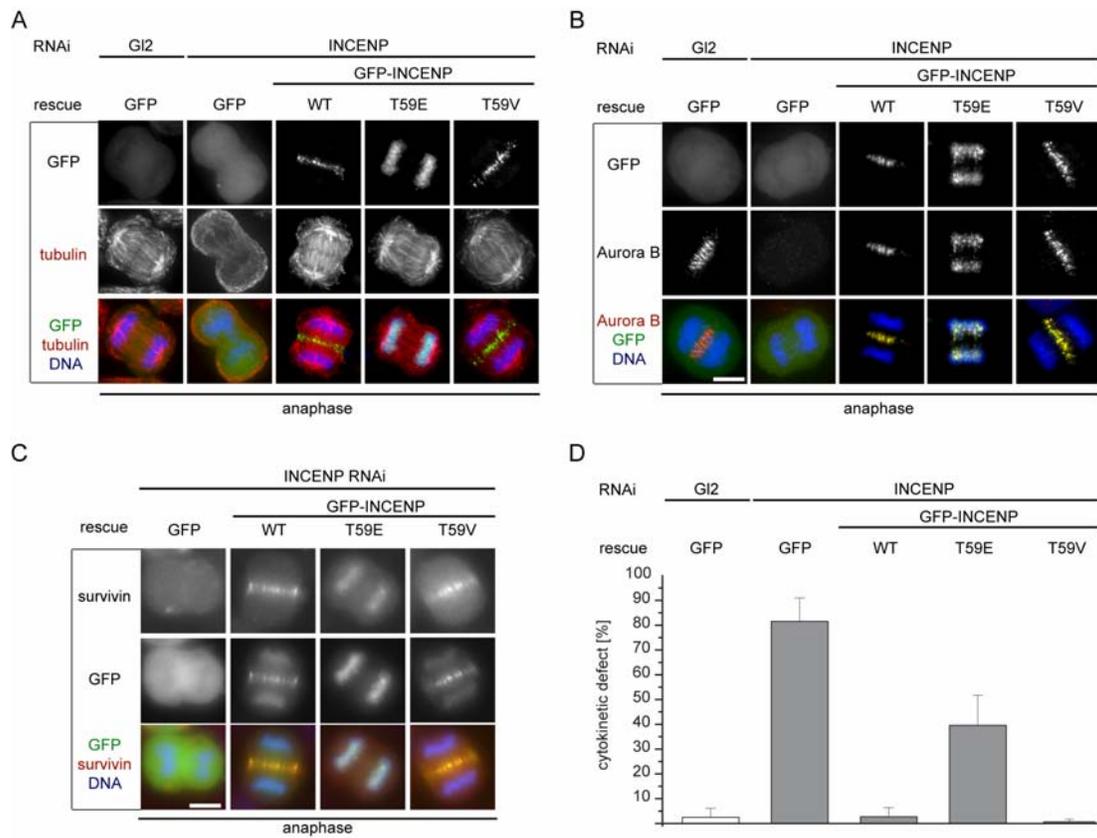
Figure 17. The phospho-mimic mutant of INCENP (T59E) does not complement the function of the CPC in cytokinesis.

(A) Immunofluorescence images of anaphase HeLa cells transfected with the indicated RNAi duplexes and rescue constructs and stained for DNA (blue), GFP (green), and α-tubulin (red). Bar, 10µm. **(B)** Immunofluorescence images of anaphase HeLa cells treated as in (A). DNA, GFP-constructs and Aurora B are shown in blue, green and red, respectively. Bar, 10 µm. **(C)** HeLa cells transfected with the indicated RNAi duplexes and rescue constructs were fixed and stained. Survivin is shown in red, GFP in green, and DNA in blue. Bar, 10 µm. **(D)** Quantification of live-cell recordings of cells, treated as in Figure 16.F. For each condition at least four independent experiments were performed, analyzing a minimum of 120 cells. Bars represent the percentage of transfected cells that failed to complete cytokinesis and exited mitosis as binucleated cells. Data were averaged and error bars represent SD.

1.4 The phospho-mimic mutant of INCENP (T59E) can not restore the localization of Mklp2 at the central spindle

Next, we analyzed the localization of Mklp2 in the INCENP RNAi rescue approach. Endogenous Mklp2 efficiently accumulated at the midzone of INCENP-RNAi cells expressing GFP-INCENP^{WT} or T59V, but localized diffusely in the cytoplasm of cells expressing T59E (Figure 18.A). The failure of Mklp2 to localize correctly was not mediated by a gross defect in midzone MT organization as indicated by the correct localization of PRC1 (Figure 18.B). Collectively, these results suggest that the phosphorylation of INCENP at T59 might act

inhibitory on the transfer of the CPC to the spindle midzone, and further corroborates our model that the CPC and Mklp2 depend on each other for correct localization.
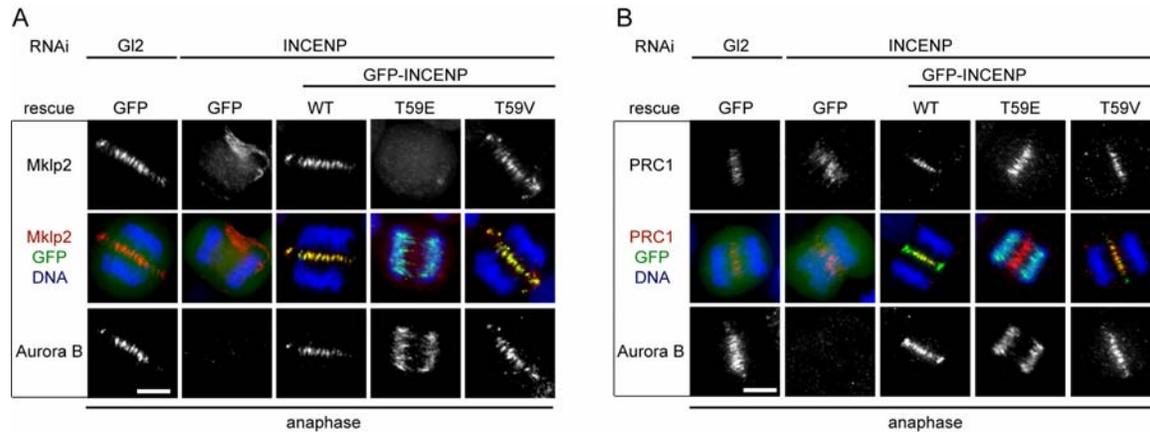
Figure 18. The phospho-mimic mutant of INCENP (T59E) can not restore the localization of Mklp2 at the central spindle.

(A) Immunofluorescence images of anaphase HeLa cells transfected with RNAi duplexes targeting INCENP or GI2 and transfected with empty GFP-vector or the indicated INCENP variants. Mklp2 is shown in red, DNA in blue, and GFP in green. The merged images do not show Aurora B for the purpose of clarity. Bar, 10 μm. **(B)** Anaphase HeLa cells treated as in A. PRC1 is shown in red, GFP in green, and DNA in blue. Bar, 10 μm.

1.5 Mklp2 and the CPC interact upon anaphase onset

Next, we analyzed the timing of the interaction between Mklp2 and the CPC in more detail. To this end, Mklp2 was immunopurified from cells released from a nocodazole block and associated proteins were analyzed by Western blotting. To monitor progression through mitosis, Cyclin B levels were determined by immunoblot analyses. As shown in Figure 19.A, INCENP and Aurora B co-precipitated with Mklp2 as soon as Cyclin B levels began to decline. This interaction was specific for Mklp2 because INCENP and Aurora B did not detectably co-precipitate when Mklp1 was immunopurified from cells in meta- or anaphase (Figure 19.B). Furthermore, the interaction between Mklp2 and the CPC was mediated by the C-terminal cargo-binding domain of Mklp2, as demonstrated by Western blotting analysis of GFP-tagged fragments of Mklp2 immunopurified from HeLa cells (Figure 19.C). Thus, anaphase onset triggers the association of the CPC with the C-terminus of Mklp2.
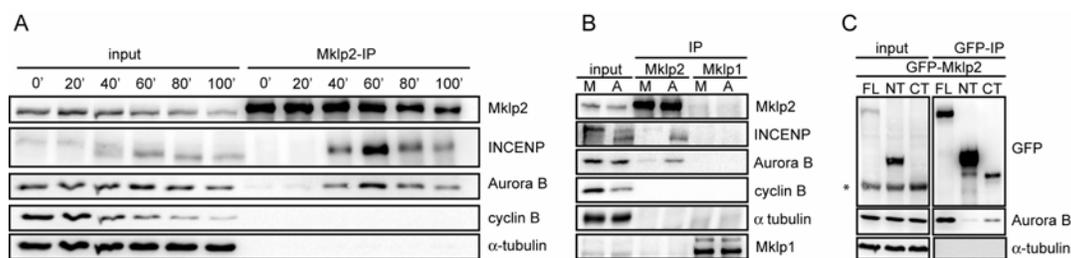
Figure 19. Mklp2 and the CPC interact upon anaphase onset.

(A) Immunoblot analysis of Mklp2 immunopurified from synchronized HeLa cells. Cells arrested in prometaphase were collected by shake-off and released from the arrest for the indicated times. Lysates (input) and immune complexes (IP) were probed with Mklp2, Aurora B, and INCENP antibodies. Cell cycle progression was monitored by immunoblotting for Cyclin B. The immunoblot for tubulin served as a loading control. **(B)** Mklp2 or Mklp1 were immunopurified from extracts (input) of HeLa cells arrested at metaphase by nocodazole treatment (M, metaphase) or released from the arrest for 60 minutes (A, anaphase). Immunoprecipitates were analyzed by immunoblotting as indicated. **(C)** Lysates (input) were prepared from HeLa cells transfected with the indicated Mklp2 fragments followed by immunoprecipitation of the fusion proteins with GFP antibodies. Western blots were probed with GFP, Aurora B, and α-tubulin antibodies. Asterisk marks a protein crossreacting with the GFP antibody.

1.6 The interaction between the CPC and Mklp2 is negatively regulated by Cdk1

Given that Mklp2 mislocalizes in INCENP depleted cells expressing T59E, we analyzed whether the phosphorylation state of T59 might be critical for the association of Mklp2 with the CPC. To this end, GFP-INCENP^{WT}, T59V, and T59E were immunopurified from anaphase cells and associated Mklp2 was detected by immunoblot analyses. Intriguingly, compared to the wildtype and non-phosphorylatable forms of INCENP, T59E was significantly less efficient in co-precipitating Mklp2. Consistent with our immunofluorescence analyses all three variants of INCENP were equally capable of binding Aurora B (Figure 20.A). In order to confirm that the interaction between Mklp2 and the CPC is indeed negatively regulated by Cdk1, we tested whether recombinant Cdk1 can dissociate an existing CPC/Mklp2 complex. To this end, Mklp2 was immunopurified from anaphase cells and the beads-bound Mklp2-precipitate was treated with recombinant active or heat-inactivated Cdk1/Cyclin B followed by a centrifugation step to separate the beads-bound fraction from the supernatant. As shown in Figure 20.B, INCENP and Aurora B remained bound to Mklp2 when the precipitate was treated with heat-inactivated Cdk1/Cyclin B. In stark contrast, Aurora B and INCENP dissociated and were detected in the supernatant when the Mklp2-precipitate was treated with active Cdk1/Cyclin B (Figure 20.B). To exclude that a contaminant kinase co-purifying with recombinant Cdk1 accounts for the observed dissociation of Mklp2 and the CPC, we repeated the assay using roscovitine to specifically inactivate Cdk1. As expected, incubation of the Mklp2-beads with Cdk1/Cyclin B in the presence of the Cdk inhibitor roscovitine prevented the dissociation of Aurora B from Mklp2

(Figure 20.C). Aurora B was not inhibited by roscovitine addition, as indicated by its electrophoretic upshift characteristic of autophosphorylated, active Aurora B (Figure 20.C). Collectively, these data demonstrate that the association between the CPC and Mklp2 is negatively regulated by Cdk1 activity and that T59 of INCENP, a reported Cdk1 phosphorylation site, is critical for this interaction.
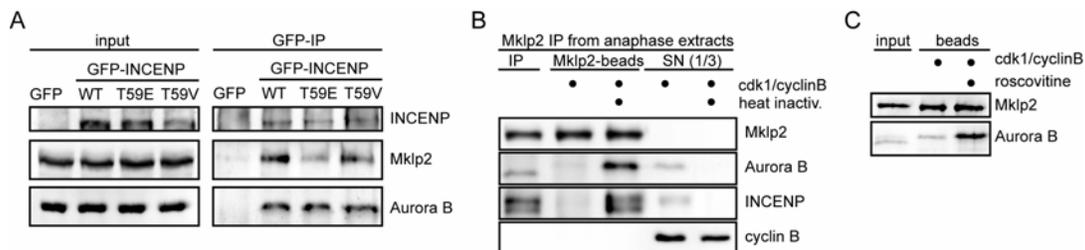
Figure 20. The interaction between the CPC and Mklp2 is negatively regulated by Cdk1.
(A) Lysates (input) were prepared from anaphase HeLa cells transfected with empty GFP-vector or the indicated INCENP variants followed by immunoprecipitation of the fusionproteins with GFP antibodies. Western blots were probed with INCENP, Aurora B and Mklp2 antibodies. **(B)** Mklp2 was immunoprecipitated from anaphase extracts prepared as described in A (input) and the precipitate was incubated with ATP and recombinant active or heat-inactivated Cdk1/Cyclin B for 30 minutes at 25°C. The reaction was separated in a bead-associated (Mklp2-beads) and supernatant fraction (SN) by centrifugation followed by immunoblotting for Mklp2, Aurora B, INCENP, and Cyclin B. **(C)** Mklp2 was immunoprecipitated from anaphase extracts prepared as described above and the precipitate was incubated with ATP and recombinant Cdk1/Cyclin B for 30 minutes at 25°C in the presence or absence of roscovitine. Bead associated Aurora B was detected by Western blotting.

1.7 Binding of the CPC and Mklp2 to MTs is negatively regulated by Cdk1

According with our immunofluorescence data, anaphase onset should be accompanied with an increase in the affinity of Mklp2 and the CPC for MTs. To test this, we performed spin-down assays with ectopically added MTs. Specifically, extracts were prepared from metaphase or anaphase cells, the cytosol was collected by centrifugation and removal of the pellet. The cytosol was then supplemented with taxol-stabilized MTs, and MT-associated proteins were detected by Western blotting after sedimentation. Consistent with their cell cycle dependent localization *in vivo*, Mklp2 and the CPC efficiently associated with MTs in anaphase but not in metaphase extracts (Figure 21.A). Immunoblotting for α-tubulin confirmed that the sedimentation of both Mklp2 and the CPC was dependent on MTs. Since anaphase onset is accompanied with a drop in Cdk1 activity, we analyzed whether this is sufficient to increase the affinity of the Mklp2/CPC complex for MTs. For this purpose, anaphase extracts were supplemented with non-degradable Cyclin B (Δ90) in order to restore Cdk1 activity. Under these conditions, the association of both Mklp2 and the CPC with taxol-stabilized MTs was abolished, while the control buffer had no effect (Figure 21.B). Immunoblotting for histone H3 confirmed that the cytosolic fraction was efficiently depleted of

chromosomes (Figure 21.B), suggesting that Cdk1 might interfere with the association of the CPC and Mklp2 to MTs, rather than with the dissociation of the CPC from chromatin. Consistently, we observed that the expression of non-degradable Cyclin B (Cyclin B^{KtoR}) interfered with the association of the CPC with Mklp2 in anaphase, as indicated by the localization of the CPC to segregating chromosomes, and diffusely localized Mklp2 (Figure 21.C). As expected, Cyclin B^{KtoR} had no effect on the localization of the CPC and Mklp2 in metaphase (Figure 21.C). Taken together, Cdk1 activity not only interferes with the interaction between Mklp2 and the CPC, but it also prevents their efficient binding to MTs.
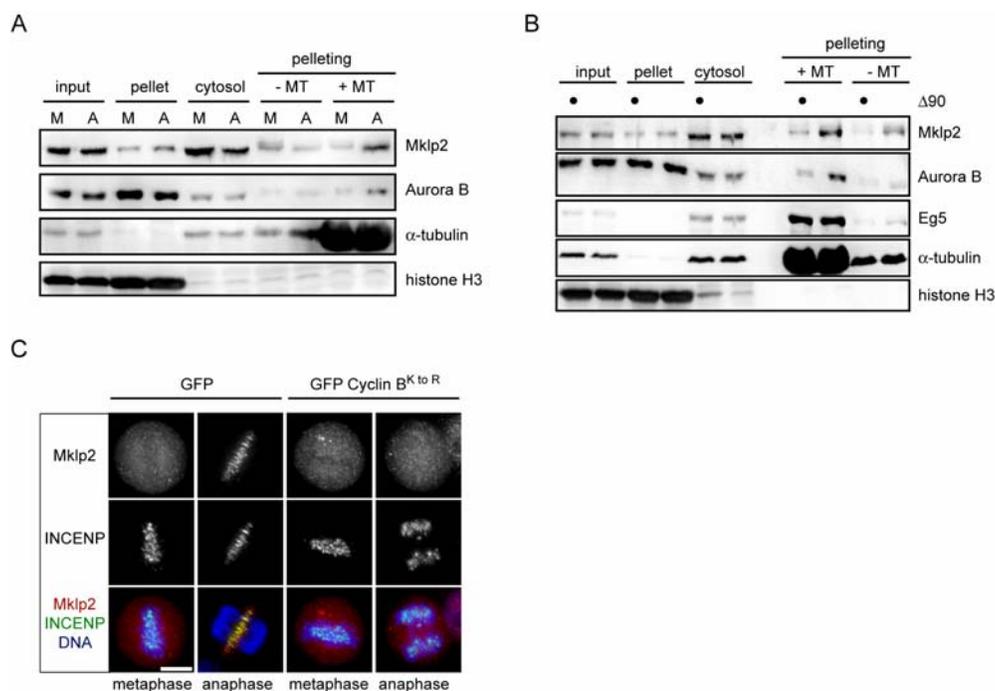
Figure 21. Binding of the CPC and Mklp2 to MTs is negatively regulated by Cdk1

(A) Lysates (input) from HeLa cells arrested at metaphase by nocodazole treatment (M, metaphase) or released from the arrest for 60 minutes (A, anaphase) were separated by centrifugation and the cytosolic fraction retained. Taxol-stabilized MTs were added to the cytosolic fraction and sedimented by centrifugation. Immunoblotting was carried out for Mklp2, Aurora B, histone H3 and α-tubulin. **(B)** Lysates of anaphase extracts (input) were supplemented with non-degradable Cyclin B (Δ90) or buffer. Pellet and cytosolic fractions were separated by centrifugation and taxol-stabilized MTs were added to the cytosolic fraction. Following centrifugation, MT-associated proteins were detected by immunoblotting. **(C)** HeLa cells transfected with GFP-tagged non-degradable Cyclin B (GFP-Cyclin B$^{K to R}$) or GFP-vector control were fixed and stained for Mklp2 (red), INCENP (green), and DNA (blue). Bar, 10 µm.

1.8 INCENP is required to localize Mklp2 close to the ends of stable MTs in cells with low Cdk1 activity

Our *in vivo* results demonstrate that the CPC and Mklp2 depend on each other for binding to midzone MTs. Since MTs ends are concentrated at the midzone, we sought for an approach that allowed us to analyze the binding of the CPC and Mklp2 to the tips of MTs. Therefore, we treated cells arrested in metaphase (by treatment with the proteasome inhibitor MG-132), with the potent Eg5 inhibitor VS-83 (Sarli et al., 2005) to induce monoasters with easily discernable MT tips. Consistent with previous reports (Murata-Hori et al., 2002), inactivation of Cdk1 with roscovitine was not sufficient to efficiently recruit the CPC or Mklp2 to MTs *in vivo* (Figure 22.A, panel 2). Thus, additional changes besides the drop in Cdk1 activity have to occur in order to enable midzone localization of the Mklp2/CPC complex at anaphase onset. Since it has been reported that MT dynamics are dramatically reduced when cells exit mitosis (Glotzer, 2009), we were wondering if co-suppression of MT dynamics by taxol is able to mimic the scenario at anaphase onset. Our immunofluorescence analysis revealed that indeed, the CPC and Mklp2 specifically accumulate at the tips of taxol-stabilized MTs (Figure 22.A, panel 4). This localization is reminiscent of the situation in anaphase where the CPC and Mklp2 accumulate in a narrow zone on midzone MTs. The association of the CPC with MTs was dependent on Mklp2, since INCENP was detected on chromatin in Mklp2 depleted cells (Figure 22.A, panel 6). Intriguingly, in INCENP depleted cells, Mklp2 failed to accumulate at the tips of MTs but localized instead to the lattice of taxol-stabilized MTs (Figure 22.A, panel 8). Thus, by the addition of taxol, we increased Mklp2's affinity for MTs enabling us to observe three phenotypes: no binding (low Cdk1 activity, panel 2), tip binding (low Cdk1 activity and stable MTs, panel 4), and lattice binding (low Cdk1 activity, stable MTs in the absence of INCENP, panel 8).
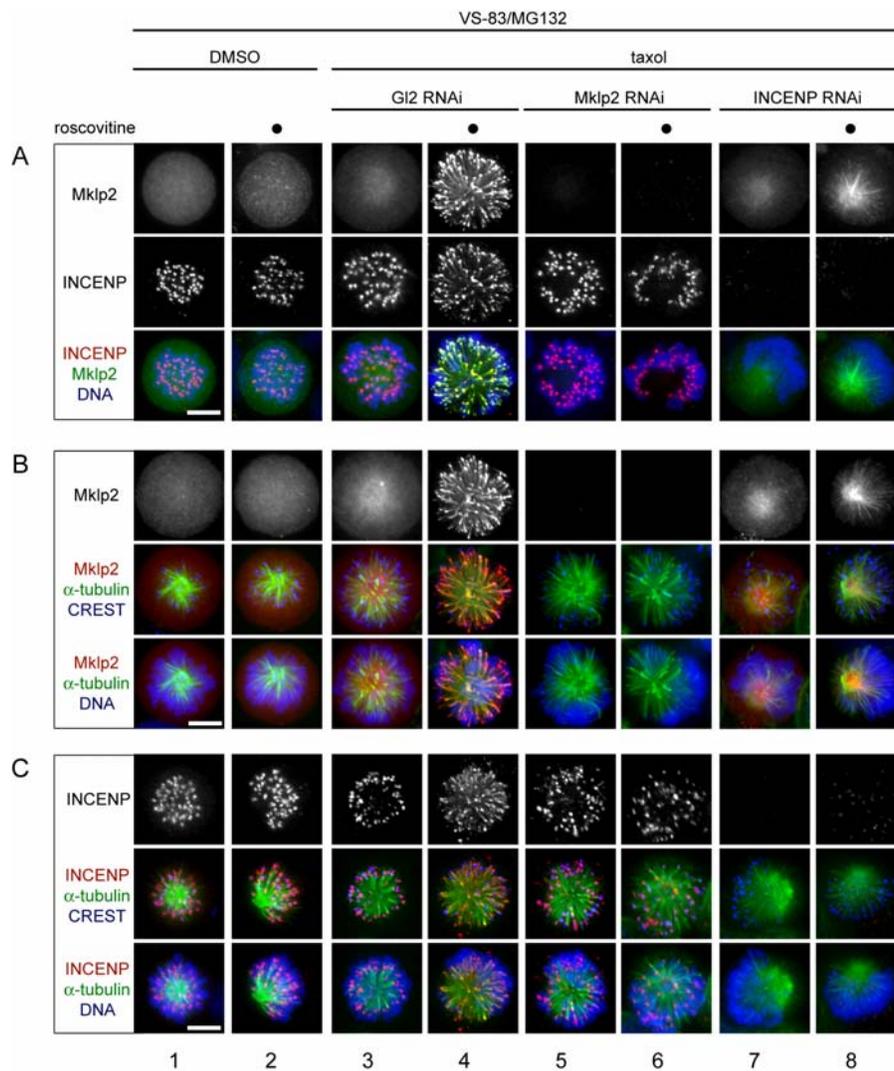
Figure 22. INCENP is required to localize Mklp2 close to the ends of taxol-stabilized MTs in roscovitine treated cells.
Immunofluorescence images of HeLa cells arrested in mitosis with 50 µM VS-83 and 20 µM MG132 in the presence of 1 µM taxol and 100 µM roscovitine or DMSO as solvent control and transfected with the indicated RNAi duplexes targeting INCENP, Mklp2 or Gl2. Mklp2 is shown in green, INCENP in red and DNA in blue **(A)**. In **B** and **C** cells were stained for Mklp2 or INCENP in red and these images were merged with either tubulin (green) and CREST (blue) or tubulin (green) and DNA (blue). Bar, 10 µm.

In order to test if the interaction between Mklp2 and the CPC is prerequisite for the tip binding of the Mklp2/CPC complex, we made use of the phospho-mimicking mutant of INCENP (T59E). In this scenario, Mklp2 remained bound to the MT lattice and failed to accumulate to the tips of stable MT plus-ends (Figure 23). Thus, only if the interaction between Mklp2 and the CPC can be achieved, binding of Mklp2 to the MT lattice upon reduced Cdk1 activity can be converted into a plus-end localization.
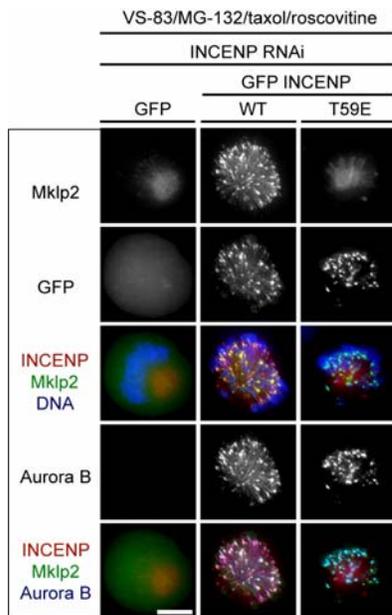
Figure 23. The phospho-mimic mutant of INCENP (T59E) cannot restore the localization of Mklp2 at MT plus ends.
Immunofluorescence images of HeLa cells treated like in Figure 22 and transfected with RNAi duplexes targeting INCENP and the indicated rescue constructs. Mklp2 is shown in green, INCENP in red and either DNA or Aurora B in blue. Bar, 10 µm.

1.9 Aurora B activity is required for the correct localization of the Mklp2/CPC complex in cells undergoing monopolar cytokinesis

Our analyses of VS-83/taxol-treated cells suggest that the stabilization of MTs is necessary for the recruitment of the CPC and Mklp2. In order to test if the CPC has a direct role in locally stabilizing these MTs at the midzone, we analyzed the localization of the CPC and Mklp2 in the absence of taxol in cells undergoing monopolar cytokinesis. Since inhibition of Eg5 activates the SAC, mitotic exit in VS-83 arrested cells was induced by a prolonged inhibition of Cdk1. The resulting monopolar spindle structures allow easy visualization of MT plus-ends, as was described previously (Hu et al., 2008). In this scenario, Mklp2 and the CPC co-localized to the ends of MTs in the region of the forming cleavage furrow (Figure 24). In support of our observation that the localization of the Mklp2/CPC complex depends on the presence of stable MTs, it has been reported that specifically these MT ends that are growing towards the furrow are stabilized by a so far unknown mechanism (Hu et al., 2008). The polar extrusions expand over the time of the treatment and are mediated by MTs as shown by their absence in nocodazole treated cells (Figure 24). In order to test if the localization of the Mklp2/CPC complex is dependent on the activity of Aurora B, we treated cells with the kinase inhibitor ZM447439. In line with previous reports, inactivation of Aurora B abolished the formation of these extrusions and strikingly, Mklp2 co-localized with the CPC near the chromosomes (Figure 24). In agreement with these results, inhibition of Aurora B results in significantly shorter MTs that only rarely elongate towards the cell cortex (Hu et al., 2008). Thus, it is interesting to speculate that the absence of stable MT plus-ends near the cell cortex is the cause for the delocalization of the Mklp2/CPC complex and it will be interesting to see in the future if this hypothesis can be proven.
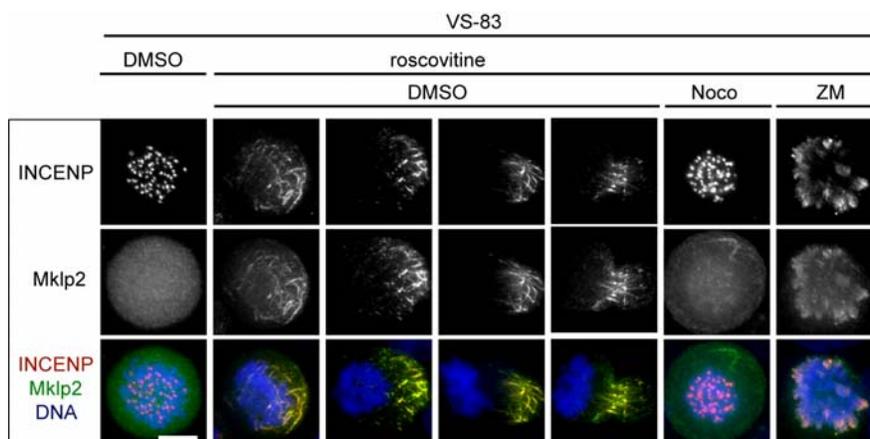
Figure 24. Localization of Mklp2 in cells undergoing monopolar cytokinesis.
Immunofluorescence images of HeLa cells undergoing monopolar cytokinesis. Cells are arrested in mitosis with 100 µM VS-83 were treated with 100 µM roscovitine and 20 µM ZM447439 (ZM) or 500 nM nocodazole (Noco) or DMSO as solvent control. Mklp2 is shown in green, INCENP in red and DNA in blue. Bar, 10 µm.

Conclusion 1

Taken together, we uncovered a regulatory network that ensures the specific localization of Mklp2 and the CPC to stable MT plus-ends of the spindle midzone at anaphase onset. Starting from the observation that the CPC and Mklp2 are interdependent for proper midzone localization, we could demonstrate that the interaction between the CPC and Mklp2 is prerequisite for their correct localization. This interaction, as well as the binding of Mklp2 and the CPC to MTs, is negatively regulated by Cdk1 and thus, the drop in Cdk1 activity at anaphase onset is required for the correct localization of the Mklp2/CPC complex. In addition, analyzes of VS-83-treated cells revealed that in the absence of Cdk1 activity, stable MTs are prerequisite for the localization of the Mklp2/CPC complex to MTs plus-ends. Furthermore, using this experimental setup, we showed that in the absence of INCENP, Mklp2 binds to the lattice of stable MTs upon Cdk1 inactivation. This led us to conclude that the drop in Cdk1 activity at anaphase onset enables the binding of Mklp2 to the lattice of stable MTs and the formation of the Mklp2/CPC complex, resulting in their localization to MT plus-ends of the spindle midzone. Finally, analyzes of cells undergoing monopolar cytokinesis revealed that the Mklp2/CPC complex specifically binds to the subset of stable MTs at the site of the future cleavage furrow. Interestingly, the presence of this type of MTs is dependent on Aurora B (Hu et al., 2008) and inhibition of the kinase activity consequently abolished the localization of the Mklp2/CPC complex. It is interesting to speculate that following the drop in Cdk1 activity, the stabilization of MTs, required for the correct localization of the Mklp2/CPC complex, is mediated by the intrinsic activity of Aurora B.

Results 2: The function of Mklp2 in late cytokinesis

Mklp2 is essential for the localization of the CPC to the central spindle upon anaphase onset (Gruneberg et al., 2004). While the requirement of the CPC for the completion of cytokinesis has been intensively studied (Ainsztein et al., 1998; Carmena, 2008; Eckley et al., 1997; Ruchaud et al., 2007; Schumacher et al., 1998; Tatsuka et al., 1998; Terada et al., 1998; Wheatley and Wang, 1996), the role of the Mklp2-mediated localization of the CPC and its function during cytokinesis remains far less understood. Considering that Mklp2 originates much later in evolution than the CPC (Glotzer, 2009), and that the requirement for Mklp2 in cytokinesis seems to differ depending on the studied species (Cesario et al., 2006; Gruneberg et al., 2004), it remains to be addressed which CPC-mediated functions in cytokinesis require Mklp2 dependent localization to the central spindle.

2.1 Mklp2 depletion by RNAi causes a failure in late cytokinesis

To explore in detail the function of Mklp2 in cytokinesis, we performed RNAi experiments to examine the depletion phenotype. For these experiments, two RNAi duplexes were used, targeting either the 3'-untranslated region (UTR) (Mkpl2 #1) as described above or the ORF (Mkpl2 #2) of Mklp2 as described previously (Neef et al., 2003). RNAi depletion experiments were carried out according to the scheme shown in Figure 14. Quantification of Western blot signals from cells processed in this way showed an efficient depletion of Mklp2 with both RNAi-duplexes (Figure 25.B). In line with these results, immunofluorescence analysis of Mklp2 depleted cells revealed no detectable staining for Mklp2 in anaphase cells and consequently the CPC remained bound to the chromosomes in these cells (Figure 25.B). However, in later stages of cytokinesis, residual amounts of Mklp2 could be detected at the central spindle, which was accompanied with a partial localization of the CPC to this region (Figure 25.A). Quantification of the phenotype by live cell microscopy revealed a robust defect in cytokinesis with both RNAi oligonucleotides (45% Mklp2 #1, 60% Mklp2 #2) (Figure 25.C). In contrast to previous reports (Neef et al., 2003), describing an early failure in cytokinesis, our live-cell analyses revealed an almost exclusive late defect, characterized by the formation of a cleavage furrow that ingressed but regressed before the final separation of the two daughter cells (Figure 25.C).
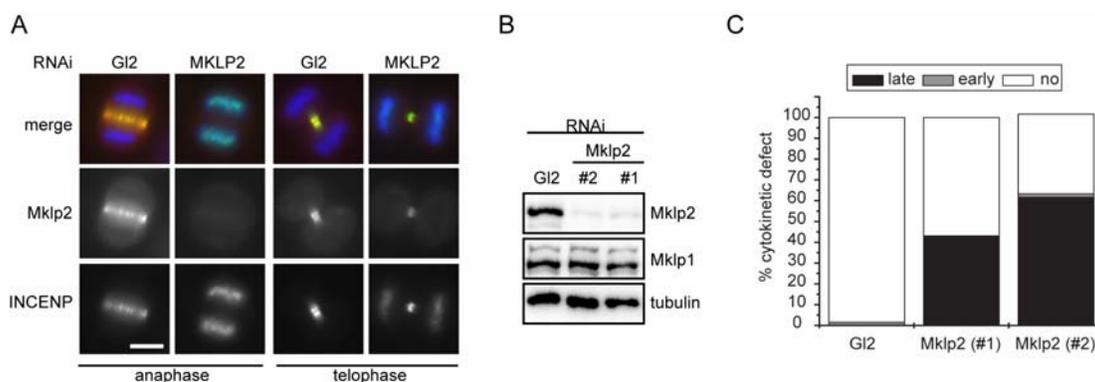
Figure 25. Late cytokinesis defect upon Mklp2 depletion by RNAi.
(A) Immunofluorescence analyzes of Mklp2 RNAi cells. Representative images of cells in anaphase and telophase fixed 10 h after the release from thymidine (see Figure 14). Cells were stained with for Mklp2 (red), INCENP (green) and DNA (blue). **(B)** Immunoblot analyzes of Mklp2 RNAi cells. Whole cell lysates were prepared from cells treated like in (A) analyzed by Western blotting with Mklp2 and Mklp1 antibodies. The α-tubulin immunoblot serves as a loading control. **(C)** Quantification of the Mklp2 RNAi phenotype by live cell analyzes. Mklp2 RNAi was performed as described in Figure 14 prior to image acquisition. The phenotype was classified as cells with normal progression through cytokinesis (no), cells that do not ingress the cytokinetic furrow (early) and cells that ingress but fail to pinch into two daughter cells (late). Bar, 10 µm.

2.2 Delocalization of vimentin to the cytokinetic bridge in Mklp2-depleted cells

Vimentin phosphorylation is required for normal progression through cytokinesis (Izawa and Inagaki, 2006). Phosphorylation of vimentin by Aurora B was shown to induce the depolymerization of the filament in order to ensure its equal segregation into the newly formed daughter cells (Goto et al., 2003; Yokoyama et al., 2005). Specifically, serine 72 on vimentin was shown to be phosphorylated by Aurora B after mitosis (Goto et al., 2003; Yasui et al., 2001). This correlates timely with the Mklp2-dependent recruitment of the CPC to the central spindle. Therefore, we asked whether the delocalization of Aurora B in Mklp2 depleted cells could impair the phosphorylation induced depolymerization of the IF vimentin, and thus, explain the observed failure in late cytokinesis.

To test this hypothesis, we first monitored the localization pattern of vimentin and S72-phosphorylated vimentin (pS72). In agreement with previous reports (Goto et al., 2003; Yasui et al., 2001), control (Gl2-depleted) cells displayed filamentous structures of vimentin along the entire cell cortex and these filaments were phosphorylated at S72 in the cortex region adjacent to the central spindle (Figure 26.A, Figure 26.B and Figure 26.D). We could not detect total vimentin at the central spindle where conversely Aurora B localizes. In order to confirm that Aurora B kinase activity is indeed required for the phosphorylation and disassembly of the filament at the central spindle, we treated cells in telophase for a short time with the Aurora B kinase inhibitor ZM447439 (Ditchfield et al., 2003). Immunofluorescence analyses revealed that Aurora B inhibition strongly reduced the staining

for pS72 and induced the accumulation of vimentin at the central spindle (Figure 26.A). Thus Aurora B kinase activity is required to phosphorylate and subsequently disassemble vimentin filaments at the central spindle, confirming previous reports (Goto et al., 2003).
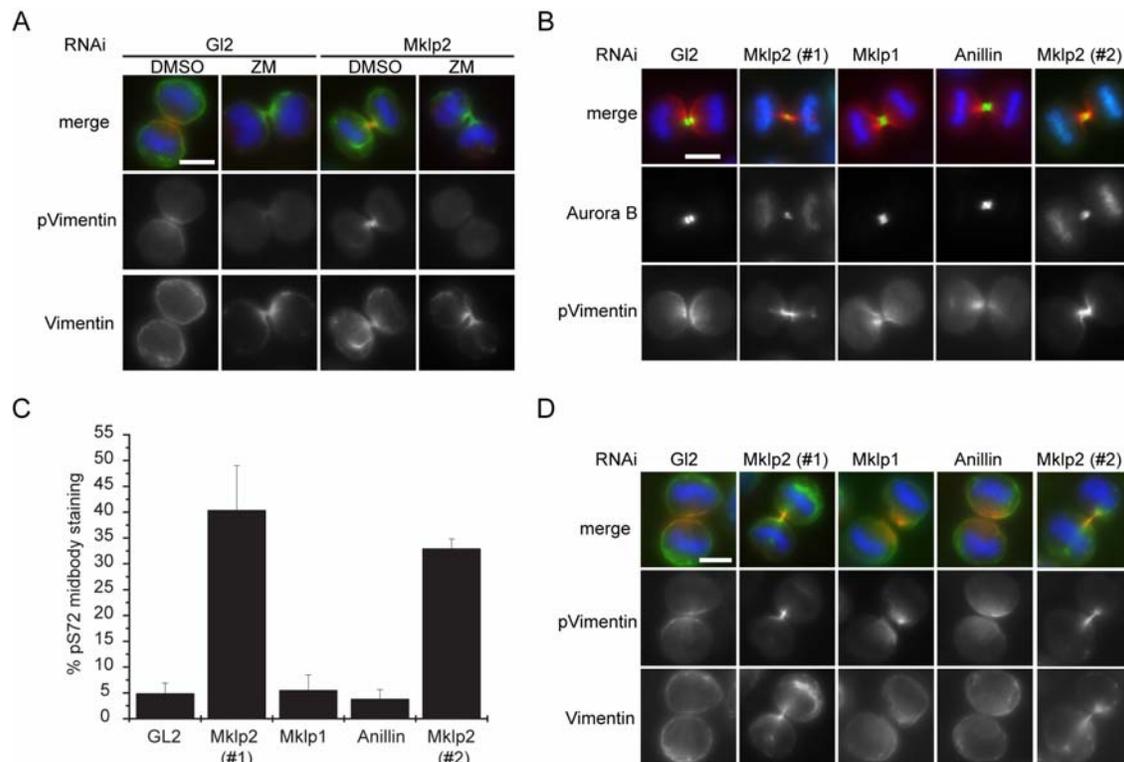
Figure 26. Delocalization of vimentin to the cytokinetic bridge in Mklp2-depleted cells.
(A) Localization of vimentin and pS72 in telophase cells treated with the Aurora kinase inhibitor ZM447439. Cells were treated with the indicated RNAi oligos and 14 hours after the release from a thymidine block (see Figure 14) treated for 20 minutes with ZM447439 (ZM) or DMSO as solvent control and subsequently fixed and immunostained for vimentin (green), pS72 (red) and DNA (blue). **(B)** Localization of Aurora B and pS72 of vimetin in telophase. Cells were treated with the indicated RNAi oligos and fixed 10 h after the release from the thymidine block (see Figure 14). Cells were immunostained for Aurora B (green), pS72 (red) and DNA (blue). Bars, 10 μm. **(C)** Quantification of cells with pS72 positive staining at the central spindle in telophase. Cells were processed as described in (B) and data of three independent experiments with more than 100 cells per experiment were averaged. Error bars represent SD. **(D)** Cells treated as desribed in (B) were fixed and immunostained for pS72 (red), vimentin (green) and DNA (blue).

Next, we analyzed the localization of vimentin in Mklp2-depleted cells. In contrast to control-depletd (Gl2) cells, total vimentin was readily visible at the central spindle of Mklp2-depleted cells (Figure 26.A and Figure 26.D). Notably, these filaments contained S72-phosphorylated vimentin (Figure 26.A, Figure 26.B and Figure 26.D). These results indicate that in Mklp2-depleted cells, vimentin gets phosphorylated on S72 at the central spindle but the subsequent depolymerization of vimentin does not occur. Depletion of Mklp2 by the second

RNAi duplexes could confirm these results (Figure 26.B and Figure 26.D). Furthermore, neither Mklp1 nor Anillin depletion resulted in a similar defect, indicating that this phenotype is not due to a general failure in cytokinesis but specific to the Mklp2 depletion (Figure 26.B and Figure 26.D). Finally, quantification of this phenotype revealed pS72 vimentin positive filaments at the central spindle in about 45% of the cells depleted for Mklp2 in comparison to 2% in control treated cells (Figure 26.C). This perfectly matches the failure in late cytokinesis observed under these experimental conditions (Figure 26.C and Figure 25.C).

In summary, Aurora B levels at the central spindle are reduced in Mklp2 depleted cells. Although phosphorylation of vimentin at S72 by Aurora B occurs at the central spindle on these cells, total vimentin accumulates in this region, indicative of partial phosphorylation and incomplete disassembly of the filament. As it happens in unperturbed cells, phosphorylation of vimentin precedes its immediate depolymerization and that explains why we do not observe pS72 staining in the presence of high, concentrated Aurora B activity at the central spindle. In addition, this could also explain why pS72 is only detected at the central spindle adjacent cortex in control cells (Gl2-depleted), but decorates the central spindle of Mkpl2-depleted cells, where Aurora B levels are reduced. One possibility is that phosphorylation of vimentin at S72 occurs with low amount of Aurora B (i.e. adjacent cortex of control cells or central spindle of Mkpl2-depleted cells) but that the total phosphorylation-induced depolymerization of vimentin at the central spindle requires a local high concentration of Aurora B in this region.

2.3 The phospho-mimic mutant of INCENP (T59E) can not restore the correct localization of vimentin at the central spindle

If our assumption is correct, the localization of Aurora B at the central spindle is required to dissolve vimentin in this region and thus to ensure normal progression through cytokinesis. In order to underline this, we made us of our earlier observation that expression of GFP-INCENP^{T59E} in INCENP-depleted cells prevents the transfer of the CPC to the central spindle. While we have already shown that this defect is accompanied with a failure in cytokinesis, it remained to be addressed if this occurs at an early stage before cells start to ingress or if cells first ingress but finally fail to pinch of two daughter cells. In order to determine this, we reinvestigated our life cell analyses of INCENP-depleted cells rescued with either GFP alone, GFP-INCENP^{WT} or the two mutant forms of INCENP (GFP-INCENP^{T59E}, GFP-INCENP^{T59V}). As we have shown above, the depletion of INCENP was accompanied with a destabilization of Aurora B and these cells failed in cytokinesis when rescued with GFP alone (Figure 15.B and Figure 17.D). This defect occured either early (32 %) or late in cytokinesis (42 %) (Figure 27.A). Both, the early and the late failure in cytokinesis, can be rescued by GFP-INCENP^{WT} and GFP-INCENP^{T59V} (Figure 27.A). In

contrast, GFP-INCENP^{T59E}, unable to bind Mklp2 and to transfer to the central spindle, did not restore the function of the CPC in late cytokinesis in about 35 % of the cells (Figure 27.A). Thus, in contrast to cells expressing GFP alone, the ability of GFP-INCENP-T59E to bind and stabilize Aurora B is accompanied with a rescue of the early but not the late defects in cytokinesis. This is reminiscent to the phenotype observed upon Mklp2 depletion by RNAi, where only the transfer of the CPC to the central spindle, but not the overall activity of Aurora B is affected. Notably, a similar defect in late cytokinesis has been reported for a fusion protein of INCENP with the centromere binding domain of CENP-B, which constitutively binds to the centromeric region and consequently prevents the transfer of the CPC to the central spindle but leaves the activity of Aurora B unaffected (Eckley et al., 1997).

According to our hypothesis, the late failure in cytokinesis, caused by the absence of Aurora B from the central spindle, should be accompanied with the accumulation of filamentous vimentin at the cytokinetic bridge. In order to test this hypothesis, we analyzed the localization of vimentin in cells depleted for INCENP and rescued them with either GFP alone or the different GFP-tagged versions of INCENP. In line with their ability to restore the function of the CPC in cytokinesis, the expression of either GFP-INCENP^{WT} or GFP-INCENP^{T59V} resulted in a localization pattern of pS72 that was indistinguishable from the one in control (Gl2-depleted) cells (Figure 27.B). In contrast to this, we observed a clear accumulation of vimentin at the central spindle in telophase cells when INCENP depleted cells were either rescued with GFP alone or GFP-INCENP^{T59E} (Figure 27.B). Furthermore, quantification of this defect revealed that this occurs in about 20 % (GFP) or 40 % (GFP-INCENP^{T59E}). Remeniscent to Mklp2-depeleted cells, the deolocalization of pS72 positive filaments in GFP-INCENP^{T59E} rescued INCENP-RNAi cells, closely correcaltes with the observed failure in late cytokinesis (Figure 27.A and Figure 27.C). Thus, we conclude that not only the presence, but also the correct localization of Aurora B in late cytokinesis is required for the efficient phosphorylation and depolymerization of the IF vimentin at the central spindle. If this localization is perturbed, vimentin filaments accumulate at the central spindle and cells fail at a late stage in cytokinesis.

Alongside with these results, immunofluorescence analyses of INCENP depleted cells revealed further insights into the interplay between the kinesin Mklp2 and the IF vimentin. In control (Gl2-depleted) anaphase cells, Mklp2 localized at the central spindle and vimentin structures were visible underneath the cell cortex (Figure 27.D). However, in INCENP-depleted cells Mklp2 was absent from the central spindle and we could instead detect a co-localization with vimentin positive structures (Figure 27.D). This localization was only visible in INCENP-depleted cells and might be explained by the accompanied destabilization of Aurora B, preventing the instantaneous depolymerization of vimentin after binding to the Mklp2/CPC complex. Thus, in addition to its function as kinesin motor protein, Mklp2 might

provide a physical link between the kinase Aurora B to its substrate vimentin, but the short life of this interaction disables its visualization in an unperturbed situation.
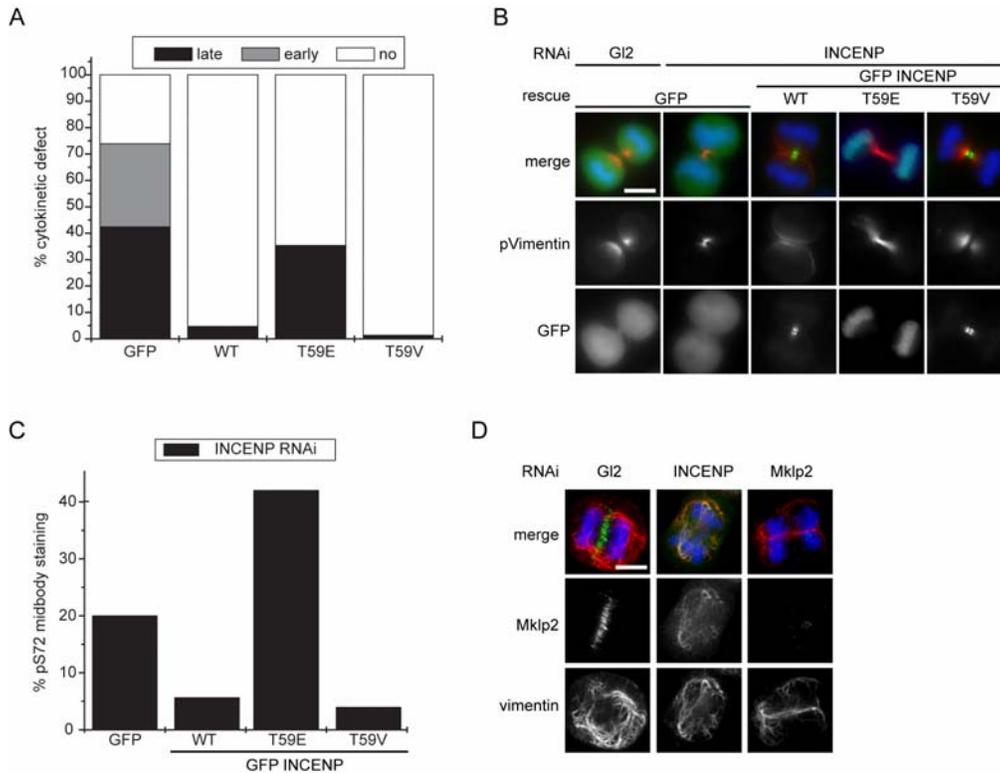
Figure 27. The phospho-mimic mutant of INCENP (T59E) can not restore the correct localization of vimentin at the central spindle.

(A) Quantification of the phenotype of cells depleted for INCENP and transfected with the indicated constructs. INCENP RNAi rescue experiment was performed as described in Figure 17 and cells were recorded by live cell microscopy. The phenotype was classified in cells with normal progression through cytokinesis (no), cells that do not ingress the cytokinetic furrow (early) and cells that ingress but fail to pinch into two daughter cells (late). **(B)** Localization of pS72 under the different RNAi-rescue conditions in telophase. INCENP- or Gl2-depleted HeLa cells expressing the indicated rescue constructs were stained for pS72 (red) and DNA (blue). Cells were processed 10 h after the thymidine release according to the scheme shown in Figure 14. Bars, 10µm. **(C)** Quantification of cells with pS72 positive midbody staining in telophase. Cells were processed as in (B). **(D)** Gl2- ,INCENP- and Mklp2-depleted cells were stained for Mkpl2 (green), vimentin (red) and DNA (blue). Bars, 10 µm.

2.4 No cytokinesis defect upon Mklp2 depletion in vimentin negative MCF-7 cells

Our data collectively demonstrate that the Mklp2-mediated phosphorylation of vimentin by Aurora B is a prerequisite for the disassembly of the filament in the cytokinetic bridge and that this defect is accompanied with a failure in late cytokinesis. However, it remains to be addressed if the unresolved vimentin filaments are the cause for the defect in cytokinesis.

In parallel to our studies in HeLa cells, we also used MCF-7 cells to analyze the RNAi-depletion phenotype of Mklp2. Western blot and immunofluorescence analysis revealed an efficient depletion of the protein (Figure 28.A and Figure 28.B). The lack of Mklp2 was accompanied with the delocalization of the CPC from the central spindle, resembling the situation observed in HeLa cells after depletion of Mklp2 by RNAi (Figure 28.A and Figure 25.A). However, in contrast to HeLa cells, the depletion of Mklp2 did not result in a failure in cytokinesis, determined by the number of binucleated cells present in fixed samples and by live cell analyses (Figure 28.C and Figure 28.D). Mklp1 depletion in HeLa and MCF-7 cells induced cytokinesis defects to a similar degree (Figure 28.C and Figure 28.D). These data indicate that Mklp2 is essential for the recruitment of the CPC to the central spindle, but is only required for successful progression through cytokinesis in HeLa but not in MCF-7 cells.
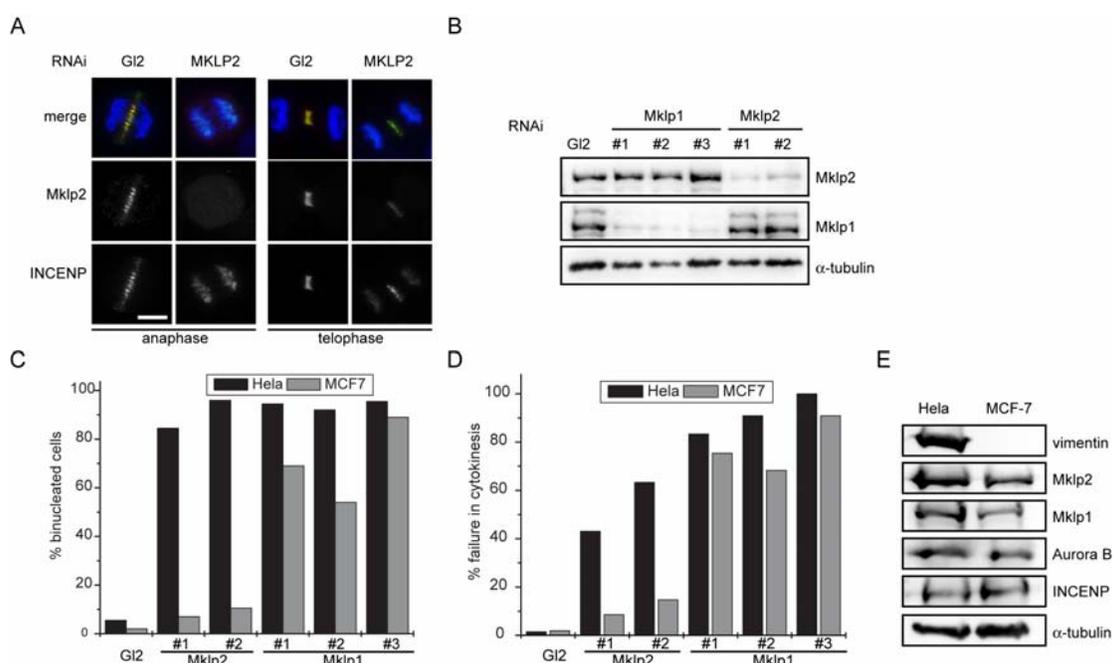
Figure 28. No cytokinesis defect upon Mklp2 depletion in vimentin negative MCF-7 cells.

(A) Immunofluorescence analyzes of MCF-7 cells depleted for Mklp2 by RNAi. Representative images of cells in anaphase and telophase fixed 10 h after the release from thymidine (see Figure 14). Cells were stained for Mklp2 (red), INCENP (green) and DNA (blue). Bar, 10µM. **(B)** Immunoblot analyzes of MCF-7 cells depleted for Mklp1 and Mklp2 by RNAi. Cells were treated as described in (A), whole cell lysates were prepared and analyzed by Western blotting with Mklp2 and Mklp1 antibodies. The α-tubulin immunoblot serves as a loading control. **(C)** Quantification of the Mklp2 RNAi phenotype in MCF-7 cells. Asynchronously growing cells were depleted for Mklp1 and Mklp2 by RNAi for 60 h, cells were fixed and the percentage of binucleated cells was determined. **(D)** Quantification of the Mklp2 RNAi phenotype in MCF-7 cells by live cell acquisition. RNAi was performed as described in Figure 14. Bars represent the percentage of cells that failed to complete cytokinesis and exited mitosis as binucleated cells. **(E)** Immunoblot analyzes of Hela and MCF-7 cells. Whole cell lysates were prepared from asynchronously growing cells and analyzed by Western blotting with the indicated antibodies.

Interestingly, it has been reported that vimentin is expressed in HeLa but not in MCF7 cells (Sarria et al., 1990). Our Western blot analyses confirmed this cell type specific expression of vimentin (Figure 28.E). Thus, the presence of vimentin correlates with the requirement for Mklp2 in late cytokinesis. It is interesting to speculate that the expression of vimentin requires an Mklp2/CPC mediated control mechanism that ensures the local disassembly of the IF at the cytokinetic bridge at the end of mitosis in order to guarantee its normal progression through cytokinesis.

Conclusion 2

Following the goal to gain further insights in the Mklp2-mediated functions of the CPC in cytokinesis, we showed that the phosphorylation-induced disassembly of vimentin at the central spindle by Aurora B in late cytokinesis is dependent on Mklp2. This conclusion is based on the observations that the delocalization of the CPC after depletion of Mklp2 or expression of GFP-INCENP^{T59E} in INCENP-depleted cells results in an accumulation of vimentin at the central spindle. Furthermore, we observed a co-localization of Mklp2 and vimentin in the absence of INCENP which might imply that Mklp2 not only ensures proper midzone localization of the CPC, but also provides a physical link between the kinase Aurora B and the substrate vimentin. Interestingly, the requirement for Mklp2 in late cytokinesis correlates with the presence of vimentin in HeLa and MCF-7 cells. Direct evidence in future studies will help to confirm the hypothesis that vimentin is a major downstream target of the Mklp2-mediated function of the CPC in late cytokinesis.

Results 3: Novel inhibitors for mitotic kinesins

The phase of cell division is highly dynamic and controlled by a complex network of regulatory processes. Thus, the study of cell division requires molecular tools with a high temporal resolution.

In this context, we aimed to identify novel potent Eg5 inhibitors which could be used to arrest cells in a prometaphase-like state without interfering with MTs. This first screen served as a pilot screen on our main goal to identify inhibitors of kinesins involved in cytokinesis, namely Mklp1, Mklp2, MPP1 and KIF4.

3.1 Screen for novel Eg5 inhibitors

Monastrol was the first identified selective kinesin inhibitor (Mayer et al., 1999). The target of monastrol is the kinesin Eg5 required for spindle bipolarity (Blangy et al., 1995). Consequently, monastrol-treated cells arrest in mitosis with a characteristic monoaster phenotype. The compound was identified in a forward chemical genetics approach, screening for compounds that arrest cells in mitosis without directly targeting MTs (Mayer et al., 1999). During recent years, its selectivity and mode of action towards Eg5 has been well characterized but the lack of potency limited its routines application. Thus, we performed a reverse chemical genetic approach to identify more potent small molecule inhibitors of Eg5.

For this purpose, the known Eg5 inhibitors monastrol and HR22C16 (Hotha et al., 2003) were used as lead compounds to synthesize a small library of 500 compounds. In the first step, this library was screened in duplicate for the inhibition of Eg5 *in vitro* using a malachite green ATPase assay. In parallel the kinesins Mklp1, Mklp2, MPP1, KIF4, KIF5a, KIF5b, CenpE and MCAK were analyzed to provide selectivity in the screening procedure. As shown in Figure 29.A, 53 out of 500 tested compounds are able to inhibit the motor activity of Eg5 to more than 50% and only 12 of these compounds significantly (>50%) affected any of the other tested kinesins. Out of the resulting 41 compounds, at this stage called selective Eg5 inhibitors, 27 were more potent than monastrol.

In parallel, all 500 compounds were tested for their ability to induce a mitotic arrest *in vivo*. For this, BSC-1 cells were released from a thymidine arrest for 14 h in the presence of the compounds and the percentage of cells in mitosis was determined by immunofluorescence microscopy. Only 9.6% (48/500) of all tested substances were able to induce a significant arrest in mitosis (Figure 29.B). Strikingly, however, almost one-third (16/53) of the compounds inhibiting Eg5 *in vitro* were able to do so (Figure 29.C). Moreover, 13 of the 27 molecules (48%) that were more potent than monastrol *in vitro* were also able to induce a mitotic arrest phenotype *in vivo* (Figure 29.C). In summary, out the 500 tested compounds,

we uncovered 13 selective Eg5 inhibitors, which were more potent than monastrol *in vitro* and induced a mitotic arrest in cells. Thus, we could demonstrate that a reverse chemical genetics approach is a valuable strategy to identify small molecule inhibitors for mitotic kinesins.
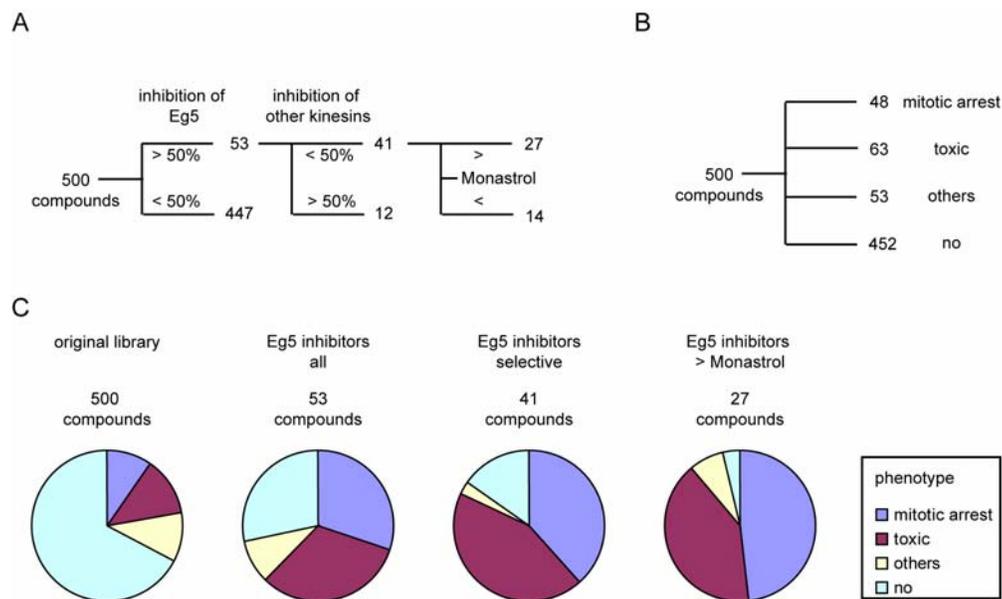
Figure 29. Screen for novel inhibitors of Eg5.

(A) Flow scheme of screening results for selective Eg5 inhibitors *in vitro*. **(B)** Results from the phenotypic analyses from the compound treatment of BSC-1 cells. **(C)** Cellular phenotype caused by the indicated subsets of compounds.

3.2 Improvement of monastrol by an applied structure activity relation (SAR) method

Out of the substances identified in this screen, the group of VS compounds caught our attention because this group of molecules efficiently inhibited Eg5 *in vitro* and caused a mitotic arrest in BSC-1 cells. The scaffold of these compounds was derived from monastrol and is characterized by a cyclisation of the side chain, reported to improve the activity of the compound via its rigidization (Sunder-Plassmann et al., 2005). Furthermore, out of our initial data set it appeared that the hydroxyl group on the 3'-position of the 3,4-dihydro-4-phenylquinazoline-2(1H)-thione skeleton is invariant for the inhibition (Figure 30.A; compare VS-1 with VS-12) and thus, only compounds matching this requirement were considered for further studies. Based on these criteria and the data obtained from the initial screen, a biased sublibrary of VS compounds was generated (Figure 30.B) and tested *in vitro* and *in vivo* for their ability to inhibit Eg5. To determine the properties of these compounds in a quantitative and comparable manner, the IC_{50} values were determined. To do so, the ATPase activity of Eg5, normalized to the solvent control (DMSO), was measured in the presence of different

concentrations of VS compounds or monastrol using the malachite green ATPase assay. As shown in Figure 30.C, all tested compounds were able to inhibit Eg5 in a dose dependent manner and the calculation of the IC$_{50}$ values revealed a decrease from 20 µM in the case of monastrol to a minimum of 2 µM in the case of VS-83 (Figure 30.D).
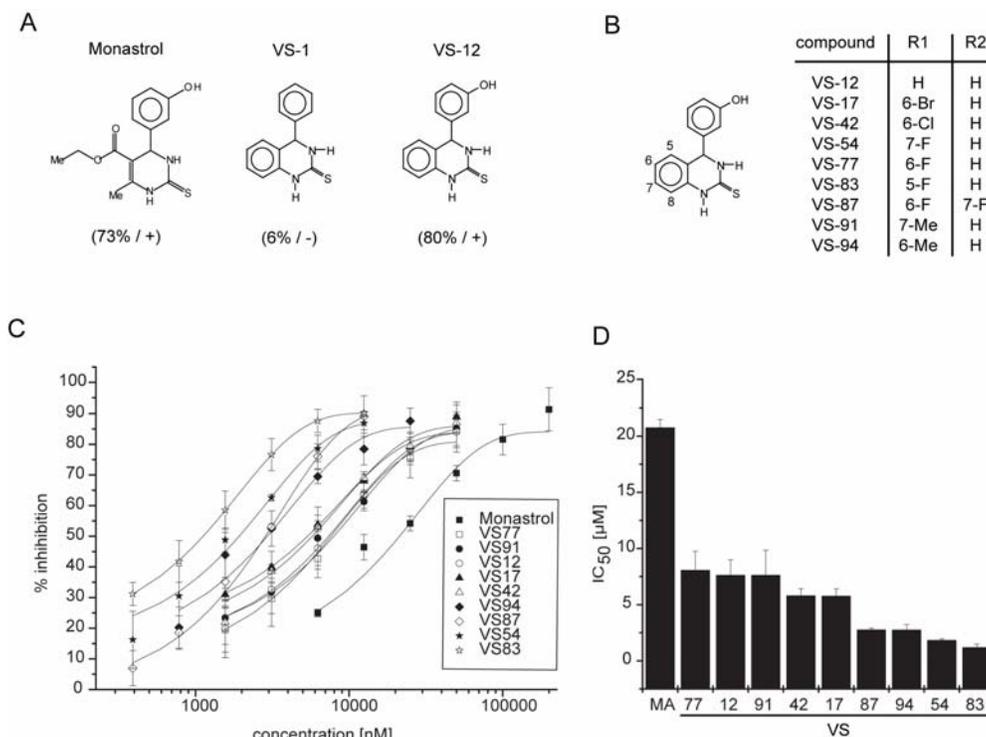
Figure 30. VS-83 – a potent Eg5 inhibitor *in vitro*.

(A) Chemical structure of monastrol and the indicated VS compounds. The numbers in brackets show the percentage of Eg5 inhibition in the initial screening as determined in the ATPase assay, and the ability to induce a mitotic arrest is indicated with (+). **(B)** Sublibrary of VS compounds. The core structure of VS compounds is shown on the left and the synthesized derivates are summarized in the table. The substitutions (R1 and R2) are made at the indicated positions. **(C)** Inhibition of the motor activity of Eg5 at different concentrations of the indicated compounds. Error bars represent SD. **(D)** The IC$_{50}$ values were determined from the data obtained in (B) and blotted as bars for each compound. Error bars represent SD.

In order to determine if this increased potency *in vitro* is also reflected in a stronger phenotype *in vivo*, BSC-1 cells arrested in G1/S by thymidine were released for 10 h into the indicated compound concentrations and the cell-cycle profiles were determined by flow cytometry. The obtained data reveal that an efficient mitotic arrest, comparable to the one after treatment with 500 nM nocodazole, could only be achieved with 200 µM monastrol, but already with 10 µM of the most potent VS compounds (Figure 31.A and Figure 31.B). In comparison to monastrol, VS-83, the most potent Eg5 inhibitor *in vitro*, was also 20 times more potent in cells (Figure 31.B).
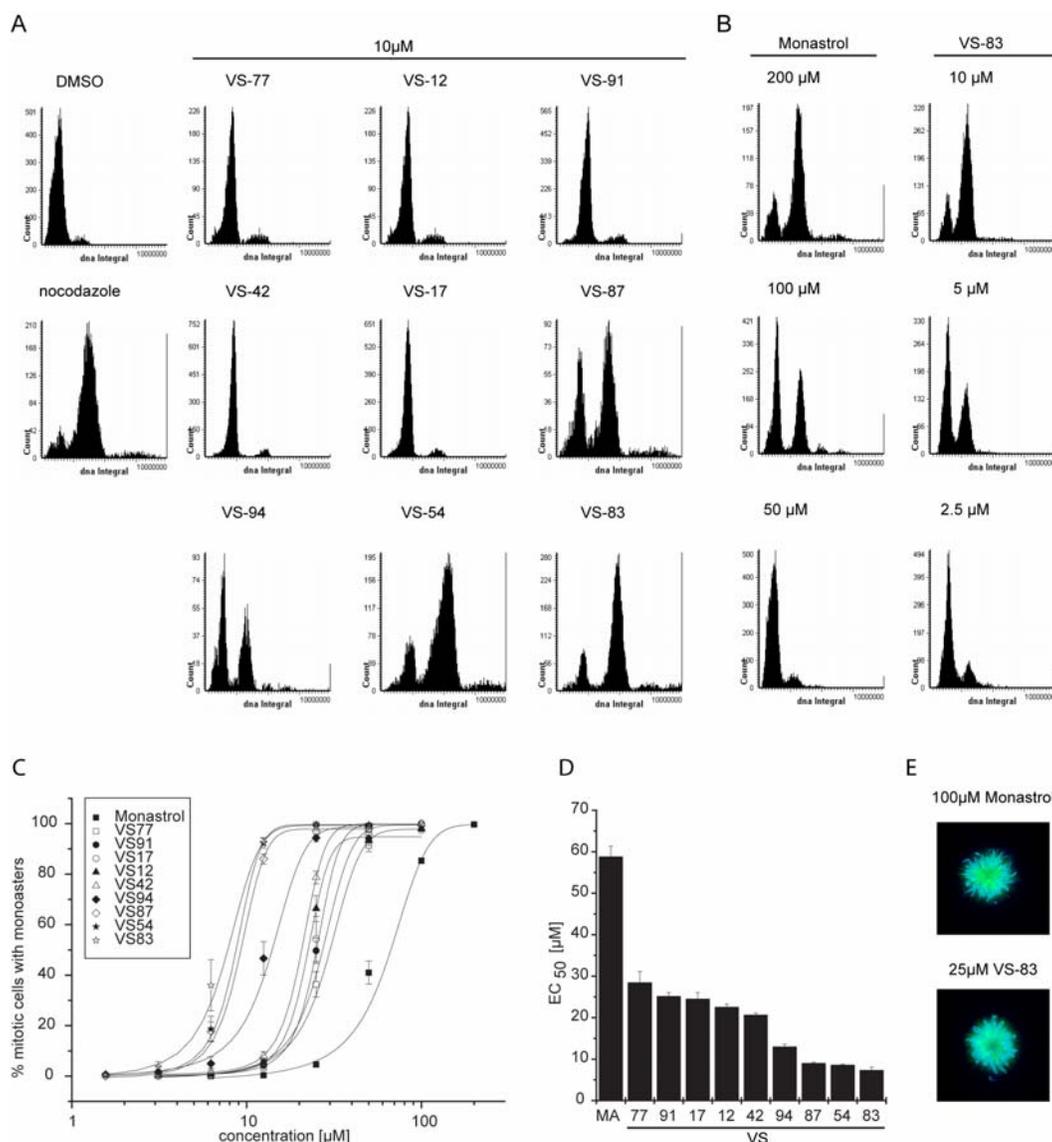
Figure 31: VS-83 – a potent Eg5 inhibitor *in vivo*.

(A) FACS analysis of BSC-1 cells treated with the indicated compounds. BSC-1 cells released from a thymidine block were treated with 10 µM of the compounds and fixed 12 h later. The DNA content was measured using an LSC. DMSO and Nocodazole (500 nM) were used as positive and negative controls, respectively. **(B)** Comparison of the mitotic arrest phenotype of monastrol and VS-83 treated BSC-1 cells by FACS analyzes. Cells were treated with different concentrations of both compounds and processed as described in (A). **(C)** Analysis of the monoaster phenotype in mitotic cells. BSC-1 cells released from a thymidine block were treated with the different concentrations of the indicated compounds, fixed 8 h later and processed for immunofluorescence analyses. Bars represent the number of mitotic cells with a monoaster phenotype. Error bars represent the SD. **(D)** EC$_{50}$ values were calculated from the data in (C) and are blotted for each compound. Error bars represent the SD. **(E)** Immunofluorescence analyses of BSC-1 cells treated with 100 µM monastrol or 25 µM VS-83. DNA is shown in blue and α-tubulin in green.

To further confirm that the induced cellular phenotype correlated with the inhibition of Eg5 *in vivo*, we analyzed the spindle morphology of compound-treated mitotic cells (Figure 31.E). In

order to do this in a quantitative manner, we determined the effective concentration *in vivo* (EC_{50}), at which 50 % of the mitotic cells displayed the typical monoaster phenotype. As shown in Figure 31.C, all tested compounds were able to induce a monoaster phenotype in a dose dependent manner. Furthermore, the EC_{50} values of the individual compounds perfectly matched the potency of these compounds *in vitro* (Figure 31.D and Figure 30.D). In summary these data demonstrate that the VS-compounds display the same selectivity towards Eg5 *in vivo* and *in vitro* as the lead compound monastrol, but being up to 20 times more potent.

3.3 Novel inhibitors for kinesins in cytokinesis

Having established a method for identification of biological active kinesin inhibitors in a reverse chemical genetic approach, we next thought to identify novel inhibitors for kinesins required in cytokinesis. In the first step, 22.000 substances were screened in duplicate for the inhibition of the kinesins Mklp1, Mklp2, MPP1 and KIF4 *in vitro* using the aforementioned malachite green ATPase assay. To select for more specific inhibitors, compounds were screened in parallel on the unrelated kinesins 5A and 5B. In order to process the obtained data, only compounds that were able to inhibit one kinesin with more than 50 % (inhibition > 50 %) while not inhibiting more than one other kinesins to more than 50 % (selective inhibition), were considered for further analyses (Fig 32.A).

Since a failure in cytokinesis ultimately leads to the formation of binucleated cells, we used the binuclear phenotype as readout for the functionality of the compounds *in vivo*. For this purpose, HeLa cells were released from a thymidine arrest in the presence of the compounds and analyzed for the formation of binucleated cells. Following this protocol, we were also able to identify and sort out compounds inducing phenotypes unrelated to the function of the according kinesin target, e.g. affecting entry into mitosis. As shown in Figure 32.A, only a small number of compounds were able to induce a binucleated phenotype *in vivo*. After retesting these compounds *in vivo* and in *vitro* three compounds remained that inhibit the ATPase activity of Mklp2 and MPP1 and induce a binucleated phenotype in cells. (Figure 32.A, validated compounds).

In summary, out of 22.000 compounds initially tested, three compounds targeting Mklp2 and Mpp1 that induced a binucleated phenotype *in vivo* could be identified. A fourth substance was originally identified during an earlier screen (S. Hümmer, Diplomarbeit, 2004). Thus, we have discovered four structurally unrelated compounds *via* a reverse chemical genetic screen combined with a subsequent analyzes *in vivo* and named them SH1-4 (Figure 32.B).
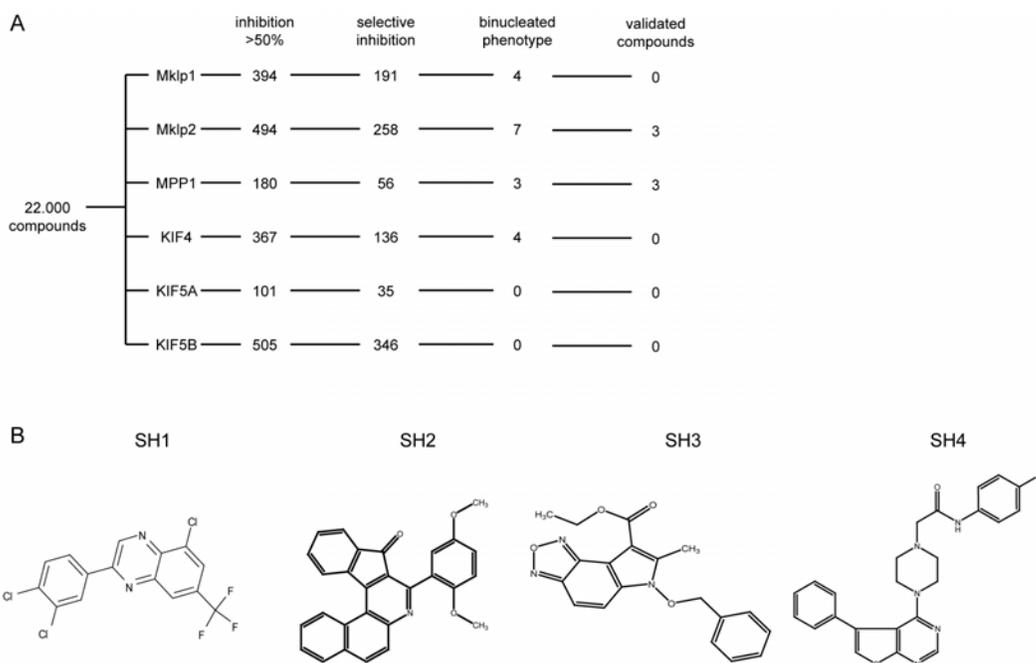
Figure 32. Screen for inhibitors of cytokinetic kinesins.
(A) Flow scheme of screening results for inhibitors of cytokinetic kinesins. **(B)** Chemical structure of SH compounds.

3.4 SH compounds inhibit Mklp2 and MPP1 *in vitro* and induce a cytokinesis defect *in vivo*

To further validate these inhibitors, we first determined their IC_{50} and EC_{50} values. This basic characterization is mainly represented by studies on SH1 and SH2, since the four identified substances represent similar properties which are summarized in Figure 33.C.

The IC_{50} value was determined by measuring the ATPase activity in the presence of different concentrations of SH compounds using the malachite green assay as described above. SH substances were able to inhibit Mklp2 and MPP1 in a dose dependent manner whereas Mklp1, despite being member of the same kinesin family, was not significantly affected at the tested concentrations (Figure 33.A). SH2 was slightly more potent in inhibiting Mklp2 and MPP1 than SH1. However, both compounds did not show any significant specificity towards either Mklp2 or MPP1 (Figure 33.A and Figure 33.C).

The EC_{50} values were determined by the quantitative analyses of compound-treated HeLa cells. The number of binucleated cells in SH treated cells was normalized to the control (DMSO-treated) and blotted against the concentration of the compounds. While both compounds were able to induce a binucleated phenotype in a dose dependent manner, the EC_{50} values revealed that SH2 was more potent than SH1 *in vivo*, consistent with the *in vitro* data.

In order to improve the specificity and/or potency of SH1, we also characterized derivates of the compound, but we could so far neither achieve a significant increase in the potency nor improve the selectivity towards Mklp2 or MPP1 (data not shown).

In summary, SH1 and SH2 are cell permeable, small molecule inhibitors that despite being structurally unrelated, display similar properties *in vivo* and *in vitro*.
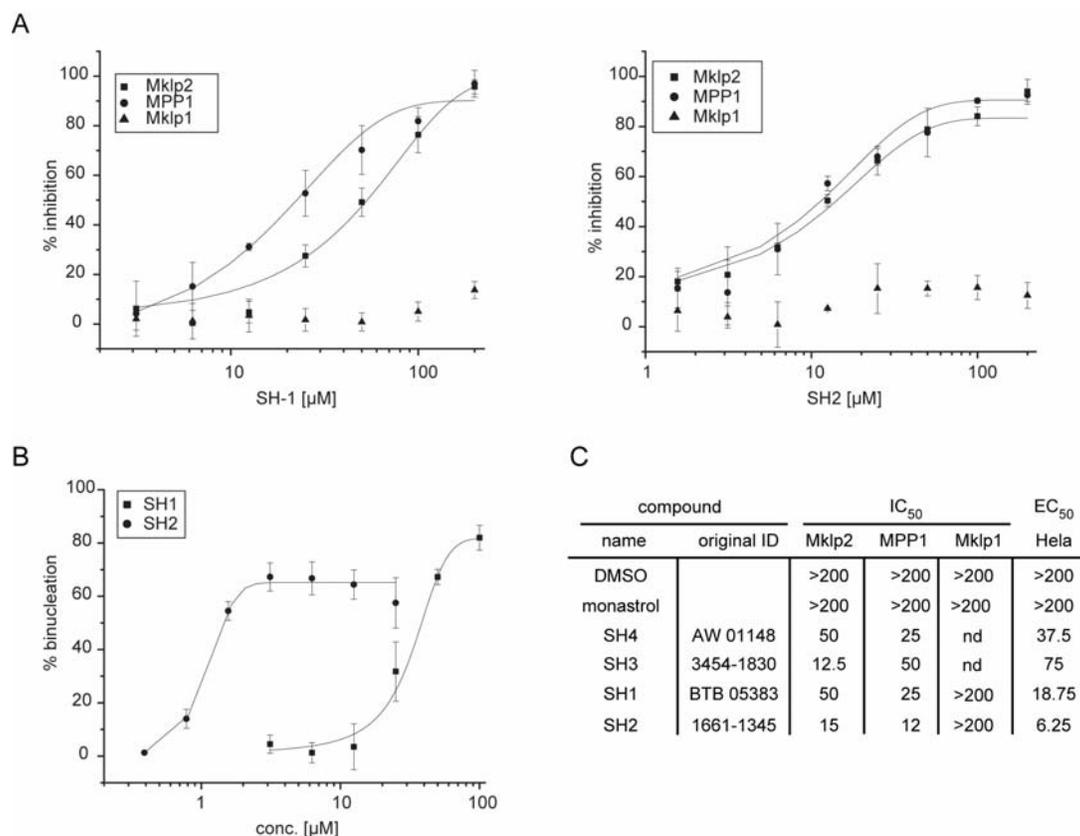
Figure 33. Initial characterization of SH compounds.

(A) SH1 (left) and SH2 (right) inhibit Mklp2 and Mpp1 but not Mklp1 *in vitro*. Inhibition of the ATPase activity of the kinesins, normalized to DMSO as solvent control is plotted against the concentration of the compounds. **(B)** SH1 and SH2 induce a binucleated phenotype *in vivo*. Hela cells released from a thymidine block were treated with different concentrations of the compounds or DMSO as solvent control and fixed 14 h later. The percentage of binucleated cells was determined and blotted against the concentration of the compounds. Error bars represent SD. **(C)** Table showing the characteristics of SH compounds *in vitro* and *in vivo*. Monastrol and DMSO were used as positive and negative controls, respectively.

3.5 SH1 does not interfere with Mklp2/MPP1 independent cellular processes

SH compounds inhibit Mklp2 and MPP1 *in vitro* and induce a binuclear phenotype *in vivo*. Since both proteins are reportedly required for normal progression through cytokinesis (Abaza et al., 2003; Hill et al., 2000), it was plausible that Mklp2 and MPP1 are the relevant targets of SH1 and SH2 *in vivo*. To collect further evidence that SH1 and SH2 are selective

in their mode of action, we analyzed cellular structures and processes known to be independent of Mklp2 and MPP1. Due to the similar characteristics of all SH compounds *in vitro* and *in vivo*, we focused on the initially identified molecule SH1 for these analyses.

The cytoskeleton of the cell, composed of actin and MTs, is the structural basic of many cellular processes including cytokinesis. Its structure is based on its dynamic behavior, as well as the functionality of a number of associated proteins. Immunofluorescence analyses of both actin and MT cytoskeleton in interphase cells revealed no differences between SH1 or DMSO treated cells, excluding that the cytoskeleton or any of the proteins required for its structure is affected by the compound (Figure 34.A).

As MTs and their associated motor proteins are involved in the correct cellular localization of organelles such as lysosomes or the Golgi apparatus (Hirokawa, 1998), we tested whether SH1 affects Golgi or lysosome structures in cells. While the disassembly of the MT network by nocodazole resulted in fragmentation and displacement of these structures, the localization of the Golgi apparatus and the lysosomes in SH1-treated cells was similar to the one in the DMSO control (Figure 34.B). Thus, these results imply that none of the proteins involved in the assembly and localization of these MT dependent organelles is affected by SH1.

Cell migration is a process that requires the interplay between actin, MTs and their associated proteins, including motor proteins, to guide the movement of a cell in a specific direction (Ridley et al., 2003). To analyze if any of the proteins, involved in this process is affected by the treatment of cells with SH1, we induced a cut in the cell layer of compound treated BSC-1 cells and monitored the time required to close this gap (wound healing assay). (Rodriguez et al., 2005). While cells treated with nocodazole were not able to close the gap within 22 hours after applying the cut, there was no obvious difference in the efficiency in healing when comparing SH1 or DMSO treated cells (Figure 34.C). Thus SH compounds do not interfere with the function of any protein that is required for this process.
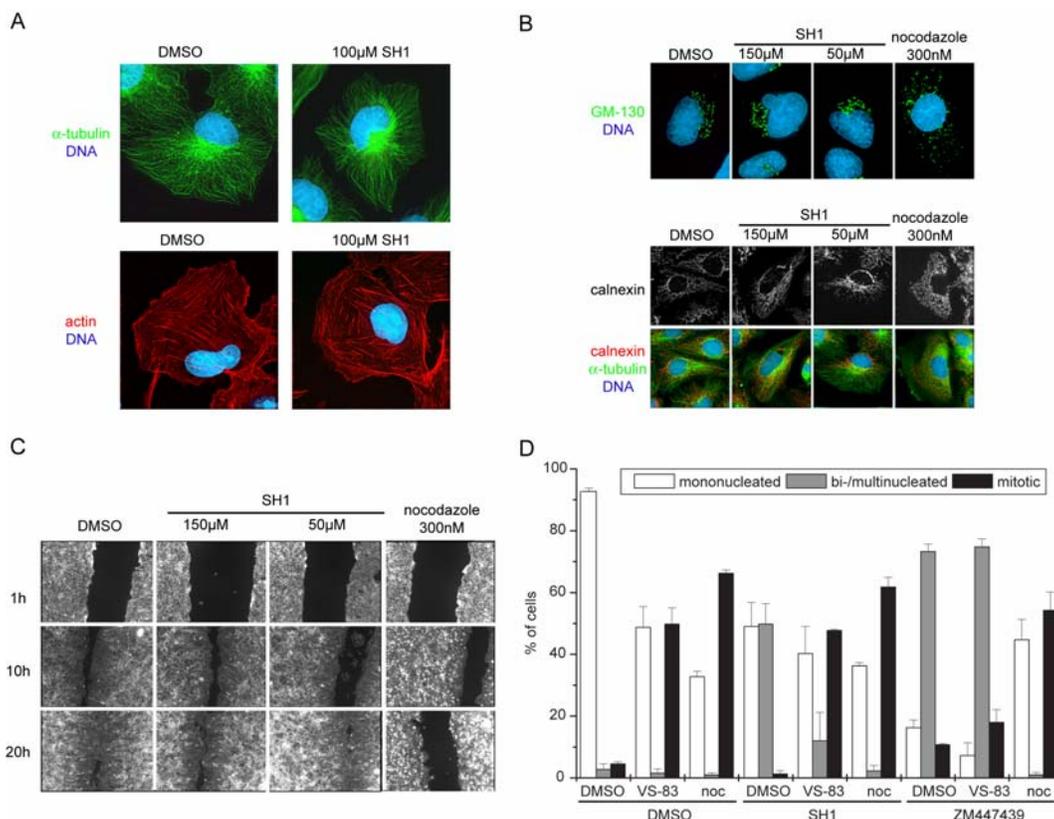
Figure 34. Specificity analysis of SH1.

(A) SH1 does not affect the interphase cytoskeleton. Immunofluorescence analysis of BSC-1 cells treated with 100 µM SH1 or DMSO as solvent control. Tubulin is shown in green (upper panel), actin in red (lower panel) and DNA in blue. **(B)** SH1 does not affect the localization of the golgi apparatus and lysosomes. BSC-1 cells treated with the indicated concentrations of SH1, nocodazole, or DMSO as solvent control were fixed and analyzed by immunofluorescence. GM-130 as marker protein for the golgi apparatus is shown in green (upper panel) and calnexin as marker for lysosomes in red (lower panel) and DNA is shown in blue. Cells in the lower panel were also stained for α-tubulin. **(C)** SH1 does not affect wound healing. A cut was introduced in a layer of BSC-1 cells treated with the indicated compounds (0 h) and the ability to close this gap was monitored at 1 h, 12 h and 20 h. **(D)** SH1 treatment neither causes a mitotic arrest nor overrides the SAC. Hela cells were treated with the combinations of the indicated compounds after the release from thymidine and fixed after 14 h. The percentage of interphase cells with one nucleus (mononucleated) and more than one nucleus (bi-/multinucleated) as well as the percentage of mitotic cells was determined. Error bars represent SD.

The SAC senses incorrect attachment of chromosomes to the mitotic spindle apparatus and delays anaphase onset until error free segregation of the genome into the daughter cells can be ensured (Musacchio and Salmon, 2007). Since neither Mklp2 nor MPP1 have a described role during early mitotic progression, SH treatment should not lead to defects in this process. In order to prove this, compound treated HeLa cells were released for 16 h from a thymidine arrest and the mitotic index, describing the ratio of cells in mitosis compared to other stages of the cell cycle, was determined by immunofluorecence. As expected, VS-83 as well as

nocodazole treatment, known to delay mitotic progression by the activation of the SAC, lead to an increase in the mitotic index (Figure 34.D). In contrast, SH1-treated cells progress normally through mitosis and the mitotic index was similar to that of cells treated with DMSO as solvent control (Figure 34.D). Moreover, there was a clear increase in the number of binucleated interphase cells after of SH treatment confirming that the compounds were active under the experimental conditions (Figure 34.D). Thus we can rule out that SH drugs interfere with the functionality of proteins known to be required for normal mitotic progression.

Defects in chromosome segregation can induce the formation of binucleated cells (King, 2008). Thus, we investigated whether the SH1-induced binuclear phenotype is due to the override of the SAC. In order to test this possibility, the spindle assembly checkpoint was activated by either nocodazole or VS-83 and the maintenance of the checkpoint was analyzed in the presence of SH1. As a positive control we used ZM447439 which inhibits Aurora B kinase, whose activity is required to sustain the SAC in the presence of mal-attached chromosomes (Ditchfield et al., 2003). As shown in Figure 34.D, the mitotic index of nocodazole- or VS-83-treated cells treat did not change significantly in the presence of SH1 or DMSO, indicating that the SAC can be efficiently sustained in the presence of SH1. In contrast, ZM447439 clearly affected the mitotic arrest induced by VS-83 but not the treatment of nocodazole arrested cells, as reported (Ditchfield et al., 2003) (Figure 34.D).

In summary, SH1 seems not to affect any of the analyzed Mklp2- or MPP1-independent cellular processes.

3.6 Binding of SH compounds to the target proteins is mediated by a kinesin 6-family specific insertion in the motor domain

Kinesin-6 family members are characterized by specific extension in the highly conserved motor domain (Hizlan et al., 2006; Miki et al., 2005) (Figure 35.A). Since all inhibitors identified in the screen inhibited Mklp2 and MPP1 but not other kinesins, we speculated that the kinesin-6 specific insertion in the motor domain might be critical for the inhibitory activity of the compounds.

Therefore, we created a deletion mutant of the Mklp2 motor domain lacking the residues 193-295 (Mklp2$^{\Delta\text{-loop}}$, Figure 35.B). Since the overall sequence of the kinesin motor domain is highly conserved, and mutation in this domain could possibly impair its function, we first determined the activity of Mklp2$^{\Delta\text{-loop}}$ by measuring its ATPase activity. The data obtained from these measurements revealed that Mklp2$^{\Delta\text{-loop}}$ is active with a slight reduction in its turn-over rate compared to the wild type protein (Figure 35.C). This is in line with a previous report, showing that this characteristic extension is not involved in the basic function of the motor domain of Zen4, the *C. elegans* homolog of Mklp1 (Hizlan et al., 2006).
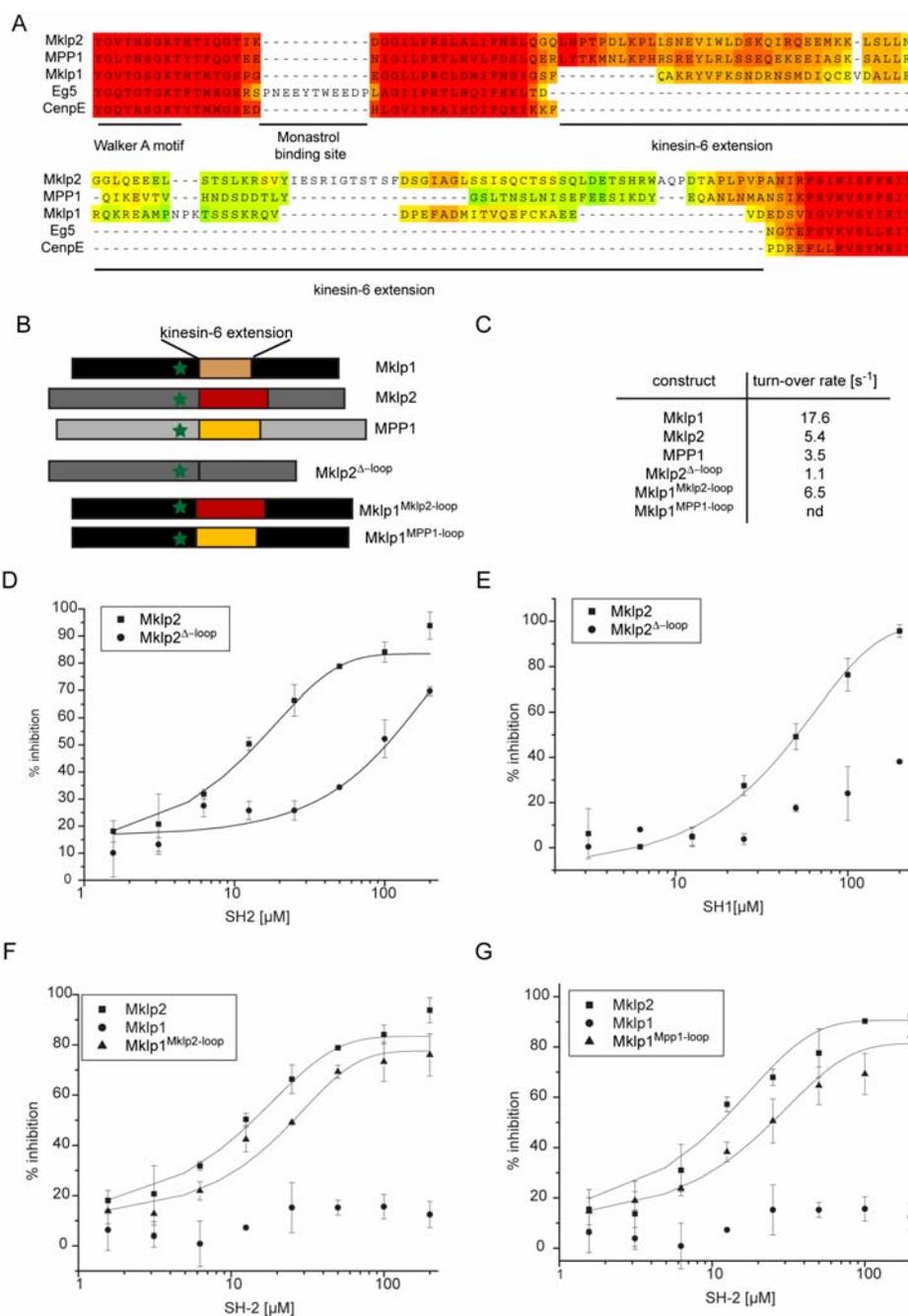
Figure 35. Kinesin-6 extension mediates inhibition by SH compounds.

(A) Sequence alignment of the region of the motor domain of Mklp1, Mklp2 and MPP1 in comparison to the non kinesin-6 family members Eg5 and CenpE. The conserved walker A motif is indicated, the kinesin-6 familiy specific extension is underlined and the binding site of monastrol in Eg5 is shown. **(B)** Schematic drawing of the motor domain of Mklp1, Mklp2 and MPP1 showing the location of the kinesin-6 specific extension in relation to the Walker A motif (green star). The deletion constructs of Mklp2 and MPP1 as well as the chimera of Mklp1 are shown below. **(C)** Table showing the turn-over rates [s^{-1}] for the indicated constructs. **(D-G)** Graphs showing the inhibition of the ATPase activity of the indicated constructs by SH1 or SH2. Data obtained from the ATPase activity measurements were normalized to the solvent control DMSO and the percentage of inhibition is blotted against the concentration of the compounds. The curves of the wildtype constructs are blotted for comparison and are identical to the one presented in Figure 33.

59

Having approved the functionality of this construct, we next asked if SH compounds could still inhibit Mklp2$^{\Delta\text{-loop}}$. As shown in Figure 35.D and 35.E, Mklp2$^{\Delta\text{-loop}}$ is significantly less sensitive to both compounds compared to the wild type. Similarly, MPP1 lacking the kinesin-6 specific extension was significantly less inhibited by SH1 and SH2 (data not shown). Thus this extension seems to be required for the inhibition by SH compounds. As we have shown above, Mklp1 with the smallest extension in the kinesin-6 family (65aa compared to 79aa in MPP1 and 102aa in Mklp2), was not targeted by the compounds *in vitro.* Therefore, it was tempting to speculate, that Mklp2 and MPP1 contain additional residues critical for the mode of action*.* In order to test this hypothesis, we replaced the extension of Mklp1 (aa 146-211) with the one from Mklp2 (aa 193- 295) or MPP1 (aa 186-265) resulting the Mklp1 chimeras Mklp1$^{\text{Mklp2-loop}}$ and Mklp1$^{\text{MPP1-loop}}$, respectively (Figure 35.B). The enzymatic measurement showed that the turn-over rate of Mklp1$^{\text{Mklp2-loop}}$ was similar to the one of wild type Mklp1 (Figure 35.C). While Mklp1 was not inhibited by SH2, the chimera Mklp1$^{\text{Mklp2-loop}}$ was nearly as efficiently inhibited by SH2 as Mklp2 itself (Figure 35.F). This effect could be also repeated with the chimera of Mklp1$^{\text{MPP1-loop}}$ (Figure 35.G) and for both chimeras with with SH1 (data not shown), underlying a common mode of action of the SH compounds in the inhibition of Mklp2 and MPP1. Taken together, these data imply that the extensions of Mklp2 and MPP1, different from the one in Mklp1, are required for the inhibition by the SH drugs, and that the transfer of this region to Mklp1 is sufficient to sensitize Mklp1 for the SH compounds.

3.7 The expression profile and RNAi phenotype of MPP1 do not correlate with a potential target of SH compounds *in vivo*

Our *in vitro* studies identified SH1 and SH2 as inhibitors of both Mklp2 and MPP1 raising the question of whether SH1 and SH2 also target both kinesins *in vivo.* To address this question, we first analyzed the expression of the kinesin-6 family members in different cell lines. For this purpose, cell lysates from exponentially growing cultures were prepared and the expression levels of the individual kinesins were analyzed by Western blotting. While Mklp1 and Mklp2 were expressed in all analyzed cell types to comparable levels, MPP1 was barely expressed in HeLa cells as determined by Western blot analyses using two antibodies directed against different domains of the protein (Figure 36.A). Since the expression level of MPP1 appeared to be similar in all other tested cell lines, this difference seemed to be specific for HeLa cells. Thus, either the remaining amount of MPP1 in HeLa cells is sufficient to induce the cytokinesis defect when inhibited by SH compounds or another target protein, different than MPP1, causes this phenotype. To test this further, we depleted MPP1 from HeLa cells by RNAi and compared the defect in cytokinesis to control cells (Gl2-depleted) and cells depleted for Mklp1 or Mklp2. In contrast to Mklp1 and Mklp2, the depletion of MPP1 in HeLa cells by four different RNAi oligos did not induce a failure in cytokinesis and its

subsequent binucleated phenotype (Figure 36.B). Due to the undetectable levels of MPP1 in HeLa cells, we could not determine the degree of depletion by western blot or immunofluorescence analyses. However, MPP1 depletion in other cell lines resulted in a clear reduction of MPP1 protein levels (Figure 36.C, MPP1 RNAi in MCF-7 cells) and yet we did not observe any significant defect in cytokinesis in any of the tested cells (Figure 36.B and data not shown). Although we can not exclude that cytokinesis can be efficiently achieved with very low amounts of MPP1, it is plausible that MPP1 is not required for cytokinesis in the analyzed cell lines. These results suggest that MPP1 is not the relevant target of SH compounds in cells.
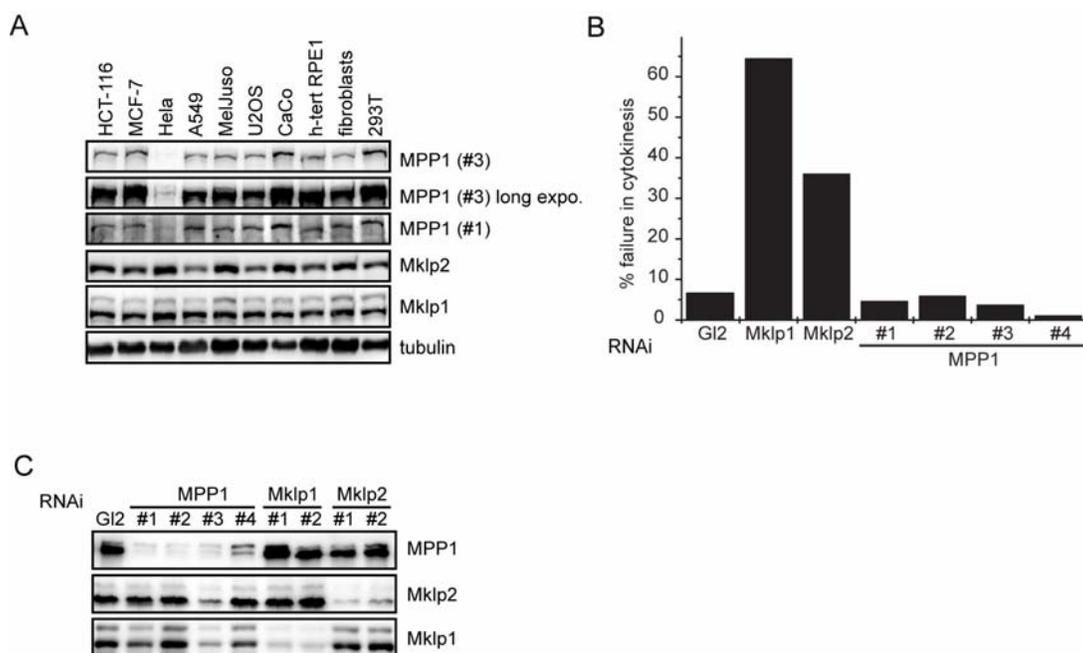
Figure 36. Depletion of MPP1 by RNAi does not cause a cytokinesis defect in HeLa cells.
(A) Expression of MPP1, Mklp2 and Mklp1 in different cell lines. Whole cell lysates were prepared from asynchronously growing cells and analyzed by Western blotting with the antibodies for MPP1 (#1) and MPP1 (#3) as well as for Mklp1 and Mklp2. The immunoblot for α-tubulin serves as loading control. **(B)** Quantification of live-cell recordings of Hela cells depleted for Mklp1, Mklp2 or MPP1. Bars represent the percentage of cells that failed to complete cytokinesis and exited mitosis as binucleated cells. **(C)** MCF-7 cells depleted for the indicated proteins by RNAi were processed for Western blot analyses with the indicated antibodies.

3.8 SH2 treatment correlates with the RNAi phenotype of Mklp2 in HeLa and MCF-7 cells

If MPP1 is not the likely target of SH compounds *in vivo*, we sought for additional evidence that SH cause a cytokinesis defect by inhibiting Mklp2. As shown above, depletion of Mklp2 in HeLa but not in MCF-7 cells induced a cytokinesis failure. Thus, MCF-7 cells should be

resistant to SH treatment assuming that Mklp2 is the relevant target of these compounds. To examine the effect of the compounds on the different cell lines in detail, SH-treated cells were analyzed by live-cell microscopy. Notably, SH1 caused a cytokinesis defect in both cell lines, whereas SH2 was only effective in HeLa but not in MCF-7 cells (Figure 37.A and Figure 37.B). Thus, SH2 unlike SH1 seems to selectively target Mklp2 in cells.
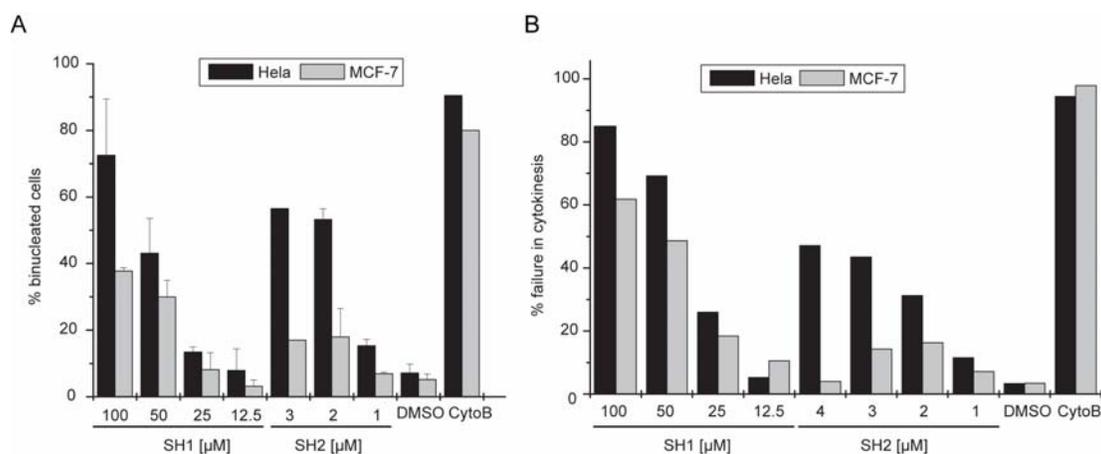
Figure 37. SH2 does not cause a cytokinesis defect in MCF-7 cells.
(A) MCF-7 cells do not show a cytokinesis defect upon SH2 treatment. Asynchronously growing Hela and MCF-7 cells were treated for 48 h with different concentrations of SH1 and SH2, cells were fixed and the number of binucleated cells was quantified by immunofluorescence microscopy. DMSO and 2 µM cytochalasin B (CytoB) were used as positive and negative control respectively. **(B)** Quantification of defective cytokinesis in SH1 or SH2 treated cells by live cell microscopy. Hela and MCF-7 cells were released from a thymidine block and treated with different concentrations of SH1 and SH2 as well as DMSO and cytochalasin B. Bars represent the percentage of transfected cells that failed to complete cytokinesis and exited mitosis as binucleated cells.

3.9 SH treatment does not interfere with the localisation of the target proteins *in vivo*

Finally we tested, if the inhibition of the motor activity of Mklp2 by SH2 results in a similar delocalization from the central spindle as we could observe for the motor dead versions of the protein (Figure 14.D). Even though the motor activity of the tested mutants is affected by different means (no ATP binding: Mklp2^{ATPm} and rigor type MT binding: Mklp2^{SIlm}), both mutants are absent from the central spindle in anaphase (Figure 14.D), suggesting that the motor activity of Mklp2 is required for the correct localization of Mklp2 to the central spindle in anaphase. However, immunofluorescence analysis of HeLa and MCF-7 cells, treated with either of the SH compounds did not reveal any significant differences in the localization of Mklp2 compared to the DMSO control (and MPP1 and Mklp1 were also not affected) (Figure 38.A and Figure 38.C). At first, these results would argue against Mklp2 as the relevant target of SH2 in cells. However, the localization of Eg5 was also unaffected in cells treated with VS-83 compared to control treated cells (Figure 38.B). Thus, it is also plausible to

assume that dependent on the mode of inhibition of the ATPase activity, either by small molecules or by mutation of critical residues in the motor domain, the localization of these motor proteins is affected differently. Since it remains unaddressed how motor dead versions of Eg5 are localized in the RNAi background, this hypothesis remains to be proven.
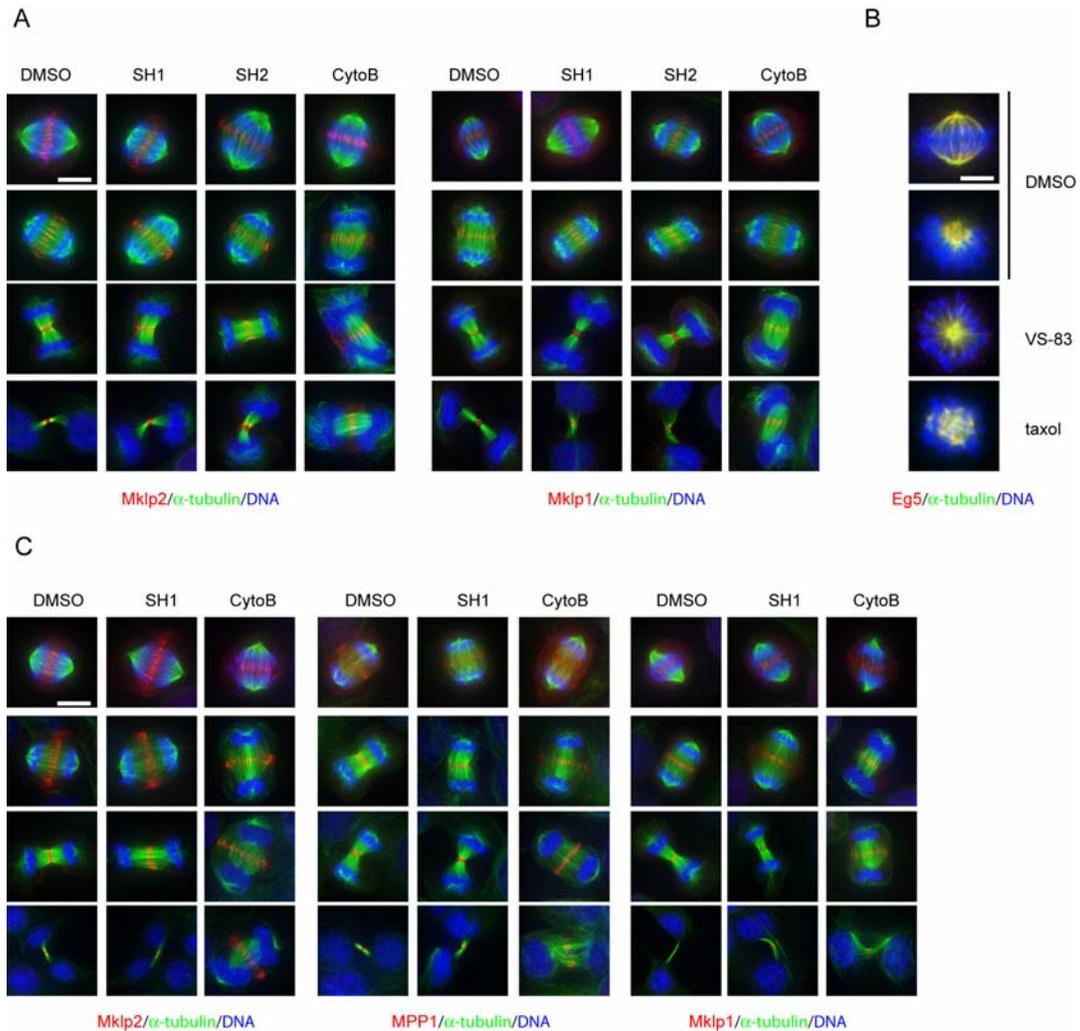
Figure 38. SH compounds do not delocalize the target proteins.
(A) Localization of MPP1, Mklp1 and Mklp2. HeLa cells were treated with 100 µM SH1 or 20 µM SH2 were fixed and immunostained for Mklp2 or Mklp1 (red) and α-tubulin (green) and DNA (blue). DMSO and cytochalasin B (2 µM) were used as negative and positive controls, respectively. **(B)** MCF-7 cells were treated with 25 µM VS-83, 1 µM taxol or DMSO as solvent control. Cells were fixed and stained for Eg5 (red), α-tubulin (green) and DNA (blue). **(C)** MCF-7 cells treated and processed as described in (A) were stained for Mklp2 or MPP1 or Mklp1 (red) and α-tubulin (green) and DNA (blue).

Conclusion 3

To further study the role of kinesins in cellular progression, we sought to identify specific inhibitors for kinesins via a reverse chemical genetics approach. The successful establishment of such an approach was proven by the discovery of the potent Eg5 inhibitor VS-83. Using this approach, we could uncover four structurally unrelated novel inhibitors for cytokinetic kinesins, called SH compounds. All inhibitors displayed the same mode of action/inhibition of the kinesins Mklp2 and MPP1 *in vitro*, and induction of a binucleated phenotype *in vivo*. The specificity of SH1 was confirmed by analyses of target independent cellular functions. Furthermore, we could also demonstrate that SH compounds act by inhibiting the ATPase activity of these kinesins targeting a family specific extension in the motor domain. Finally, we have collected the first evidences pinpointing Mklp2 as the relevant target of SH2 in cells, although future research will be required to rigorously confirm this point and to mechanistically clarify how the inhibition of the motor activity *in vitro* is transmitted to a failure in cytokinesis *in vivo*.

Discussion

1 Cdk1 negatively regulates midzone localization of Mklp2 and the CPC

The translocation of the CPC from centromeres to the spindle midzone at anaphase onset is critical for the completion of cytokinesis (Ainsztein et al., 1998; McCollum, 2004; Schumacher et al., 1998; Tatsuka et al., 1998; Terada et al., 1998; Wheatley et al., 2001). The mitotic kinesin like protein Mklp2, a member of the kinesin 6-family, is essential for the binding of the CPC to the spindle midzone (Gruneberg et al., 2004). However, the molecular mechanism regulating the binding of Mklp2 to MTs has remained unknown.

1.1 MT binding of Mklp2 at anaphase onset is mediated by its motor domain

The transition from metaphase to anaphase marks the association of Mklp2 with MTs (Figure 14.A, (Hill et al., 2000)). Our analyses of ATP-binding mutants of Mklp2 suggested that the affinity of the motor domain for MTs might control the localization of Mklp2 during mitotic progression (Figure 14.D).

In an earlier study, it has been reported that efficient binding of Mklp2 to MTs requires not only the motor domain but also its C-terminus (Gruneberg et al., 2004). While this conclusion was drawn from analyses of deletion constructs, we investigated the role of the motor domain in the binding of Mklp2 to MTs generating point mutations in the context of the full-length protein. Strikingly, Mklp2^{ATPm}, carrying a mutation in the ATP binding motif, does not localize to the central spindle upon anaphase onset (Figure 14.D). These results imply that the interaction of Mklp2 with MTs *in vivo* is likely to be mediated by the affinity of the motor-domain for MTs and that the proposed MT binding site in the non-motor region (Echard et al., 1998) is not sufficient for the binding of Mklp2 to MTs *in vivo*. Furthermore, Mklp2^{SIIm}, a rigor-type Mklp2 mutant, can bind prematurely to MTs, supporting the notion that motor-mediated MT binding is probably sufficient for the association of Mklp2 with MTs *in vivo*. It is plausible that the binding of Mklp2 to MTs of the spindle midzone is mainly mediated by the affinity of the motor-domain for MTs and that the potential MT binding site in the non-motor-domain may have an assisting but not essential function.

1.2 Mklp2 and the CPC are mutually dependent on each other for midzone localization

Mklp2 is essential for the binding of the CPC to the spindle midzone (Gruneberg et al., 2004). Strikingly, depletion of INCENP by RNAi resulted in a delocalization of Mklp2 from the central

spindle (Figure 15.A), arguing that Mklp2 and the CPC are mutually dependent on each other for midzone localization. Since Mklp2 was also miss-localized in INCENP depleted cells expressing GFP-INCENP[T59E] (Figure 18.A), a mutant form of INCENP which is unable to bind to Mklp2 (Figure 20.A), we conclude that the interaction between Mklp2 and the CPC is prerequisite for their efficient localisation to the spindle midzone. In analogy to this, the members of the centralspindelin complex Mklp1 (Zen-4) and MgcRacGAP (Cyk-4) are shown to be mutually dependent on each other for efficient binding to the central spindle (Jantsch-Plunger et al., 2000). Cyk-4 interacts with the neck-linker region of the kinesin Zen4 and only in this configuration, Zen4 is able to bind and bundle anti-parallel MTs (Mishima et al., 2002). The neck linker region, known to be essential for the directed movement of kinesins along MTs, is up to five times longer in members of the kinesin-6 family compared to other kinesins (Mishima et al., 2002). Interestingly, a similar mode of interaction seems to be also preserved in the Mklp2/CPC complex, since the C-terminus of Mklp2, containing the neck linker region, was able to bind to the CPC (Fig 19.C). Therefore, it is likely, that integration of two events, cargo binding and activation of the motor activity, mediated by the interaction of the cargo protein with the neck linker region, is a common mechanism for the regulation of the kinesin-6 family.

1.3 The phospho-mimicking mutant of INCENP (T59E) as a tool to uncouple the early from the late functions of the CPC in mitosis

INCENP was shown to be phosphorylatated at T59 by Cdk1 until the onset of anaphase, but the function of T59 phosphorylation remained unknown (Goto et al., 2006). The phosphomicking mutant of INCENP (T59E) was able to rescue the function of the CPC in early mitosis but failed to transfer to the central spindle upon anaphase onset and did not support the post-metaphase function of the CPC (Figure 16 and Figure 17). Underlining these results, several previous reports already indicate that the phosphorylation status of INCENP at T59 might be dispensable for the function of the CPC during mitosis but critical for the transfer of the CPC to the central spindle. First, phosphorylation of INCENP at T59 by Cdk1 is not essential for the function of the CPC in early mitosis (Goto et al., 2006). Second, dephosphorylation of Sli-15, the budding yeast homolog of INCENP, is required for the spindle transfer at anaphase onset (Pereira and Schiebel, 2003). Third, high Cdk1 activity in anaphase prevents the spindle transfer of the CPC member Aurora B in human cells (Murata-Hori et al., 2002). Fourth, a mutant form of INCENP, in which the amino acids 53-63 are randomly exchanged by mutagenesis, fails to transfer to the central spindle (Ainsztein et al., 1998). Thus, in line with the published literature, we concluded that the phosphorylation status at T59 is critical for the transfer of the CPC to the central spindle in anaphase.

Therefore, the phosphomimicking mutant T59E provided us the thought of tool to dissect the early from the late functions of the CPC.

Notably, the non-phosphorylatable mutant was created by exchanging threonine 59 to valine (T59V) and not to alanine (T59A) as described before (Goto et al., 2006). It is known that structural changes in the N-terminus of INCENP impair the transfer of the CPC to the central spindle in anaphase (Jeyaprakash et al., 2007). Therefore, we exchanged threonine to valine to minimize the difference in size between the two amino acids, trying to avoid major structural changes. A similar amino acid change (threonine to valine) had been reported in the case of the phosphorylation site T210 in the activation loop of Plk1 (Kothe et al., 2007). INCENP^{T59V} rescued the function of the CPC in early and late mitosis, indicating its functionality. Furthermore, INCENP^{T59V} rescued the localisation of Mklp2 in anaphase and was consequently able to interact with Mklp2 (Figure 18.A and Figure 20.A). None the less, the interaction of Mklp2 with GFP-INCENP^{T59V} was slightly weaker compared to the wild-type protein in its un-phosphorylated state (anaphase extract) (Figure 20.A). This might be explained by the remaining differences between these amino acids (i.e. the lack of the hydroxyl group on valine), which might be important for the interaction with Mklp2. Thus INCENP^{T59V} represents the best approximation so far, towards a non-phosphorylated form of INCENP at T59.

1.4 The interaction between the CPC and Mklp2 is negatively regulated by Cdk1

The formation of the Mklp2/CPC complex is prerequisite for its binding to the spindle midzone. This interaction in turn, is negatively regulated by Cdk1 during mitosis. In support of this, we could show that Mklp2 and the CPC only interact with each other after anaphase onset when Cyclin B levels begin to decline (Figure 19.A). Furthermore, GFP-INCENP^{T59E} was unable to bind to Mklp2 (Figure 20.A). The disassembly of a pre-existing Mklp2/CPC complex by Cdk1 *in vitro* finally confirmed that this interaction is indeed negatively regulated by Cdk1 (Figure 20.B and Figure 20.C). Similarly, it has been shown that phosphorylation of Ect2 by Cdk1 during mitosis prevents its association with the centralspindlin complex and a non-phosphorylatable mutant of Ect2 (T342A) was shown to bind to Cyk-4 prematurely (Yuce et al., 2005). Furthermore, the interaction between Plk1 and PRC1 is negatively regulated by Cdk1 (Neef et al., 2007). Binding of Plk1 to PRC1 requires a priming phosphorylation which is carried out by Plk1 itself (self-docking). This priming phosphorylation is prevented by Cdk1 phosphorylation of PRC1 until the onset of anaphase (Neef et al., 2007). Thus, the negative regulation of protein interactions by Cdk1 phosphorylation during early mitosis appears as a common mechanism of regulation to prevent the premature formation of protein complexes with specific post mitotic functions.

1.5 Binding of the CPC and Mklp2 to MTs is negatively regulated by Cdk1

In order to explore how Cdk1 activity affects the binding of Mklp2 and the CPC to MTs, we performed MT-pulldown experiments with taxol-stabilized MTs form cell extracts. Mklp2 and the CPC co-precipitated with MTs in anaphase cell extracts, but did not do so in extracts prepared from metaphase cells (Figure 21.A), or when Cdk1 activity was restored in anaphase extracts by the addition of non-degradable Cyclin B (Figure 21.B). Furthermore, overexpression of a non-degradable version of Cyclin B, prevented midzone localization of the Mklp2/CPC complex (Figure 21.C). Thus, Cdk1 activity not only interferes with the interaction between Mklp2 and the CPC, but also prevents their efficient binding to MTs. In line with these results, it has been previously reported (Murata-Hori et al., 2002) that microinjection of a non degradable version of Cyclin B in Ptk1 cells prevents the transfer of Aurora B to the central spindle. Furthermore, it was shown by work in budding yeast that dephosphorylation of the yeast homolog of INCENP (sli-15) by cdc14 is required for the binding to the spindle midzone (Pereira and Schiebel, 2003). While an essential role for cdc14 at the exit of mitosis in higher eukaryotes remains to be clarified (Queralt and Uhlmann, 2008), it is interesting to note, that PP1 has been recently identified as the major Cdk1 counteracting phosphatase at mitotic exit of human cells (Wu et al., 2009). It will be interesting to see in the future, if the activity of PP1 is also required for the transfer of the Mklp2/CPC to the spindle midzone.

1.6 INCENP is required to localize Mklp2 close to the ends of stable MTs in the absence of Cdk1 activity

Thus far, our data demonstrated that the drop in Cdk1 activity at anaphase onset is required for the efficient binding of the Mklp2/CPC complex to MTs. But consistent with previous reports (Murata-Hori et al., 2002), we also noticed that inactivation of Cdk1 was not sufficient to efficiently recruit the CPC or Mklp2 to MTs *in vivo* (Figure 22.A, panel 2), suggesting that additional changes have to occur in order to enable midzone localization of the Mklp2/CPC complex at anaphase onset. It has long been recognized that the highly dynamic status of MTs during mitosis is only kept until anaphase onset, when in parallel to Cdk1 inactivation the turnover of MTs in the spindle midzone is dramatically decreased (Saxton and McIntosh, 1987; Saxton et al., 1984). Simultaneous inactivation of Cdk1 and stabilization of MTs finally resulted in an accumulation of Mklp2 and the CPC at the ends of stable MTs, a scenario reminiscent to the central spindle localization in anaphase (Figure 22.A, panel 4). Thus, inactivation of Cdk1 and stabilization of MTs at the onset of anphase ensures proper midzone localization of the Mklp2/CPC complex. But, even though inactivation of Cdk1 alone is not sufficient for the binding of the Mklp2/CPC complex to the spindle midzone, Cdk1 activity might be essential to ensure that premature binding of the Mklp2/CPC complex to

MTs is prevented during mitosis. Cdk1-induced mitotic entry is accompanied with an increase in MT half-life from more than 3 min in interphase to 10 - 20 s in mitosis (Saxton et al., 1984). Thus, by increasing MT dynamics, key mechanism for the formation and maintenance of the mitotic spindle (Desai and Mitchison, 1997), Cdk1 probably prevents the association of the Mklp2/CPC with spindle MTs during mitosis.

Strikingly, the accumulation of Mklp2 at the plus ends of stable MTs was abolished when INCENP was depleted by RNAi (Figure 22, panel 8) or when INCENP depleted cells were rescued with GFP-INCENP[T59E] (Figure 23), underlining the importance of the Mklp2/CPC interaction for proper midzone localization. Under these experimental conditions, Mklp2 was instead bound to the lattice of stable MTs upon inactivation of Cdk1. This indicates that high Cdk1 activity not only prevents the interaction between the Mklp2 and the CPC, but also interferes with the interaction of Mklp2 with stable MTs. Likewise, the binding of Mklp1 to MTs is also negatively regulated by Ckd1, preventing its premature association with the mitotic spindle (Mishima et al., 2004). It remains to be addressed if, like in the case of Mklp1, direct phosphorylation of Mklp2 negatively regulates the binding of Mklp2 to MTs or if another Cdk1 dependent player is involved in the recruiting cascade of the Mklp2/CPC complex to the central spindle.

Importantly, lattice binding of Mklp2 after Cdk1 inactivation in the absence of INCENP was dependent on the addition of taxol (Figure 22, panel 7 and panel 8). It has been reported, that in an unperturbed anaphase, astral MTs remain highly dynamic, while MTs of the spindle midzone are particularly stable (Foe and von Dassow, 2008; Murthy and Wadsworth, 2008). Thus, local stabilization of MTs might be a key mechanism for the exclusive localization of Mklp2 to the MT plus-ends of the spindle midzone. The potential role of Aurora B in such a mechanism is discussed below. It is finally worth mentioning, that also Mklp1 is exclusively localized to the MTs of the spindle midzone. It is tempting to speculate that the requirement for stable MTs is the third common regulatory mechanism, besides cargo binding and Cdk1 inhibition, which controls proper midzone localization of both Mklp1 and Mklp2.

1.7 A potential feedback loop mechanism for the localization of Mklp2 and the CPC to the spindle midzone

Efficient localization of the Mklp2/CPC complex to the spindle midzone requires inactivation of Cdk1 and the stabilization of MTs. Hence, these two events need to be intimately linked to ensure proper midzone localization of the Mklp2/CPC complex. We speculate that the kinase Aurora B, integral member of the CPC and known regulator of MT dynamics (Andersen et al., 1997; Gadea and Ruderman, 2006; Ohi et al., 2004; Ruchaud et al., 2007), could be the potential regulator of MT dynamics at the spindle midzone in anaphase. Supporting this hypothesis, we could show that the localization of the Mklp2/CPC complex in cells

undergoing monopolar cytokinesis is dependent on the kinase activity of Aurora B (Figure 24). While other possibilities (e.g. phosphorylation of Mklp2, regulation of other recruiting factors etc.) are plausible, several observations support the idea that the absence of stable MTs could account for this defect. First, we showed that the Mklp2/CPC complex requires stable MTs for its localization (Figure 22). Second, it has been shown that under these experimental conditions, MTs are shorter and appear less stable when Aurora B is inhibited (Hu et al., 2008). Third, MTs are instable in the absence of Aurora B kinase activity during mitosis (Adams et al., 2001b; Gassmann et al., 2004) and depletion of the CPC by RNAi results in a disorganized central spindle with MTs that are much more sensitive to MT depolymerizing agents (Chen et al., 2006; Giet and Glover, 2001). And fourth, the MT depolymerase MCAK is specifically phosphorylated at the central spindle and thus inactivated by Aurora B (Fuller et al., 2008) and Op18, a MT stabilizing protein, is absent from the central spindle after depletion of the CPC by RNAi (Chen et al., 2006). We propose that the activity of Aurora B ensures proper localization of the Mklp2/CPC complex to the spindle midzone in anaphase by stabilizing MTs in this region. This suggests that a positive feedback loop, initiated by the drop in Cdk1 activity and maintained by the activity of Aurora B, is required proper midzone localization of the Mklp2/CPC complex (Figure 39). This in turn may explain, why the transfer of the CPC form the centromeres (metaphase) to the MTs of the spindle midzone (anaphase) occurs without any detectable intermediate localization (e.g. cytoplasm or other MTs). Notably, a similar feedback mechanism has been proposed for the local control of Aurora B activity in anaphase (Fuller et al., 2008). It will be interesting to see in the future if elucidation of mechanistic details provides the missing evidence for this model.
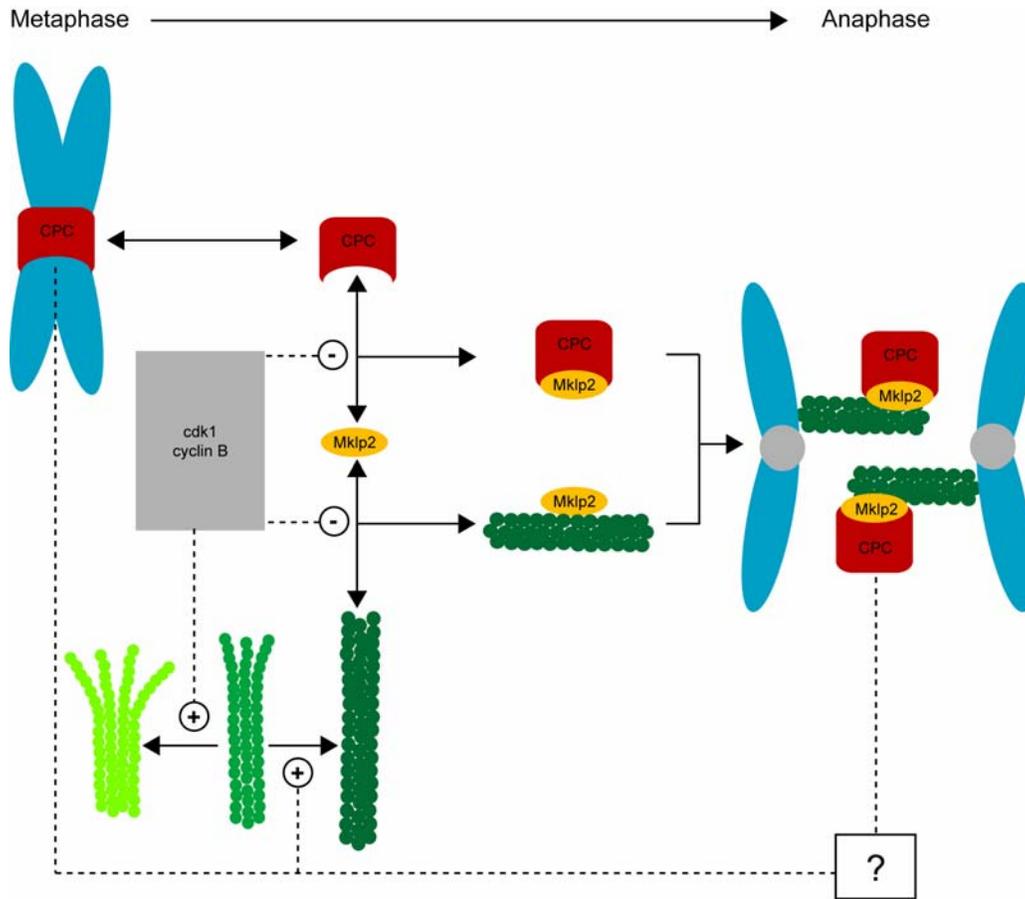
Figure 39. Proposed model for the localization of Mklp2 and the CPC to the spindle midzone.

1.8 The role of stable MTs in cleavage furrow positioning

The position of the cleavage furrow and its activation have to be tightly coupled to chromosome segregation in space and time in order to ensure genomic integrity of the forming daughter cells. But up to date, 40 years after Rappaport proposed for the first time that the position of the mitotic spindle determines the site of the future cleavage furrow, it remains under debate, which part of the spindle transmits the signal – the central spindle or the spindle poles. Even though our work did not aim in solving this important question, analyses of cells undergoing monopolar cytokinesis revealed novel hints for the underlying molecular mechanism. In contrast to an unperturbed situation, cleavage furrow positioning in cells undergoing monopolar cytokinesis occurs in the absence of a bipolar mitotic spindle and polar extrusions, reminiscent of the cleavage furrow, are formed (Hu et al., 2008). Since in this experimental setup the proposed signal modules, astral MTs and chromosomes, are initially uniformly radial, and antiparallel MTs of a spindle midzone are absent, neither of this modules alone can be sufficient for the initiation of this process (Figure 40). In contrast, the presence of MTs is absolutely essential, since these polar extrusions were not formed in the

presence of nocodazole (Figure 24). The Mklp2/CPC complex binds to stable MT plus ends and therefore, can be used as a marker to discriminate between different subsets of MTs (see above). Using this readout, we could show that the position of the cleavage furrow correlated with the existence of stable MTs underneath the cell cortex (Figure 24). It has been also shown, that taxol-stabilized MTs are sufficient for the induction of a cleavage furrow (Shannon et al., 2005). Hence, it is plausible to speculate that these MTs underneath the cell cortex are rather cause than consequence of the cleavage furrow positioning process. We further hypothesize that these stable MTs are created by an Aurora B dependent mechanism as described above. Supporting this hypothesis, inhibition of Aurora B resulted in the absence of stable MTs as determined by the delocalization of the Mklp2/CPC complex (Figure 24). Consequently, cleavage furrow formation and cell polarization is abolished (Hu et al., 2008).

In order to close the gap between stable MTs and the initiation of the cleavage furrow, a signal has to be transmitted from these specific types of MTs towards the cell cortex. This mechanism is possibly carried out by the centralspindilin/Ect2 complex that integrates directed movement along MTs via the kinesin subunit Mklp1, and stimulation of RhoA activity via an interplay between MgcRacGAP and Ect2 (Glotzer, 2005; Miller and Bement, 2009; Mishima et al., 2002). Interestingly, the localization of the centralspindelin complex to the spindle midzone is dependent on the kinase activity of Aurora B (Giet and Glover, 2001; Hauf et al., 2003; Hu et al., 2008). But up to now, no Aurora B phosphorylation site on any of the members of the centralspindelin complex has been reported that could explain this dependency. While it remains possible that the critical phosphorylation site has not been identified yet, it is also tempting to speculate that in analogy to Mklp2, the absence of stable MTs after inactivation of Aurora B might account for this defect.

However, despite stable MTs could be a sufficient source for the initiation of the cleavage furrow, the radial symmetry of a monopolar spindle would not allow creating one preferential position and therefore, a brake in the symmetry has to occur. Indeed, initiation of the cleavage furrow in cells undergoing monopolar cytokinesis is accompanied with a brake in the spindle symmetry (Hu et al., 2008). Symmetry braking typically requires a positive feedback loop to amplify a small initial signal. It was initially proposed that this feedback loop may operate from the cell cortex to MT organization (Hu et al., 2008). Alternatively or in addition, the feedback mechanism, required for the localization of Aurora B to stable MT plus-ends, may act as signaling module for the initiation of cleavage furrow formation. After a random small initial asymmetry, the Mklp2/CPC complex auto-amplifies its local concentration by stabilizing MTs in a defined area (Figure 40). These MTs in turn increase the local concentration of the centralspindelin complex and cleavage furrow formation could occur.

Since normal dividing cells are asymmetric, this brake in the symmetry is not required for cleavage furrow positioning. But since chromosomes and the CPC are positioned at the equatorial plane during metaphase, the proposed feedback mechanism would be sufficient to maintain the position of the CPC between the separating chromosomes and subsequently define the exact position of the cleavage furrow. It will be interesting to see in the future if this model appears to be valid.
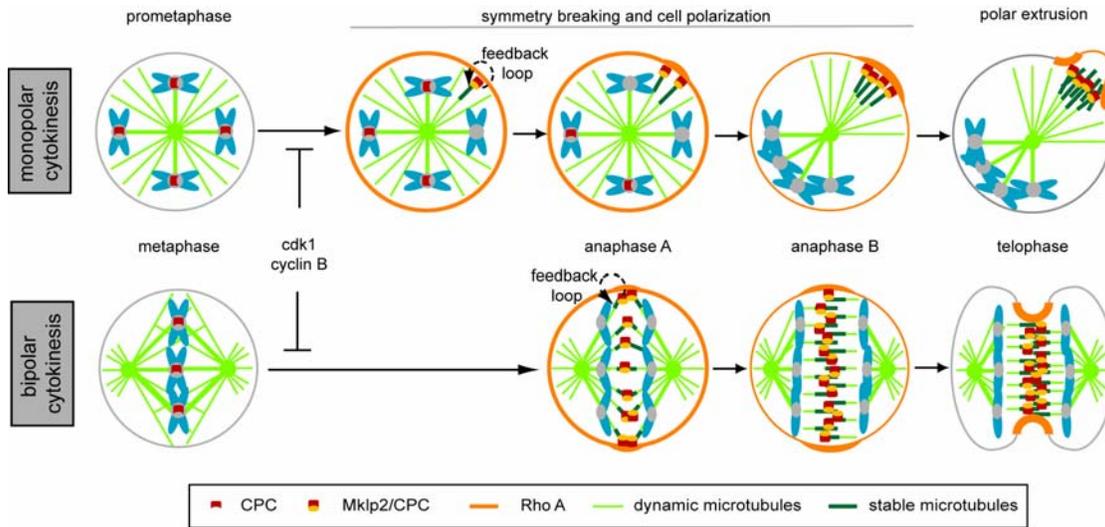
Figure 40. Comparison between proposed models for monopolar and bipolar cytokinesis.

2 The function of Mklp2 in late cytokinesis

Mklp2 is essential for the localization of the CPC to the central spindle upon anaphase onset. While the requirement of the CPC for the completion of cytokinesis has been intensively studied, the role of the Mklp2-mediated localization of the CPC in its function during cytokinesis remains far less understood.

To study more in detail the function of Mklp2 in cytokinesis, we depleted the protein from HeLa cells by RNAi. In contrast to previous reports, describing an early defect in cytokinesis after depletion of Mklp2 by RNAi (Neef et al., 2003), we could only observe a late defect in cytokinesis. Notably, a remaining amount of Mklp2 could always be detected at the spindle midzone in late cytokinesis following our RNAi protocol with two different RNAi oligos (including the previously published one (Neef et al., 2003)). Thus, an incomplete depletion of Mklp2 by RNAi may account for the different phenotypes, although it remains to be addressed if indeed the remaining amount of Mklp2 would be sufficient to fulfill the early functions of Mklp2 in cytokinesis. None the less, we could observe a robust defect in late cytokinesis (Figure 25.C) and concentrated our efforts in elucidating the function of Mklp2 in this late stage.

The IF vimentin was reported to be a critical target of Aurora B in cytokinesis. Phosphorylation of the filament by Aurora B induces its depolymerization and ensures equal segregation into the newly formed daughter cells (Goto et al., 2003; Izawa and Inagaki, 2006; Yokoyama et al., 2005). Interference with the kinase activity of Aurora B by small molecule inhibitor (ZM447439) resulted in IF bridges in between the separating cells, in agreement with the proposed role of Aurora B regulating the filament status of vimentin (Figure 26.A). However, it remained to be addressed if this is dependent on the Mklp2-mediated localization of the CPC. Strikingly, depletion of Mklp2 by RNAi resulted in filament bridges in-between the separating cells, accompanied with a failure in late cytokinesis (Figure 26). Analyses of INCENP-depleted cells, expressing GFP-INCENP[T59E], unable to bind to Mklp2 and as a consequence unable to transfer to the central spindle (see above), revealed the same defects (Figure 27). According to this data, we conclude that the Mklp2-mediated localization of the CPC at the spindle midzone might guarantee the depolymerization of the IF vimentin and therefore, proper segregation of the filament into the newly formed daughter cells.

Notably, these filaments are still phosphorylated by Aurora B at S72 as judged by staining with the phospho-specific antibody (pS72) recognizing this epitope (Figure 26). Since we observe filamentous structures, phosphorylation of vimentin seems to still occur, but depolymerization of the filament does not take place. In control cells pS72 positive filamentous structures are visible at the cortex, adjacent to the bulk of Aurora B at the central spindle. It is possible that after depletion of Mklp2 the remaining amount of Aurora B at the spindle midzone is still able to phosphorylate vimentin to a degree, which is not sufficient to

induce depolymerization, comparable to the phosphorylation of vimentin in the cortex region of control cells.

Further supporting our hypothesis, we observed a co-localization of vimentin and Mklp2 in the absence of INCENP (Figure 27.D), suggesting that Mklp2 might provide a direct link between the kinase Aurora B and the substrate vimentin. Such a physical link between the kinase Aurora B and its substrates is known for the members of the CPC complex (i.e. INCENP (Honda et al., 2003)), but has not been described for any other substrate and might explain the special requirement for Mklp2 in the phosphorylation of vimentin by Aurora B.

Unexpectedly, the requirement for Mklp2 in late cytokinesis correlates with the presence of vimentin in different cell lines. Mklp2 depletion results in a failure in cytokinesis in vimentin positive HeLa cells, but not in the vimentin negative MCF-7 cells (Figure 28). These results suggest that vimentin is the critical target of the Mklp2/CPC complex in late cytokinesis.

Among the other known substrates of Aurora B in cytokinesis, the centralspindlin complex is the most prominent one. Studies in different organisms revealed that the kinase activity of Aurora B is required for the localization of the complex to the central spindle (Giet and Glover, 2001; Hauf et al., 2003; Severson et al., 2000). However, the mechanistic details remain elusive, since particularly none of the identified phosphorylation site(s) on any of the members could explain a direct regulation by phosphorylation. However, the kinase activity of Aurora B is also important for the function of Mklp1 in late cytokinesis by other means than regulating the localization. Analyses of the reported phosphomutants of Mklp1 S802A and S911A, revealed that despite their localization at the central spindle, they failed to support cytokinesis (Guse et al., 2005; Neef et al., 2006). Phosphorylation of S911 in particular, is required to prevent premature import of Mklp1 in the nucleus before the completion of cytokinesis (Neef et al., 2006). Importantly, phosphorylation of S911 on Mklp1 by Aurora B is the only other reported case, besides our findings on vimentin, where the function of Aurora B in cytokinesis depends on its Mklp2-mediated localization. Accordingly, it has been proposed that the cooperation between Mklp2 and Mklp1 is required for the control of late stages of cytokinesis. Since both Mklp2-mediated functions of Aurora B, regulation of vimentin and Mklp1, are essential for normal progression through cytokinesis in HeLa cells, it appears surprising that depletion of Mklp2 in MCF-7 cells does not result in a failure in cytokinesis. We showed that the absence of vimentin from MCF-7 cells correlates with the different requirements for Mklp2 in late cytokinesis (Figure 28). In contrast, Mklp1 is essential for cytokinesis in MCF-7 cells (Figure 28) but the Mklp2-mediated function of Aurora B that prevents premature nuclear import of Mklp1, seems to be dispensable. Therefore, it needs to be explored in the future, how nuclear import of Mklp1 is prohibited in MCF-7 cells to ensure normal progression through cytokinesis. In addition, it will be necessary to provide direct evidence that vimentin is the major downstream target of Mklp2 in late cytokinesis in order to

rigorously rule out that the different requirements for Mklp2 in HeLa and MCF-7 cells are due to other means than the presence of vimentin.

It is interesting to note, that Mklp2 mutants in *D. melanogaster*, do not fail in cytokinesis, even though the transfer of the CPC to the central spindle is impaired, and mutants of the CPC are defective in cytokinesis (Cesario et al., 2006; Jang et al., 2005). In line with our findings in human cells, showing that the requirement for Mklp2 in late cytokinesis correlates with the presence of vimentin (Figure 28), no genes for cytoplasmic IFs (including vimentin) can be detected in the whole genome of *D. melanogaster* (Karabinos et al., 2001). In contrast to this, but in agreement with our findings in MCF-7 cells, the homolog of Mklp1 (Pav) has been shown to be essential for cytokinesis also in *D. melanogaster* (Adams et al., 1998). Future experiments will clarify if nuclear import of Pav is not essential for cytokinesis or if the regulatory mechanism controlling the nuclear import of Mklp1 is specific for vertebrates as previously suggested (Neef et al., 2006). In any case, the presence of vimentin correlates with the requirement for Mklp2 in late cytokinesis, even across different organisms.

To confirm in the future the interplay between Mklp2 and vimentin, it might be particularly important to verify that Mklp2 can indeed act as bridging module between the kinase Aurora B and the substrate vimentin, since this has not been described for any other Aurora B substrate and might explain the special requirement of Mklp2 for this function.

3 Small molecule inhibitors for cytokinetic kinesins

High temporal resolution, achieved by instantaneous activity and reversibility, is a key feature of small molecules. The process of cell division in turn, is highly dynamic. Targeting cell division specific protein functions with small molecule inhibitors would permit the study of such a highly dynamic process with the required temporal resolution. Since the role of several kinesins in cell division has been reported, we aimed to identify small molecule inhibitors for mitotic kinesins.

We applied a reverse chemical genetics approach to identify novel small molecule inhibitors of Eg5. Using this approach, we identified several small molecule inhibitors that selectively inhibited the ATPase activity of Eg5 *in vitro* and cause a mitotic arrest phenotype *in vivo* (Figure 29). Since monastrol was identified in a forward chemical genetics approach, the identification of novel Eg5 inhibitors in a reverse chemical genetics approach validated this method for the identification of small molecule inhibitors for other kinesins. Out of the novel identified inhibitors we focused on the group of VS compounds, derivates of monastrol. Based on the initial data set, a structure activity relation (SAR) study was used to generate a sublibrary of VS compounds, which were tested for the inhibition of Eg5 *in vitro* and *in vivo*. Out of these compounds, we identified VS-83 as a novel Eg5 inhibitor that is 20 times more potent than monastrol (Figure 30 and Figure 31). Due to this increase in the potency, VS-83 is now routinely used for the studies of mitotic cells with an intact MT network.

Using a similar reverse chemical genetics approach, we next aimed to identify novel inhibitors for kinesins with a function in cytokinesis. We uncovered four bioactive molecules (SH1-4), which induced a binucleated phenotype *in vivo* and inhibited the kinesins Mklp2 and MPP1 *in vitro* (Figure 32 and Figure 33). Furthermore, we could show that target independent cellular functions were not affected by SH1, approving a selective mode of action *in vivo* (Figure 34). However, in contrast to the mono-specific inhibitors of Eg5, a similar selectivity towards only one kinesin could not be achieved. This difference might be explained by the fact that there are three closely related kinesin-6 family members while Eg5 as the only member of the Kinesin-5 family has unique structural features. In addition, monastrol binds to a region in the motor domain of Eg5 that is not found in any other kinesin (Yan et al., 2004) (Figure 35.A). We could also identify a region in the motor domain of the kinesin-6 family that increases the sensitivity of Mklp2 and MPP1 for the SH compounds (Figure 35). However, this extension even though not being highly conserved in the primary sequence, is found in all members of this family (Miki et al., 2005) (Figure 35.A). Thus, in contrast to the unique properties of Eg5, the existence of more than one kinesin in the same family might hamper the identification of a mono specific inhibitor. On the other hand, the inability of these compounds to inhibit Mklp1 *in vitro*, which we could restore by replacing its family specific extension with the one of Mklp2 (Figure 35.F and Figure 35.G), implies that

specific structural features, equally present in Mklp2 and MPP1 but absent from Mklp1, account for the mode of action of SH inhibitors. Based on these data, it seems possible to increase the selectivity towards one kinesin in the future, since also the kinesin-6 specific extension in the motor domain of MPP1 and Mklp2 significantly differ from each other in their length and amino-acid composition. Furthermore, treatment of cells with SH inhibitors resulted in a late failure in cytokinesis and consequently the formation of binucleated cells (Figure 33). This correlated with the phenotype after depletion of Mklp2 but not MPP1 by RNAi in HeLa cells (Figure 36). Although, we can not rigorously rule out that the complete absence of MPP1 (i.e. knock-out mouse) would result in a similar phenotype, it currently appears unlikely that MPP1 is the target of SH drugs *in vivo*. In addition, analyses of the phenotype after treatment of HeLa and MCF-7 cells with SH compounds revealed that while SH1 is active in both cell lines, SH2 is only able to induce a binucleated phenotype in HeLa cells (Figure 37). This correlates well with the depletion of Mklp2 by RNAi, which only causes a cytokinesis failure in HeLa but not in MCF-7 cells (Figure 28). These results clearly strengthen the argument that Mklp2 is the critical target of SH2 *in vivo*. It remains to be clarified though, whether Mklp2 is indeed not essential for cytokinesis in MCF-7, which can be only proven by a stable knock-out. Finally, we did not observe a difference in the localization of Mklp2 after treatment with SH compounds (Figure 38). This is reminiscent to the observation that the localization of Eg5 is not affected after inhibition of its motor activity by monastrol. On the other hand, mutation of critical residues in the motor domain of Mklp2, resulting in the inactivation of the ATPase activity, clearly affected the localization to the central spindle (Figure 14). This might be explained by the different modes of inactivation of Mklp2s motor activity by small molecules or mutations. Since it also remains unaddressed how motor dead versions of Eg5 are localized in the RNAi background, this hypothesis remains to be proven. Thus, future work will confirm that Mklp2 is the target of SH2 compounds *in vivo,* and will validate this compound as a molecular tool for the study of cytokinesis.

In addition to its use a small molecule inhibitor of Mklp2, SH2 could be also a novel tool to study the function of other mitotic kinesins. We could show that replacement of the kinesin-6 specific extension in Mklp1 with the one from Mklp2, sensitizes Mklp1 for the inhibition by SH compounds (Figure 35.F and Figure 35.G). In a similar approach to the one invented by Kevin Shokat (Bishop et al., 2000), we could place this extension in other kinesins to make them sensitive to the compounds. This would allow the study of other mitotic kinesins during early mitosis. In the first step to validate this method, we engineered different version Eg5 that contain the kinesin-6 specific extension of Mklp2 and we are currently testing if SH compounds can inhibit the ATPase activity of this chimeric proteins *in vitro* and more importantly, if they can induce a monoaster phenotype *in vivo*.

Beyond its use as molecular tool, a selective inhibitor for Mklp2 could be also of great interest for the treatment of cancer. The broadly used MT toxins like taxol affect all proliferating cells and consequently, treatment with this drug is accompanied with a broad number of side effects. Furthermore, it appears unlikely that the novel generation of drugs, including inhibitors for mitotic kinases (such as Aurora and Plk) as well as mitotic kinesins (Eg5) may greatly improve this problem, since all this target proteins are essential for mitosis. Our above presented data imply that the function of Mklp2 depends on the cell type and correlates with the presence of vimentin in these cells. Interestingly, the expression of vimentin in non mesenchymal cells, such as epithelial cells, is one of the hallmarks of epithelial–mesenchymal transition (EMT), which in turn is implicated in tumor progression (Kokkinos et al., 2007). Thus, a selective Mklp2 inhibitor would allow targeting a subset of mitotic cells that are relevant for tumor progression.

Materials and Methods

1 Chemicals and buffers

Chemicals were at least of purity grade p.a. (*pro analysi*) and were purchased from Merck, Sigma-Aldrich, Fluka, or Roth, unless otherwise specified. Buffers and solutions were prepared with deionized water from a Milli-Q system (Millipore) which will be referred to as H_2O. Buffers and solutions were either autoclaved or filtered before use. Standard buffers are PBS (137 mM $NaCl_2$, 2.7 mM KCl_2, 10.2 mM Na_2HPO_4, 1.8 mM KH_2PO_4, pH 7.4) and TBS (10 mM Tris-HCl pH 7.6, 150 mM $NaCl_2$).

2 Cloning procedures

All constructs used in this study were PCR-amplified from a human testis cDNA library (Invitrogen). All used primers contain a restriction site for either FseI (5´) or AscI (3´). The amplified cDNAs and fragments thereof were cloned and subcloned, if not otherwise stated, into plasmids harboring engineered FseI and AscI restriction sites at the 5' and 3' end, respectively. All constructs were confirmed by sequencing at the MPI in-house DNA sequencing facility. Deletion constructs of Mklp1, Mklp2 and MPP1 (kinesin-6 extension) were generated as follows: the two DNA strands, flanking the region to delete, were PCR amplified with primers containing the sequence for the restriction sites of either FseI and Xho1 (5` and 3`) or Xho1 and Asc1 (5´ and 3`) Both fragments were first cloned separately in the pCS2-Myc-F/A plasmid (containing restriction sites for Fse1, Asc1 and Xho1) and finally subcloned into one plasmid using either the Fse1/Xho1 or the Xho1/Asc1 restriction sites. For the insertion of the kinesin-6 specific extension, this region was PCR amplified with primers containing the restriction site for Xho1 and was subcloned either at the Xho1 restriction-site of a deletion construct (other kinesin-6 family member) or at a newly generated Xho1 restriction site in the desired region of another kinesin. Nucleotide exchanges were performed by site directed mutagenesis using the QuickChange kit (Stratagene). All cloning procedures were performed according to the standard techniques as described in *Molecular Cloning, A Laboratory Manual*, 2nd Edition, Sambrook, J., Fritsch, E.F., Maniatis, T., Cold Spring Harbor Laboratory Press 1989 and *Current Protocols in Molecular Biology*, Wiley, 1999. The following standard molecular biology techniques have been used: 1) Plasmid DNA was usually purified from the *E. coli* strain TG1 using the Qiagen Mini kit according to the manufacturer's instructions. 2) DNA fragments were isolated from agarose gels using the Qiagen gel elution kit according to manufacturers' instructions. 3) Restriction digests were carried out as recommended by the suppliers (New England

Biolabs). 4) Ligation reactivons were done using T4 DNA Ligase (NEB) or using the Rapid Ligation Kit (Roche) as described by the manufacturers' instructions. 5) Polymerase chain reaction (PCR) was carried out using Pfu Turbo polymerase PCR system was used as recommended by the manufacturer (Stratagene) and reactions were carried out in a Perkin Elmer GeneAmp PCR System 9600. All DNA modifying enzymes including Klenow polymerase, T4 PKN kinase and calf-intestinal phosphatase were used from NEB according to manufacturers' instructions.

Table 1. List of primers used to clone cDNAs and fragments thereof for this study.

number	gene	sequence	purpose	comment
TUM 381	Mklp2	attaggccggcccatgtcgcaagggatcctttctcc	cloning	5' full length
TUM 382	Mklp2	attaggcgcgccgcatgcacaagctggctagc	cloning	3' motordomain
TUM 493	Mklp2	attaggcgcgcctacttttttgccaaaagg	cloning	3' full length
TUM 398	Mklp2	tatggagtcactaactcagggacagcccacacgattcaaggtac	mutagenesis	walker A: GKT to GTA
TUM 399	Mklp2	gtaccttgaatcgtgtgggctgtccctgagttagtgactccata	mutagenesis	walker A: GKT into GTA
TUM 400	Mklp2	tatggagtcactaactcagcggcagcccacacgattcaaggtac	mutagenesis	walker A: GTA into AAA
TUM 401	Mklp2	gtaccttgaatcgtgtgggctgccgctgagttagtgactccata	mutagenesis	walker A: GTA into AAA
TUM 623	Mklp2	gatctggctggctcagcgcgctgcaaagatcag	mutagenesis	switch II: E 413 to A
TUM 624	Mklp2	ctgatctttgcagcgcgctgagccagccagatc	mutagenesis	switch II: E 413 to A
TUM 474	Mklp2	gacagcaagttgactcgcgtgttccaaggtttcttc	mutagenesis	mutation of Xho1 site
TUM 475	Mklp2	gaagaaaccttggaacacgcgagtcaacttgctgtc	mutagenesis	mutation of Xho1 site
TUM 472	Mklp2	attactcgagaacattcgcttctccatctg	cloning	Deletion of Mklp2 loop
TUM 473	Mklp2	attactcgaggccttggaggctattgaag	cloning	Deletion of Mklp2 loop
TUM 483	Mklp2	attactcgagcaacttcatccaacacctg	cloning	cloning of Mklp2 loop
TUM 484	Mklp2	attactcgagtgccgggacaggtagtgg	cloning	cloning of Mklp2 loop
TUM 203	MPP1	attaggccggccaatggaatctaattttaatcaag	cloning	5' full length
TUM 204	MPP1	attaggcgcgcctcgtcttccatcaaatcttc	cloning	3' motordomain
TUM 346	MPP1	attaggccggccagatgtatcactagacagtaattc	cloning	5' after motordomain
TUM 374	MPP1	attaggcgcgccgatgtctcaagctcttgaatc	cloning	3' until coiled coil 2
TUM 466	MPP1	attactcgagagtataaaattttctgtgtgg	cloning	Deletion of MPP1 loop
TUM 467	MPP1	attactcgagttcttgaagactatcaaataatac	cloning	Deletion of MPP1 loop
TUM 478	MPP1	attactcgagattagccatattcaagttgg	cloning	cloning of MPP1 loop
TUM 479	MPP1	attactcgagagactgtatacaaagatgaacc	cloning	cloning of MPP1 loop
TUM 404	Mklp1	attaggccggcccatgaagtcagcgagagc	cloning	5' full length
TUM 405	Mklp1	attaggcgcgccttgtctacaggtcttgctac	cloning	3' motordomain
TUM 476	Mklp1	attactcgagtgaccctatactgttaaag	cloning	Deletion of Mklp1 loop
TUM 477	Mklp1	attactcgaggatagtgtctatggtg	cloning	Deletion of Mklp1 loop
TUM 176	Eg5	attaggccggcccatggcgtcgcagccaaatt	cloning	5' full length
TUM 177	Eg5	attaggcgcgccagtttctgattcacttcaggct	cloning	3' motordomain
TUM 188	KIF4	attaggccggcccatgaaggaagaggtgaaggg	cloning	5' full length
TUM 189	KIF4	attaggcgcgcctgtagcaacaagacttgtagc	cloning	3' motordomain
TUM 201	CenpE	attaggccggccgatggcggaggaaggagccg	cloning	5' full length
TUM 202	CenpE	attaggcgcgcctctatctcacttaatgtatc	cloning	3' motordomain
TUM 229	MCAK	attatggccggccaatggccatggactcgtcgc	cloning	5' full length
TUM 230	MCAK	attatggcgcgcctggggccgtttcttgctgc	cloning	3' motordomain
TUM 254	KIF5A	attggccggccaatggcggagactaacaacgaatgc	cloning	5' full length
TUM 255	KIF5A	attggcgcgccatggatgagttgtcattcacagg	cloning	3' motordomain

TUM 304	KIF5B	attaggccggccgatggcggacctggccgagtgc	cloning	5' full length
TUM 307	KIF5B	attaggcgcgccgccactgaatagtgttccgcagg	cloning	3' motordomain
TUM 739	INCENP	attaggccggcccatggggacgacggccccaggg	cloning	5' full length
TUM 740	INCENP	taatggcgcgcctcagtgcttcttcaggctgtagg	cloning	3' full length
TUM 746	INCENP	gccagagctgatgcccaaagaaccttctcagaagaaccgac	mutagenesis	T59E
TUM 747	INCENP	gtcggttcttctgagaaggttctttgggcatcagctctggc	mutagenesis	T59E
TUM 882	INCENP	gccagagctgatgcccaaagtaccttctcagaagaaccgac	mutagenesis	T59V
TUM 883	INCENP	gtcggttcttctgagaaggtactttgggcatcagctctggc	mutagenesis	T59V

Table 2. List of plasmids engineered for this study:

number	gene	insert	insert specfication	vector	tag
TUM 718	Mklp2	wt, fl		pCS2-GFP-F/A	GFP
TUM 719	Mklp2	mut, fl	Walker A: GKT to AAA	pCS2-GFP-F/A	GFP
TUM 873	Mklp2	mut, fl	Switch II: E413A	pCS2-GFP-F/A	GFP
TUM 726	Mklp2	wt, ct	508-890	pCS2-GFP-F/A	GFP
TUM 727	Mklp2	wt, nt	1-508	pCS2-GFP-F/A	GFP
TUM 581	Mklp2	wt, nt	1-508	pQE80-His-F/A	His
TUM 684	Mklp2	mut, nt	1-508, Xho1 side mutated	pQE80-His-F/A	His
TUM 686	Mklp2	mut, nt	1-508, delta 193-295	pQE80-His-F/A	His
TUM 332	MPP1	wt, nt	1-533	pQE80-His-F/A	His
TUM 681	MPP1	mut, nt	1-533, delta 185-265	pQE80-His-F/A	His
TUM 547	MPP1	wt, ct	501-715	pQE80-His-F/A	His
TUM 600	Mklp1	wt, nt	1-444	pQE80-His-F/A	His
TUM 688	Mklp1	mut, nt	1-444, delta 146-212	pQE80-His-F/A	His
TUM 710	Mklp1	mut, nt	1-444, delta 146-212, plus MPP1 185-265	pQE80-His-F/A	His
TUM 733	Mklp1	mut, nt	1-444, delta 146-212, plus Mklp2 193-295	pQE80-His-F/A	His
TUM 224	Eg5	wt, nt	1-371	pQE80-His-F/A	His
TUM 345	KIF4	wt, nt		pQE80-His-F/A	His
TUM 346	CenpE	wt, nt		pQE80-His-F/A	His
TUM 415	MCAK	wt, fl		pQE80-His-F/A	His
TUM 417	KIF5A	wt, nt		pQE80-His-F/A	His
TUM 413	KIF5B	wt, nt		pQE80-His-F/A	His
TUM 1118	INCENP	wt, fl		pCS2-GFP-F/A	GFP
TUM 1119	INCENP	mut, fl	T59E	pCS2-GFP-F/A	GFP
TUM 1242	INCENP	mut, fl	T59V	pCS2-GFP-F/A	GFP

3 Purification of His-fusion proteins from *E. coli*

The constructs for polyhistidine-tagged fusion proteins were expressed in JM109[RIL] cells and bacteria were grown at 37°C in LB-media to OD 0.5 before inducing with 0.5 mM IPTG for 15 hours at 18°C. Cells were harvested by centrifugation (3000g, 30min, 4°C) and the cell pellet was re-suspended (25 mM Tris-HCl pH 7.8, 5 mM Imidazole, 300 mM $NaCl_2$, 0.2 % Triton-X-100 and protease inhibitors (Roche)). Cells were lysed by high pressure treatment in a french-press-apparatus and the lysate was clarified by centrifugation at 25000 rpm for 30 min at 4 °C. His-fusion proteins were then affinity purified using $Ni2^+$NTA resins (Quiagen) (0.25 - 0.5 ml resin per liter culture). Beads were incubated for 2 h at 4 °C, washed with 100 - 200

resin volumes (25 mM Tris-HCl pH 7.8, 20 mM Imidazole, 300 mM $NaCl_2$, 0.2 % Triton-X-100) ("batch-washing") and eluted (25 mM Tris-HCl pH 7.8, 200 mM Imidazole, 300 mM $NaCl_2$) in fractions of one resin volume. Fractions containing the eluted proteins were pooled, dialyzed (20 mM Tris-HCl at pH 7.4, 300 mM $NaCl_2$, 10 mM β-mercaptoethanol and 10 % glycerol) and flash frozen and stored at - 80°C. For the purification of kinesin motor domains, all buffers contained 1 mM ATP and 5 mM $MgCl_2$.

4 Purification of tubulin and generation of stabilized MTs

4.1 Purification of tubulin from pig brains

Tubulin was purified from pig brain. Pig brains were purchased from a local slaughter. Pig brains (about 1kg; 50 brain-halves) were transported in ice cold PBS. Brains were cleaned at 4 °C by removal of blood vessels and meninges. Brains were collected in DB-buffer (50 mM MES pH 6.6, 1 mM $CaCl_2$) in a 1:1 ratio (w/v). Brains were homogenized in a mixer and homogenate was cleared by centrifugation (29000 g, 1h, 4 °C). The supernatant (SN) was supplemented with one volume glycerol and one volume pre-warmed (37 °C) HMPB-buffer (1 M K-Pipes pH 6.8, 10 mM $MgCl_2$, 20 mM EGTA). To this suspension, 1.5 mM ATP and 0.5 mM GTP was added. MTs were polymerized at 37 °C in a water bath for 1 h and pelleted at 150000 g for 30 min at 37 °C. The MT pellet was re-suspended in ice cold DB buffer (1/10 of volume used for the homogenization) and kept at 4 °C for 30 min and the suspension was cleared by centrifugation (70000 g, 30 min 4 °C). The supernatant was again supplemented with one volume glycerol, one volume MMPB, 1.5 mM ATP and 0.5 mM GTP and incubated in a water bath for 30 min at 37 °C. The polymerized tubulin was pelleted at 150000 g for 30 min at 37 °C and the pellet was re-suspended in ice cold BRB80 (80 mM K-Pipes, pH 6.8, 1 mM $MgCl_2$ and 1 mM EGTA) and homogenized by douncing on ice for 30 min. The homogenate was cleared by centrifugation (100000 g, 30 min, 4 °C) and the tubulin containing supernatant was separated. The tubulin concentration was determined by measuring the absorbance at 280 nm in BRB80 using the extension coefficient of (ε=115000 $M^{-1}cm^{-1}$). The concentration of the purified tubulin was adjusted to 10 mg/ml, aliquoted, snap frozen and stored at - 80 °C.

4.2 Preparation of taxol-stabilized MTs

Tubulin, purified as described above, was cleared by centrifugation (20000 g, 4 °C, 10 min), supplemented with 25 % Glycerol in BRB80 and 1 mM GTP and polymerised for 30 min at 37 °C. After addition of 40 µM taxol, MTs were polymerised for additional 30 min and pelleted in an ultracentrifuge (90000g, 30 min, 30 °C). The pellet was resupended in BRB80

containing 25 µM taxol and the concentration of tubulin in the stabilized MT suspension was determined by measuring the absorbance at 280 nm in 6 M guanidine-HCl using an extinction coefficient of (ε=115000 M^{-1}cm^{-1}).

5 Antibodies

5.1 Antibody production

For generating rabbit polyclonal antibodies against human kinesins, His-fusion proteins expressed in *E. coli* as described above (section 3) were used as antigens. The following antigens were used: Mklp2 (His-Mklp2 (aa 1-508) for rabbit # 1375), Mklp1 (His-Mklp1 (aa 1-444) for rabbit # 1378), MPP1 (His-MPP1 (aa 1-533) for rabbit # 1416 and His-MPP1 (aa 501-715) for rabbit # 1518).

After purification of the His-fusion proteins, soluble protein was obtained by centrifugation (20000 g, 10 min, 4 °C) and the purity and concentration of the protein preparation was controlled by SDS-PAGE and Coomassie staining. The concentration of the soluble, pure His-fusion proteins was at least 0.5 mg/ml.

These fusion proteins were then used for the immunization of New Zealand white rabbits (animal facility, MPI). Before immunization, test blood was obtained from each rabbit to exclude rabbits whose serum showed inespecific signal. Blood was first kept for 1 - 2 h at RT and then stored overnight at 4 °C. Serum was cleared by centrifugation (3000 g, 30 min, 4 °C) and supernatant was supplemented with 0.02 % sodium azide and stored at 4 °C. Serum was tested by western blot analyzes (20 µg total HeLa cell extract) and by immunofluorescene of asynchronously growing cells processed as described below. Serum was tested at different dilutions (1:300, 1:1000, 1:3000). For the first immunization, 250 µg antigen in a total volume of 500 µl were used (dilution with PBS) and a emulsion with 500 µl Titermax Gold adjuvant (Sigma) was prepared in the following way. Two disposal syringes with 250 µl protein solution and 500 µl adjuvants were prepared and connected by an adaptor module. The antigen-adjuvant emulsion was prepared by mixing forth and back for 10 min. Additional 250µl protein solution was uptaken in a syringe and mixed with the emulsion for further 10 min. For the following injections, 100 µg antigen in a total volume of 500 µl and 500 µl Freunds adjuvant (Sigma) were used and emulsion was prepared as described above. Routinely, rabbits were injected 3 - 4 times after the initial injection and injections were done every 4 weeks. Test blood was obtained from each rabbit 10 days after the injection (1 ml) and processed as described above. Serum was tested at different dilutions (1:300, 1:1000, 1:3000) by Western blot analysis (1 - 100 ng recombinant protein and 20 µg HeLa cell extract from mitotic and asynchronies cells) as well as by immunofluoresence (asynchronously growing HeLa cells, processed as described below). 10

days after the last injection, final bleed was obtained and processed as described above. Serum was aliquoted (2 ml), snap frozen and stored at - 80 °C.

5.2 Antibody purification

Antibodies were affinity purified from the desired serum over a HiTrap NHS activated sepharose column (1 ml column volume, Amersham Biosciences) coupled to the antigen. The antigen was dissolved in amid-free buffer (typically storage buffer: 20 mM HEPES pH 8.3, 300 mM $NaCl_2$). The columns were shipped filled with isopropanol. To remove the isopropanol and prepare the column for coupling the antigen, the column was washed with 2 times 3 ml ice cold 1 mM HCl. After washing with storage buffer, the solution containing the antigen (1 mg/ml) was directly applied to the column and incubated for one hour at room temperature. After coupling the unbound fraction was removed by washing the column with 6 ml buffer A (0,5 M ethanolamine, 0,5 M $NaCl_2$, pH 8,3), 6 ml buffer B (0,1 M acetate, 0,5 M $NaCl_2$, pH 4,0) and 6 ml buffer A. After incubation of the column with buffer A for 1 h at RT, column was washed again with 6 ml buffer B, 6 ml buffer A, 6 ml buffer B and finally neutralized with TBS. The columns may be stored at this point in TBS at 4 °C. Before the serum was applied to the column, the column was washed with 5 ml TBS, 3 ml elution buffer (0,15 M $NaCl_2$, 0,2 M Glycin pH 2,3) and neutralized with TBS. Serum was cleared by centrifugation (20000g, 10 min, 4°C), diluted 1:1 in TBS and circulated over the column over night at 4 °C. Before elution of the antibodies the column was again washed with 5 ml TBS, 3 ml wash buffer (20 mM Tris pH 7,5, 500mM NaCl, 0,2 % Triton-X-100) and 3 ml TBS. The antibodies were eluted in 500 µl fractions with elution buffer. The tubes for fraction collection were pre filled with the required volume of 1 M Tris pH 8.5 to neutralize the pH of the elution buffer (approx. 100 µl). The pH was checked for neutrality and further adjusted if necessary. Initially, the fractions were tested by spotting 1 µl on nitrocellulose membrane followed by Ponceau staining. Protein containing fractions were examined by SDS-PAGE and the desired fractions were dialyzed against PBS and stored at 4°C. Protein concentration was determined by measuring the absorbance at 280 nm and the following approximation (absorbance of 1.35 at 280 nM equals an IgG concentration of 1 mg/ml).

5.3 Antibody coupling and crosslinking

For immunoprecipitation experiments, antibodies were coupled to beads. Rabbit polyclonal antibodies were bound to 20 µl Affiprep protein A beads (Biorad) and mouse polyclonal antibodies were coupled to protein G beads (Pierce). For immunoprecipitation of endogenous proteins, 2 - 5 µg rabbit polyclonal antibodies were used for 500 µg cell extract. For immunoprecipitation of GFP-tagged proteins, 0.25 µl rabbit polyclonal serum (Abcam,

ab-290) or 1 µg mouse monoclonal antibodies (Abcam, ab-1218) were used for 500 µg cell extract. Coupling was carried out as follows. Beads were washed with 3 - 4 times with PBS in a 500 µl Eppendorf tube, antibodies diluted in PBS were added in a total volume of 500 µl to the beads and incubated over night at 4 °C. After washing 3 - 4 times with PBS, beads may be stored at 4 °C in PBS with 0.02 % Na-Azide. To covalently cross-link antibodies to the matrix, beads were washed twice with 500 µl PBS and twice with 500 µl 0.2 M Na-Borat (pH 9.0) and than incubated with the same buffer containing 20 mM dimethyl-pimelimidate for 30 min at RT on a rotating wheel. The beads were twice washed with 500 µl 0.2 M Ethanolamine (pH 8.0), followed by an incubation in the same buffer for 2 h at RT on a rotating wheel. Finally beads were washed 3 - 4 times with PBS and may be stored as described above. To test the coupling efficiency, 2 µl beads were taken before and after the cross-linking procedure, boiled in sample before and were examined by SDS-PAGE.

6 Cell culture, synchronization and compound treatment

Cells (HeLa, MCF-7, BSC-1, 293T, HCT-116, A549, U2OS, Mel-Juso, CaCo, h-tert RPE1, primary forskin fibroblasts) were grown at 37 °C under 5 % CO_2 in Dulbecco's modified Eagle's medium (DMEM) (Gibco), supplemented with 10 % FCS and penicillin-streptomycin (100 U/ml and 100 µg/ml, respectively).

6.1 Metaphase – Anaphase synchronization

In order to obtain cell populations enriched for cells in metaphase or anaphase, Hela cells were plated at a density of $2x10^7$ cells per 15 cm plate in cell culture medium containing 5 mM thymdine (Sigma) to pre-synchronize cells at G1/S. If the protocol was combined with transient transfections, cells were plated 24 h before transfection at a density of $1x10^7$ cells per 15 cm plate and thymidine (2 mM) was added to the medium 8h after transfection. After 18 – 20 h, cells were released from the thymidine arrest by washing two times with pre-warmed PBS and 1x with cell culture medium. Two hours after the release, medium was replaced by medium containing 200 nM nocodazole (Sigma). After 12 – 14 h mitotic cells were collected by shake-off, followed by centrifugation (500 g, 5 min, RT). To obtain cells in anaphase, cell pellets of shaked-off cells were washed with pre-warmed PBS (2x) and medium (1x). For each wash step 20 ml PBS or media per 15 cm plate was used and cells had to be well re-suspended (vortex gentle). After washing, cell pellets were re-suspended in media and cells were re-plated. Medium volume and plate size should be kept minimal. (Shaked-off cells from one 15 cm plate should be re-plated in 1 well of a 6 well plate containing 1.5 ml media). Cells were incubated (37 °C, 5 % CO_2) for 60 min to enrich cells in anaphase or for the indicated time points to obtain cells in other stages. Cells were finally

harvested and washed once with PBS before further processed. The cell cycle status was controlled by immunofluorescence microscopy directly after harvesting. For this, cell suspension was mixed with a fixation buffer containing Hoechst dye to stain the DNA (50% glycerol in PBS, 0.1 % Triton-X-100, 4 % Formaldehyde and 2 mg/ml Hoechst). A droplet (2 µl) of the mixture was placed on a glass slide, covered with a cover-slide and analyzed by immunofluorescence microscopy.

6.2 Compound treatments

To determine the number of mitotic cells with monoasters and for cell cycle profile analyses, cells were synchronized using a double thymidine block. In brief, BSC-1 cells were plated on coverslips and cultured in the presence of 2 mM thymidine for 18h. Six hours after the first release from the first thymidine block, cells were treated again with 2 mM thymidine for 18 h. After the second release coverslips were transferred to a 24 well plate, containing 300 µl culture media, supplemented with chemical compounds or DMSO as a solvent control. Plates were returned to the incubator and after 12 hours cells were fixed, stained and analyzed by immunofluorescence microscopy.

To analyze defects in cytokinesis, cells (Hela and MCF-7) were synchronized using a thymidine block. In brief, cells were plated on coverlips ($2x10^6$ cells / 10 cm plate) and cultured in the presence of 2 mM thymidine for 18 h. Cells were released and coverslips were transferred to a 24 well plate containing 500 ul culture media supplemented with chemical compounds (SH compounds; see screening below) or DMSO as control. After 14 - 16 h after the release, cells were fixed, stained and the number of binucleated cells was analyzed by immunofluorescence.

For life cell analyzes cells were plated on 12 well plates ($5x10^4$). Cell synchronization was carried out as described above. 6 h after the release from thymidine, culture medium was replaced by life cell medium containing the chemical compounds or DMSO as control. Cells were filmed for 18 h.

6.3 VS-83 treatment for the study of Mklp2/CPC localization

Cells were plated 24 - 30 hours before treatment. When combined with RNAi or RNAi rescue experiments, drug treatments were carried out after 36 h of RNAi in an asynchronous cell population or 8 h after the release from thymidine in synchronized cells (see above). In order to enrich for mitotic cells with a monopolar mitotic spindle, asynchronous cells were treated first for 2-4 hours with 30 µM VS-83. Alternatively, thymdine pre-synchronized cells were treated with 30 µM VS-83 before cells enter mitosis (8h). When a sufficient amount of cells is

arrested in mitosis, cells were treated with 1 µM taxol or DMSO as solvent control for 30 min followed by the treatment with 20 µM MG132 and 100 µM roscovitine or DMSO for 20 min. Cells were fixed, stained and analyzed by immunofluorescence.

For the analyses of cells undergoing monopolar cytokinesis, VS-83 arrested cells were treated with 100 µm roscovitine for 30 - 40 min. Nocodazole (500 nM) or ZM447439 (20 µM) were added simultaneously. Cells were fixed, stained and analyzed by immunofluorescence.

7 Transient transfection, RNAi and rescue experiments

7.1 Plasmid transfection

The plasmids used for the transient overexpression of proteins are listed above (table 2). The plasmid encoding non-degradable Cyclin B (GFP-Cyclin B^{KtoR}) was a gift from Prof. Olaf Stemmann.

For immunofluorescence microscopy, cells were seeded on coverslips in a 10 cm plate at a density of $2x10^6$ cells 24 – 36 h and transferred to 6-well plate before the transfection. For the transfection of cells in one well of a 6-well plate, the following mixture was prepared according to the manufactures instruction (Roche): 3 µl Fugene6 (Roche), 1.5 µg of pure plasmid DNA (preferentially from a "mini-prep" with a concentration of 0.5 µg/µl) in 200 µl Optimem (Gibco). After transfection for 6 - 8 h medium was replaced with fresh media and cells were fixed after 36 h.

For immunoprecipitation experiments of GFP-tagged proteins from anaphase cell extracts, $1x10^7$ cells were seeded in a 15 cm plate containing 20 ml media 24 h before transfection. For transfection the same mixture as described above was used but taking 10 fold of the indicated amounts. After transfection for 8 - 10 h, medium was replaced by medium containing 2 mM thymidine. Synchronization to enrich cells in anaphase was performed as described above.

7.2 RNAi

The RNAi duplexes used in this study are listed below. All duplexes were diluted to 20 µM with buffer provided by Dharmacon Research and annealed. Annealing was carried out in a PCR machine (1 min at 90 °C followed by 1 h at 37°C) and annealed oligos were stored at -20 °C until use.

Table 3. List of RNAi oligonucleotides, used in this study:

gen	oligo name	sequence	targeting	reference
Mklp2	#1 (TUM 26)	5'-ccacctatgtaatctcatg-3'	3´ UTR	
Mklp2	#2 (TUM 31)	5'-gatcagggttgtgtccgta-3'	ORF	Neef et al., 2003
Mklp1	#1 (TUM 27)	5'-gcagtcttccaggtcatct-3'	3' UTR	
Mklp1	#2 (TUM 28)	5'-cagctggagatgcagaata-3'	ORF	
Mklp1	#3 (TUM 30)	5'-cgacataacttacgacaaa-3'	ORF	Yüce et al., 2005
MPP1	#1 (TUM 18)	5'-aggacagagtcgtctgatt-3'	ORF	Abaza et al., 2003
MPP1	#2 (TUM 26)	5'-ccaggtttgtcttcgaata-3'	ORF	
MPP1	#3 (TUM 26)	5'-aaaccaagatgacctacta-3'	ORF	
MPP1	#4 (TUM 26)	5'-atacgtccatcatctaaga-3'	ORF	
MPP1	#5 (TUM 26)	5'-gagaaagatagtgaccttc-3'	ORF	
MPP1	#6 (TUM 26)	validated sequence (Quiagen)		
INCENP	(TUM 53)	5'-ggcttggccaggtgtatat-3'	3' UTR	Klein et al., 2006
Anillin	#2 (TUM)	5'-gcaactgcagcctcctcag-3'	ORF	Straight et al., 2005
Gl2	(TUM)	5'-cgtacgcggaatacttcga-3'	ORF	Elbashir et al. 2001

Cells were seeded at a density of 2×10^6 cells on glass-coverslips in a 10 cm plate 24 – 36 h before the RNAi. Coverslips were transferred to a 6-well plate before the RNAi. For life cell analysis, cells were seeded in a 12 well plate at a density of 4×10^4 cells / well. For the RNAi of cells in 1 well of a 6 well plate containing 2 ml media the following mixture was prepared according to the instruction of the manufacture (Invitrogen): 4 µl oligofectamine (Invitrogen), 6 µl RNAi oligo (20µM) in 200 µl Optimem. For the RNAi of cells in 1 well of a 12 well plate, ½ of the amounts were used. RNAi was performed for 36 – 48 h.

For RNAi experiments combined with cell synchronization, cells seeding and RNAi mixture was prepared as above. After RNAi for 8 h, medium was replaced with medium containing 2 mM thymidine and RNAi mixture was added again. Cells were released after 18 h by washing with PBS and medium and then either analyzed by life cell imaging (6 h), fixed and stained for immunofluorescence (10 h) or harvested, lysed and processed for Western blotting (10 h).

7.3 RNAi rescue experiments

For rescue experiments cells were seeded in 12 well plates at 4×10^4 cells / well 24 - 36 h before transfection. Plasmids and RNAi duplexes were transfected simultaneously according to the protocol described above. After 8h medium was replaced and 2 mM thymidine and RNAi duplexes were added again. Cells were released after 18h by washing with PBS (2 times) and medium (2 times) and then either analyzed by life cell imaging (6 h), fixed and stained for immunofluorescence (10 h) or harvested, lysed and processed for Western blotting (10 h).

8 Immunofluorescence microscopy and live cell imaging

8.1 Fixed samples

Cells were grown on coverslips and fixed and permeabilized for 10 min in fixation buffer (100 mM Pipes pH 6.8, 10 mM EGTA, 1 mM $MgCl_2$, 0.2 % Triton X-100, 4 % formaldehyde). Samples were washed with TBS + 0.1% Triton X-100 (TBST) and incubated for 1 h in TBST + 2 % BSA (Sigma). Coverslips can be stored at this point at 4 °C. All antibody incubations were carried out for 1 h at room temperature in blocking solution, followed by three washes in TBST. For DNA stain, samples were first washed with TBS, DNA was stained with 4,6-diamidino-2-phenylindole (DAPI; 2 µg/ml) in TBS and TBS washed samples were embedded in mounting media (20mM TrisHCl pH 8,8; 0,5% phenylendiamine; 90% glycerol).

Table 4. List of antibodies used for immunofluorescence:

Antigen	species	dilution	generated/purchased from:	comment
Mklp2	rabbit	1:1000	Home-made	serum and affinity purified (0.3 µg/µl)
Mklp1	rabbit	1:1000	Home-made	serum and affinity purified (0.8 µg/µl)
MPP1	rabbit	1:1000	Home-made (#1, rabbit 1416)	serum and affinity purified (0.5 µg/µl)
MPP1	rabbit	1:1000	Home-made (#3, rabbit 1518)	serum and affinity purified (0.5 µg/µl)
Eg5	rabbit	1:1000	Home-made	serum
α-tubulin	mouse	1:500	Sigma (DM1α)	
α-tubulin (FITC labeled)	mouse	1:500	Sigma (DM1α)	
Aurora B	mouse	1:250	BD Biosience (AIM-1)	
INCENP	mouse	1:10	Abcam (ab 23956)	
INCENP	rabbit	1:500	Abcam (ab 36453)	
survivin	rabbit	1:500	Abcam (ab-469)	
PRC1	rabbit	1:250	Santa Cruz	
CREST	human	1:5000	Immunovision	
vimentin	mouse	1:1000	Sigma (V9)	
vimentin pS72	rabbit	1:1000	Epitomics (EP1070Y)	

Immunofluorescence microscopy was performed using a Zeiss Axioplan II microscope (Zeiss, Jena, Germany) with Apochromat and 63x oil immersion objectives.

To determine the cell cycle profile, cells stained for chromatin were analyzed on a light scanning microscope (CompuCyte) equipped with a 20x lens. Prior to the analysis, the settings were defined by measurement of standard samples. The following standardizations were used: cells treated with 500 nM nocodazole (G2/M), thymdine (G1/S). Cell cycle profiles were analyzed using the ComuCyte software.

For high-resolution images, a DeltaVision microscope (Applied Precision) on an Olympus IX71 base, equipped with a PlanApo 60X/1.40 oil immersion objective, and a Cool SNAP HQ camera (Photometrics) was used for collecting 0.2 µm distanced optical sections in the z

axis. Images at single focal planes were processed with a deconvolution algorithm, and optical sections were projected into one picture by using Softworx software (Applied Precision). Images were cropped in Adobe Photoshop 6.0, and then sized and placed in figures using Adobe Illustrator 10 (Adobe Systems).

8.2 Live cell imaging

For live-cell imaging, cells were grown in 12 well plates and processed as described above. Before live cell imaging medium was replaced by CO_2 independent medium (Gibco, supplemented with 10 % FCS, penicillin-streptomycin (100 U/ml and 100 µg/ml, respectively) and 1x Glutamax (Gibco)) and the culture dish was placed onto a heated sample stage within a heated chamber (37 °C). Live cell imaging was performed using a Zeiss Axiovert microscope (Zeiss) with a Plan Apo 20x/0.95 objective. Images were captured with 50-100 millisecond exposure times in 5 minutes intervals for 18 hours. MetaMorph software was used to collect and process data.

9 MT pull-down from cell extracts

Cell synchronization (metaphase / anaphase) was performed as described above (section 6.1). Per experimental condition, one 15 cm plate of cells was used. After harvesting, cells were collected by centrifugation (500g, 5min, RT) and washed once with PBS. Cells were lysed on ice for 20 min (10 mM Pipes pH 6.8, 115 mM KCl, 0.5 % Triton-X 100, 300 mM Succrose, 5 mM $MgCl_2$, 1 mM ATP, 1 mM EGTA, 20 mM β-Glycerophsaphate, 0.3 mM Sodiumvanadate, 0.1 mM Sodiumfluoride, 100 nM Okadaic Acid, 1 µM Dithiothreithol, complete inhibitor tablets (Roche)). Shaked-off cells from one 15 cm plate ($2x10^7$ cells) were lysed in 500 µl lyses buffer resulting in an extract concentration of approximately 5 mg/ml. After lysis, extracts were centrifuged for 10 min at 2000 g (4 °C) and supernatant (cytosol) was separated from the pellet. The cytosolic fraction was cleared by an additional centrifugation (30 min, 20000 g, 4 °C) and kept on ice until use.

Taxol-stabilized MTs were prepared as described above. Before using them in spindown assays, 100 µM MTs were diluted 1/10 in BRB80 containing 20 µM taxol and pelleted by centrifugation (30 min, 20000 g, RT). Supernatant was removed and MTs were re-suspended in the same buffer to a concentration of 10 µM. The cytosolic fraction was brought to room temperature before the addition of taxol-stabilized MTs (per condition 400 µl cytosol). The cytosol was supplemented with taxol (20 µM) and ATP (1 mM) and taxol-stabilized MTs (1 µM). Following incubation at RT for 30 min on a rotating wheel, one reaction volume of lyses-buffer was added as cushion and MTs were pelleted (30 min, 20000

g, RT). SN was removed and pellet was resolved in sample buffer (1/10 reaction volume) and analysis of MT-bound proteins was carried out by western blotting.

In order to restore Cdk1 activity in anaphase extract, recombinant Cyclin B$^{\Delta 90}$ ($\Delta 90$) was used as follows. Cyclin B$^{\Delta 90}$ was purified by Eva Hörmanseder from Sf9 cells following the protocol provided by Prof. Olaf Stemmann. Cells were enriched in anaphase (section 6.1) and lysed as described above. After lysis for 20 min on ice, 40 µl Cyclin B $\Delta 90$ (1.2 µg/µl) or dialyzes buffer and 1 mM ATP were added to 400 µl extract with a concentration of about 5 µg/µl. After incubation for 30 min at 4 °C on a rotating wheel, the above described protocol, starting with the centrifugation at 2000 g for 10 min at 4 °C, was followed.

10 Immunoprecipitations

For co-immunoprecipitations, HeLa cells were synchronised as described above (section 6.1), harvested and lysed in lysis buffer (25 mM Tris-HCl pH 7.5, 300 mM NaCl$_2$, 5 mM EDTA, 0.5 % Triton-X-100, DNAse 20 µg/ml, RNAse 20 µg/µl, 20 mM β-Glycerophsaphate, 0.1 mM PMSF, 0.3 mM Sodiumvanadate, 0.1 mM Sodiumfluoride, 100 nM Okadaic Acid, 1 µM Dithiothreithol, complete inhibitor tablets (Roche) for 30 min on ice. Shaked-off cells from one 15 cm plate (2×10^7 cells) were routinely lysed in 500 µl lyses buffer, resulting in an extract concentration of about 5 mg/ml. Extracts were cleared by centrifugation (20000g, 10min, 4°C). Antibody coupling was carried out as described above. The coupled antibodies were incubated with the extract for 3h at 4°C on a rotating wheel. After protein capture, beads were washed 5-times with lyses buffer buffer and finally re-suspended in gel sample loading buffer. Co-precipitation experiments were analyzed by western blotting.

11 Cdk1 kinase assay on immunoprecipitated Mklp2

Mklp2 was immunoprecipitated from anaphase extract as described above. Beads were first washed 5 times with lysis buffer and then washed 3 times with kinase buffer (25 mM Tris-HCl pH 7.4, 150 mM NaCl$_2$, 10 mM MgCl$_2$, 5 mM EDTA, 20 mM β-Glycerophsaphate, 1 mM Sodiumvanadate, 0.1 % Triton-X-100). Kinase reactions were carried out in 100 µl kinase assay buffer containing 20 µl Mklp2-beads, 4 ng/µl Cdk1/Cyclin B (Millipore) and 1 mM ATP. Heat-inactivation of Cdk1 as control was done for 10 min at 96 °C. Alternatively, the reaction mixture was supplemented with either 1 mM roscovintine or DMSO as solvent control. After incubation at 30 °C for 30 min in an eppendorf shaker (800 rpm), supernatant and bead fractions were separated and beads were washed 5-times with kinase buffer and finally re-suspended in gel sample loading buffer.

12 Western blotting analysis

For Immunoblot analyzes, protein samples, dissolved in sample buffer, were loaded on SDS-page gels. Separated proteins were transferred to Nitrocellulose membranes (Schleicher & Schuell). After transferring, membranes were washed with blocking buffer (5% low-fat dry milk in PBST (PBS, 0.1% Tween)) for 1 h at RT. Primary antibodies were diluted in blocking buffer. Dilution of the antibodies, as well as incubation times and conditions, are listed below (table 5). After incubation with the primary antibodies, membranes were washed 3 times in PBST, following incubation with the HRP conjugated secondary goat-anti mouse or or goat-anti rabbit antibodies (1:3000, Pierce) for 1 h at RT. After 3 washes with PBST, bound antibodies were detected by ECL solution using a digital Fujifilm LAS-1000 camera attached to an intelligent Darkbox II (Raytest).

Table 5. List of antibodies used for Western-blotting in this study:

Antigen	species	dilution	procedure	generated/purchased:	comment
Mklp2	rabbit	1:1000	1h, RT	Home- made	serum and affinity purified (0.3 µg/µl)
Mklp1	rabbit	1:1000	1h, RT	Home-made	serum and affinity purified (0.8 µg/µl)
MPP1	rabbit	1:1000	1h, RT	Home-made (#1)	serum and affinity purified (0.5 µg/µl)
MPP1	rabbit	1:1000	1h, RT	Home-made (# 3)	serum and affinity purified (0.5 µg/µl)
Eg5	rabbit	1:1000	1h, RT	Home-made	serum
α-tubulin	mouse	1:500	1h, RT	Sigma (DM1α)	
histone H3	mouse	1:1000	1h, RT	Millipore	
Cyclin B	mouse	1:1000	1h, RT	Abcam (ab-72)	
Aurora B	mouse	1:250	o.n., 4 °C	BD Biosience (AIM-1)	
INCENP	mouse	undiluted	o.n., 4 °C	Abcam (ab 23956)	
vimentin	mouse	1:1000	1h, RT	Sigma (V9)	

13 ATPase assay for kinesins and high-throughput screening

13.1 Malachite green assay

The ATPase activity of the kinesin motor domains was measured using the malachite green assay. Saturated ATP and MT concentrations were chosen (200 µM and 200 nM, respectively). The reactions were typically performed in total reaction volume of 60 µl in assay buffer (BRB80, 0.1 mg/ml BSA, 0.1 µM taxol) supplemented with 200 nM taxol-stabilized MTs. In each experiment, each reaction condition was done in duplicate. The concentration of the individual motor proteins was determined as the concentration at which a linear ATPase activity could be guarantied over the time of the experiment (0.01 - 0.02 absorbance units at 650 nm / min). Tested compounds were pre-incubated with the reaction mixture for 10 min at RT before the start of the assay. The reactions were started by the

addition of 200 µM ATP and incubated at room temperature. At individual time points (normally every 6 min over a time of 18 min) 10 µl of the reaction mix was pipetted in 40 µl perchloric acid (2 M) in a 384 well plate (Nunc). After the last time point 40 µl developer solution (1 M HCl, 1 mM Malachit Green (Sigma), 10 mM ammonium molybdate tetrahydrat (Sigma)) was added and after 20 min incubation at RT the absorbance at 650 nm was measured using a plate reader (Victor2, Perkin Elmer).

Data were processed in the following way. For each individual reaction, the absorbance value at 0 min (background) was subtracted from the values at the following time points. These normalized absorbance values were averaged using the duplicate for each condition in the same experiment. From these values, we subtracted at each time point the values obtained from a reaction without motor domain in order normalize for the ATP auto-hydrolyses rate. These values from three independent experiments were averaged and blotted in a graph against the time of the experiment using Microsoft Excel or Origin 6.1. The slope of these curves, determined by linear fitting of the data points, represents the velocity of the reaction in the unit [absorbance/s].

The ATP hydrolyses rate per time was determined as follows. The absorbance values of defined concentrations of free phosphate in solution was determined and blotted in a graph. The slope of this curve was determined by linear fitting. According to this standard curve, an absorbance value of 0.1 equals a concentration of 15 µM free phosphate in the solution. Using this conversion, the velocity of the reaction could be determined as phosphate release per time [µM/s] which represents the ATP hydrolyses rate per time. The turn-over rates [s^{-1}] were finally calculated as velocity [µM/s] per concentration of motor protein [µM].

The inhibitory effect of small molecule inhibitors and the IC_{50} values were determined as follows. The velocity [absorbance/s] of the ATP hydrolysis in the linear range of the reaction was determined as described above in the presence of different concentrations of the small molecule inhibitors or DMSO as solvent control. The value from the control reaction in each experiment was set to 100 % activity (0 % inhibition) and the ATPase activity in the presence of the different concentrations of small molecule inhibitors was determined accordingly. The obtained values were blotted in a graph against the concentration of the inhibitor in the log scale using Origin 6.1 and fitted sigmoid, when possible. The IC_{50} was determined as the concentration of the small molecule inhibitors at which the ATP hydrolysis rat was 50 % of the one from the DMSO control.

13.2 High-throughput screening

The screen for small molecule inhibitors of mitotic kinesins was based on the malachite green assay. The MT dependent ATPase activity of the motor domain of different kinesins in the presence of small molecules was used as measurement to identify novel small molecule

inhibitors. The screen was carried out for the following kinesins: Eg5, Mklp1, Mklp2, MPP1, KIF4, CenpE, MCAK, KIF5A and KIF5B. The 25.000 tested substances were purchased from (ChemDiv, Maybridge and from our collaborator A. Giannis). The substances were stored in sealed 384 well plates (Matrix) at - 40 °C. Different copies of the original library with different concentrations were made and stored separately. Plates were thawed up before use in a cabinet desicator and centrifuged for 1 min at 3000 g to avoid spill over.

For the screening procedure, an endpoint measurement in 384 well plates (Nunc) using a modified version of malachite green assay was applied. The kinesin reaction was carried out in a total volume of 20 µl in assay buffer (20 mM K-Pipes pH 6.8, 1 mM $MgCl_2$, 1 mM EGTA, 0.1 mg/ml BSA, 0.1 µM taxol) containing the following concentrations of motor proteins, MTs and ATP (see table 6).

Table 6. Screening conditions for the individual kinesins:

kinesin	motor domain [nM]	MTs [nM]	ATP [µM]
Eg5	48	80	50
Mklp2	344	500	50
MPP1	10	30	200
Mklp1	42	25	50
KIF4	19	140	100
CenpE	66	280	40
MCAK	180	120	120
KIF5A	65	125	50
KIF5B	22	220	40

The screening was carried out as follows. 20 µl of the reaction mixture were dispensed in the 384 well reaction plates using an automated dispenser (Multidrop, Thermolabs) and plates were shortly centrifuged (3000g, 10s). The chemical substances were transferred from the storage plate to the reaction plate using a "pintool" (BiomeckFX, Beckman). Each reaction was done in duplicate for each substance. The reaction plates were shortly centrifuged and incubated for 15 min at RT. The reaction was started by the addition of 10 µl ATP solution (kinesin dependent ATP concentration in assay buffer) using the automated dispenser. Plates were shortly centrifuged and incubated for 12 min at RT. Using the pipetting robot (BiomekFX, Beckman), the reaction was stopped and the color reaction was started by the addition of 70 µl perchloric acid/develover solution (1 M perchloric acid / 0.5 M HCl, 0.5 mM Malachit Green, 5mM ammonium molybdate tetrahydrat). The plates were shortly centrifuged and after 20 min incubation the absorbance at 650 nm was measured using a plate reader (Victor2, Perkin Elmer).

Data were collected and analyzed using Microsoft Excel. Each reaction plate was processed in the following way. First the average absorbance value of one column of the reaction plate that did not contain any motor protein was calculated. This background value was

subtracted from all other values on the plate. Next, the average of value of one column of the reaction plate, in which DMSO was used as solvent control, was calculated. This value represents 100 % activity of the motor protein. For each substance, the % inhibitory value was calculated, taking the DMSO value as 0 % inhibition (100 % activity). The average for each compound from the two reactions (duplicate) was calculated and this value together with the corresponding compound ID was finally stored and saved in an Excel sheet. Finally, all data from the different kinesins and compounds were combined in an Excel sheet and sorted according to the desired thresholds (inhibition of one kinesin to more than 50% but not more than one other kinesin with more than 50%).

List of Abbreviations

All units are abbreviated according to the International Unit System.

aa: amino acid

ATP: adenosine 5' triphosphate

BSA: bovine serum albumin

Cdk: cyclin dependent kinase

cDNA: complementary deoxyribonucleic acid

CPC: chromosomal passenger complex

CO_2: carbon dioxid

C-terminus; carboxy-terminus

DAPI: 4´,6-diamidino-2-phenylindole

DNA: deoxyribonucleic acid

DTT: dithiothreitol

E. coli: Escherichia coli

ECL: enhanced chemiluminescence

EDTA: ethylene-dinitrilo-tetraacetic acid

EGTA: ethylene-gycol-tetraacetic acid

FACS: fluorescence activated cell sorter

FCS: Fetal calf serum

GEF: guanine nucleotide exchange factor

GFP: green fluorescent protein

GST: glutathione S-transferase IF: immunofluorescence

HCl: hydrochloric acid

Hepes: N-2-Hydroxyethypiperazine-N'-2-ethane sulfonic acid

IF: intermediate filament

h: hour

IgG: Immunoglobulin G

INCENP: inner centromere protein

IP: immunoprecipitation

IPTG: isopropyl-beta-D-thiogalactopyranoside

kDa: kilo Dalton

KIF: kinesin family member

KT: kinetochores

LB: luria broth

MES: 2-(N-morpholino) ethanesulfonic acid

min: minute(s)

Mklp: mitotic kinesin-like protein

MT: microtubule

MW: molecular weight

N-terminus: amino-terminus

OD: optical density

ORF: open reading frame

PBS: Phosphate-buffered saline

PCR: Polymerase chain reaction

PIPES: 1,4-Piperazinediethanesulfonic acid

Plk: Polo-like kinase

PMSF: phenylmethylsulfonyl fluoride

rpm: revolutions per minute

RT: room temperature

SAC: spindle assembly checkpoint

SDS-PAGE: Sodium dodecylsulfate polyacrylamid gelelectrophoresis

RNAi: small interference ribonucleic acid

T59: threonine at postion 59

wt: wildtype

References

Abaza, A., J.M. Soleilhac, J. Westendorf, M. Piel, I. Crevel, A. Roux, and F. Pirollet. 2003. M phase phosphoprotein 1 is a human plus-end-directed kinesin-related protein required for cytokinesis. *J Biol Chem*. 278:27844-52.

Adams, R.R., M. Carmena, and W.C. Earnshaw. 2001a. Chromosomal passengers and the (aurora) ABCs of mitosis. *Trends Cell Biol*. 11:49-54.

Adams, R.R., H. Maiato, W.C. Earnshaw, and M. Carmena. 2001b. Essential roles of Drosophila inner centromere protein (INCENP) and aurora B in histone H3 phosphorylation, metaphase chromosome alignment, kinetochore disjunction, and chromosome segregation. *J Cell Biol*. 153:865-80.

Adams, R.R., A.A. Tavares, A. Salzberg, H.J. Bellen, and D.M. Glover. 1998. pavarotti encodes a kinesin-like protein required to organize the central spindle and contractile ring for cytokinesis. *Genes Dev*. 12:1483-94.

Ainsztein, A.M., S.E. Kandels-Lewis, A.M. Mackay, and W.C. Earnshaw. 1998. INCENP centromere and spindle targeting: identification of essential conserved motifs and involvement of heterochromatin protein HP1. *J Cell Biol*. 143:1763-74.

Alsop, G.B., and D. Zhang. 2003. Microtubules are the only structural constituent of the spindle apparatus required for induction of cell cleavage. *J Cell Biol*. 162:383-90.

Andersen, S.S., A.J. Ashford, R. Tournebize, O. Gavet, A. Sobel, A.A. Hyman, and E. Karsenti. 1997. Mitotic chromatin regulates phosphorylation of Stathmin/Op18. *Nature*. 389:640-3.

Balasubramanian, M.K., E. Bi, and M. Glotzer. 2004. Comparative analysis of cytokinesis in budding yeast, fission yeast and animal cells. *Curr Biol*. 14:R806-18.

Barr, F.A., H.H. Sillje, and E.A. Nigg. 2004. Polo-like kinases and the orchestration of cell division. *Nat Rev Mol Cell Biol*. 5:429-40.

Bishop, A.C., J.A. Ubersax, D.T. Petsch, D.P. Matheos, N.S. Gray, J. Blethrow, E. Shimizu, J.Z. Tsien, P.G. Schultz, M.D. Rose, J.L. Wood, D.O. Morgan, and K.M. Shokat. 2000. A chemical switch for inhibitor-sensitive alleles of any protein kinase. *Nature*. 407:395-401.

Blangy, A., H.A. Lane, P. d'Herin, M. Harper, M. Kress, and E.A. Nigg. 1995. Phosphorylation by p34cdc2 regulates spindle association of human Eg5, a kinesin-related motor essential for bipolar spindle formation in vivo. *Cell*. 83:1159-69.

Brady, S.T. 1985. A novel brain ATPase with properties expected for the fast axonal transport motor. *Nature*. 317:73-5.

Brennan, I.M., U. Peters, T.M. Kapoor, and A.F. Straight. 2007. Polo-like kinase controls vertebrate spindle elongation and cytokinesis. *PLoS ONE*. 2:e409.

Bringmann, H., and A.A. Hyman. 2005. A cytokinesis furrow is positioned by two consecutive signals. *Nature*. 436:731-4.

Brinkley, B.R., E.M. Fuller, and D.P. Highfield. 1975. Cytoplasmic microtubules in normal and transformed cells in culture: analysis by tubulin antibody immunofluorescence. *Proc Natl Acad Sci U S A*. 72:4981-5.

Burkard, M.E., C.L. Randall, S. Larochelle, C. Zhang, K.M. Shokat, R.P. Fisher, and P.V. Jallepalli. 2007. Chemical genetics reveals the requirement for Polo-like kinase 1 activity in positioning RhoA and triggering cytokinesis in human cells. *Proc Natl Acad Sci U S A*. 104:4383-8.

Carmena, M. 2008. Cytokinesis: the final stop for the chromosomal passengers. *Biochem Soc Trans.* 36:367-70.

Case, R.B., D.W. Pierce, N. Hom-Booher, C.L. Hart, and R.D. Vale. 1997. The directional preference of kinesin motors is specified by an element outside of the motor catalytic domain. *Cell.* 90:959-66.

Cesario, J.M., J.K. Jang, B. Redding, N. Shah, T. Rahman, and K.S. McKim. 2006. Kinesin 6 family member Subito participates in mitotic spindle assembly and interacts with mitotic regulators. *J Cell Sci.* 119:4770-80.

Chen, Q., H. Li, and A. De Lozanne. 2006. Contractile ring-independent localization of DdINCENP, a protein important for spindle stability and cytokinesis. *Mol Biol Cell.* 17:779-88.

Colucci-Guyon, E., M.M. Portier, I. Dunia, D. Paulin, S. Pournin, and C. Babinet. 1994. Mice lacking vimentin develop and reproduce without an obvious phenotype. *Cell.* 79:679-94.

Cooke, C.A., M.M. Heck, and W.C. Earnshaw. 1987. The inner centromere protein (INCENP) antigens: movement from inner centromere to midbody during mitosis. *J Cell Biol.* 105:2053-67.

D'Avino, P.P., M.S. Savoian, and D.M. Glover. 2005. Cleavage furrow formation and ingression during animal cytokinesis: a microtubule legacy. *J Cell Sci.* 118:1549-58.

Desai, A., and T.J. Mitchison. 1997. Microtubule polymerization dynamics. *Annu Rev Cell Dev Biol.* 13:83-117.

Ditchfield, C., V.L. Johnson, A. Tighe, R. Ellston, C. Haworth, T. Johnson, A. Mortlock, N. Keen, and S.S. Taylor. 2003. Aurora B couples chromosome alignment with anaphase by targeting BubR1, Mad2, and Cenp-E to kinetochores. *J Cell Biol.* 161:267-80.

Earnshaw, W.C., and C.A. Cooke. 1991. Analysis of the distribution of the INCENPs throughout mitosis reveals the existence of a pathway of structural changes in the chromosomes during metaphase and early events in cleavage furrow formation. *J Cell Sci.* 98 (Pt 4):443-61.

Echard, A., F. Jollivet, O. Martinez, J.J. Lacapere, A. Rousselet, I. Janoueix-Lerosey, and B. Goud. 1998. Interaction of a Golgi-associated kinesin-like protein with Rab6. *Science.* 279:580-5.

Eckes, B., D. Dogic, E. Colucci-Guyon, N. Wang, A. Maniotis, D. Ingber, A. Merckling, F. Langa, M. Aumailley, A. Delouvee, V. Koteliansky, C. Babinet, and T. Krieg. 1998. Impaired mechanical stability, migration and contractile capacity in vimentin-deficient fibroblasts. *J Cell Sci.* 111 (Pt 13):1897-907.

Eckley, D.M., A.M. Ainsztein, A.M. Mackay, I.G. Goldberg, and W.C. Earnshaw. 1997. Chromosomal proteins and cytokinesis: patterns of cleavage furrow formation and inner centromere protein positioning in mitotic heterokaryons and mid-anaphase cells. *J Cell Biol.* 136:1169-83.

Eggert, U.S., T.J. Mitchison, and C.M. Field. 2006. Animal cytokinesis: from parts list to mechanisms. *Annu Rev Biochem.* 75:543-66.

Eriksson, J.E., P. Opal, and R.D. Goldman. 1992. Intermediate filament dynamics. *Curr Opin Cell Biol.* 4:99-104.

Florian, S., S. Hummer, M. Catarinella, and T.U. Mayer. 2007. Chemical genetics: reshaping biology through chemistry. *Hfsp J.* 1:104-14.

Foe, V.E., and G. von Dassow. 2008. Stable and dynamic microtubules coordinately shape the myosin activation zone during cytokinetic furrow formation. *J Cell Biol.* 183:457-70.

Franke, W.W., C. Grund, C. Kuhn, B.W. Jackson, and K. Illmensee. 1982. Formation of cytoskeletal elements during mouse embryogenesis. III. Primary mesenchymal cells and the first appearance of vimentin filaments. *Differentiation.* 23:43-59.

Franke, W.W., M. Hergt, and C. Grund. 1987. Rearrangement of the vimentin cytoskeleton during adipose conversion: formation of an intermediate filament cage around lipid globules. *Cell.* 49:131-41.

Fuchs, E., and D.W. Cleveland. 1998. A structural scaffolding of intermediate filaments in health and disease. *Science.* 279:514-9.

Fuchs, E., and K. Weber. 1994. Intermediate filaments: structure, dynamics, function, and disease. *Annu Rev Biochem.* 63:345-82.

Fuller, B.G., M.A. Lampson, E.A. Foley, S. Rosasco-Nitcher, K.V. Le, P. Tobelmann, D.L. Brautigan, P.T. Stukenberg, and T.M. Kapoor. 2008. Midzone activation of aurora B in anaphase produces an intracellular phosphorylation gradient. *Nature.* 453:1132-6.

Gadde, S., and R. Heald. 2004. Mechanisms and molecules of the mitotic spindle. *Curr Biol.* 14:R797-805.

Gadea, B.B., and J.V. Ruderman. 2006. Aurora B is required for mitotic chromatin-induced phosphorylation of Op18/Stathmin. *Proc Natl Acad Sci U S A.* 103:4493-8.

Galou, M., J. Gao, J. Humbert, M. Mericskay, Z. Li, D. Paulin, and P. Vicart. 1997. The importance of intermediate filaments in the adaptation of tissues to mechanical stress: evidence from gene knockout studies. *Biol Cell.* 89:85-97.

Gassmann, R., A. Carvalho, A.J. Henzing, S. Ruchaud, D.F. Hudson, R. Honda, E.A. Nigg, D.L. Gerloff, and W.C. Earnshaw. 2004. Borealin: a novel chromosomal passenger required for stability of the bipolar mitotic spindle. *J Cell Biol.* 166:179-91.

Gennerich, A., and R.D. Vale. 2009. Walking the walk: how kinesin and dynein coordinate their steps. *Curr Opin Cell Biol.* 21:59-67.

Giansanti, M.G., S. Bonaccorsi, E. Bucciarelli, and M. Gatti. 2001. Drosophila male meiosis as a model system for the study of cytokinesis in animal cells. *Cell Struct Funct.* 26:609-17.

Giet, R., and D.M. Glover. 2001. Drosophila aurora B kinase is required for histone H3 phosphorylation and condensin recruitment during chromosome condensation and to organize the central spindle during cytokinesis. *J Cell Biol.* 152:669-82.

Glotzer, M. 2001. Animal cell cytokinesis. *Annu Rev Cell Dev Biol.* 17:351-86.

Glotzer, M. 2004. Cleavage furrow positioning. *J Cell Biol.* 164:347-51.

Glotzer, M. 2005. The molecular requirements for cytokinesis. *Science.* 307:1735-9.

Glotzer, M. 2009. The 3Ms of central spindle assembly: microtubules, motors and MAPs. *Nat Rev Mol Cell Biol.* 10:9-20.

Goto, H., T. Kiyono, Y. Tomono, A. Kawajiri, T. Urano, K. Furukawa, E.A. Nigg, and M. Inagaki. 2006. Complex formation of Plk1 and INCENP required for metaphase-anaphase transition. *Nat Cell Biol.* 8:180-7.

Goto, H., H. Kosako, K. Tanabe, M. Yanagida, M. Sakurai, M. Amano, K. Kaibuchi, and M. Inagaki. 1998. Phosphorylation of vimentin by Rho-associated kinase at a unique amino-terminal site that is specifically phosphorylated during cytokinesis. *J Biol Chem.* 273:11728-36.

Goto, H., Y. Yasui, A. Kawajiri, E.A. Nigg, Y. Terada, M. Tatsuka, K. Nagata, and M. Inagaki. 2003. Aurora-B regulates the cleavage furrow-specific vimentin phosphorylation in the cytokinetic process. *J Biol Chem*. 278:8526-30.

Gruneberg, U., R. Neef, R. Honda, E.A. Nigg, and F.A. Barr. 2004. Relocation of Aurora B from centromeres to the central spindle at the metaphase to anaphase transition requires MKlp2. *J Cell Biol*. 166:167-72.

Guse, A., M. Mishima, and M. Glotzer. 2005. Phosphorylation of ZEN-4/MKLP1 by aurora B regulates completion of cytokinesis. *Curr Biol*. 15:778-86.

Hauf, S., R.W. Cole, S. LaTerra, C. Zimmer, G. Schnapp, R. Walter, A. Heckel, J. van Meel, C.L. Rieder, and J.M. Peters. 2003. The small molecule Hesperadin reveals a role for Aurora B in correcting kinetochore-microtubule attachment and in maintaining the spindle assembly checkpoint. *J Cell Biol*. 161:281-94.

Heald, R. 2000. Motor function in the mitotic spindle. *Cell*. 102:399-402.

Henningsen, U., and M. Schliwa. 1997. Reversal in the direction of movement of a molecular motor. *Nature*. 389:93-6.

Herrmann, H., and U. Aebi. 1998. Intermediate filament assembly: fibrillogenesis is driven by decisive dimer-dimer interactions. *Curr Opin Struct Biol*. 8:177-85.

Hill, E., M. Clarke, and F.A. Barr. 2000. The Rab6-binding kinesin, Rab6-KIFL, is required for cytokinesis. *Embo J*. 19:5711-9.

Hirokawa, N. 1998. Kinesin and dynein superfamily proteins and the mechanism of organelle transport. *Science*. 279:519-26.

Hizlan, D., M. Mishima, P. Tittmann, H. Gross, M. Glotzer, and A. Hoenger. 2006. Structural analysis of the ZEN-4/CeMKLP1 motor domain and its interaction with microtubules. *J Struct Biol*. 153:73-84.

Honda, R., R. Korner, and E.A. Nigg. 2003. Exploring the functional interactions between Aurora B, INCENP, and survivin in mitosis. *Mol Biol Cell*. 14:3325-41.

Hotha, S., J.C. Yarrow, J.G. Yang, S. Garrett, K.V. Renduchintala, T.U. Mayer, and T.M. Kapoor. 2003. HR22C16: a potent small-molecule probe for the dynamics of cell division. *Angew Chem Int Ed Engl*. 42:2379-82.

Hoyt, M.A., L. Totis, and B.T. Roberts. 1991. S. cerevisiae genes required for cell cycle arrest in response to loss of microtubule function. *Cell*. 66:507-17.

Hu, C.K., M. Coughlin, C.M. Field, and T.J. Mitchison. 2008. Cell polarization during monopolar cytokinesis. *J Cell Biol*. 181:195-202.

Inada, H., H. Togashi, Y. Nakamura, K. Kaibuchi, K. Nagata, and M. Inagaki. 1999. Balance between activities of Rho kinase and type 1 protein phosphatase modulates turnover of phosphorylation and dynamics of desmin/vimentin filaments. *J Biol Chem*. 274:34932-9.

Inagaki, M., Y. Nishi, K. Nishizawa, M. Matsuyama, and C. Sato. 1987. Site-specific phosphorylation induces disassembly of vimentin filaments in vitro. *Nature*. 328:649-52.

Izawa, I., and M. Inagaki. 2006. Regulatory mechanisms and functions of intermediate filaments: a study using site- and phosphorylation state-specific antibodies. *Cancer Sci*. 97:167-74.

Jackman, M.R., and J.N. Pines. 1997. Cyclins and the G2/M transition. *Cancer Surv*. 29:47-73.

Jang, J.K., T. Rahman, and K.S. McKim. 2005. The kinesinlike protein Subito contributes to central spindle assembly and organization of the meiotic spindle in Drosophila oocytes. *Mol Biol Cell.* 16:4684-94.

Jantsch-Plunger, V., P. Gonczy, A. Romano, H. Schnabel, D. Hamill, R. Schnabel, A.A. Hyman, and M. Glotzer. 2000. CYK-4: A Rho family gtpase activating protein (GAP) required for central spindle formation and cytokinesis. *J Cell Biol.* 149:1391-404.

Jeyaprakash, A.A., U.R. Klein, D. Lindner, J. Ebert, E.A. Nigg, and E. Conti. 2007. Structure of a Survivin-Borealin-INCENP core complex reveals how chromosomal passengers travel together. *Cell.* 131:271-85.

Jiang, W., G. Jimenez, N.J. Wells, T.J. Hope, G.M. Wahl, T. Hunter, and R. Fukunaga. 1998. PRC1: a human mitotic spindle-associated CDK substrate protein required for cytokinesis. *Mol Cell.* 2:877-85.

Juang, Y.L., J. Huang, J.M. Peters, M.E. McLaughlin, C.Y. Tai, and D. Pellman. 1997. APC-mediated proteolysis of Ase1 and the morphogenesis of the mitotic spindle. *Science.* 275:1311-4.

Karabinos, A., H. Schmidt, J. Harborth, R. Schnabel, and K. Weber. 2001. Essential roles for four cytoplasmic intermediate filament proteins in Caenorhabditis elegans development. *Proc Natl Acad Sci U S A.* 98:7863-8.

King, R.W. 2008. When 2+2=5: the origins and fates of aneuploid and tetraploid cells. *Biochim Biophys Acta.* 1786:4-14.

Klein, U.R., E.A. Nigg, and U. Gruneberg. 2006. Centromere targeting of the chromosomal passenger complex requires a ternary subcomplex of Borealin, Survivin, and the N-terminal domain of INCENP. *Mol Biol Cell.* 17:2547-58.

Kokkinos, M.I., R. Wafai, M.K. Wong, D.F. Newgreen, E.W. Thompson, and M. Waltham. 2007. Vimentin and epithelial-mesenchymal transition in human breast cancer--observations in vitro and in vivo. *Cells Tissues Organs.* 185:191-203.

Kothe, M., D. Kohls, S. Low, R. Coli, A.C. Cheng, S.L. Jacques, T.L. Johnson, C. Lewis, C. Loh, J. Nonomiya, A.L. Sheils, K.A. Verdries, T.A. Wynn, C. Kuhn, and Y.H. Ding. 2007. Structure of the catalytic domain of human polo-like kinase 1. *Biochemistry.* 46:5960-71.

Kurasawa, Y., W.C. Earnshaw, Y. Mochizuki, N. Dohmae, and K. Todokoro. 2004. Essential roles of KIF4 and its binding partner PRC1 in organized central spindle midzone formation. *Embo J.* 23:3237-48.

Lawrence, C.J., R.K. Dawe, K.R. Christie, D.W. Cleveland, S.C. Dawson, S.A. Endow, L.S. Goldstein, H.V. Goodson, N. Hirokawa, J. Howard, R.L. Malmberg, J.R. McIntosh, H. Miki, T.J. Mitchison, Y. Okada, A.S. Reddy, W.M. Saxton, M. Schliwa, J.M. Scholey, R.D. Vale, C.E. Walczak, and L. Wordeman. 2004. A standardized kinesin nomenclature. *J Cell Biol.* 167:19-22.

Lens, S.M., J.A. Rodriguez, G. Vader, S.W. Span, G. Giaccone, and R.H. Medema. 2006. Uncoupling the central spindle-associated function of the chromosomal passenger complex from its role at centromeres. *Mol Biol Cell.* 17:1897-909.

Li, R., and A.W. Murray. 1991. Feedback control of mitosis in budding yeast. *Cell.* 66:519-31.

Lowe, M., C. Rabouille, N. Nakamura, R. Watson, M. Jackman, E. Jamsa, D. Rahman, D.J. Pappin, and G. Warren. 1998. Cdc2 kinase directly phosphorylates the cis-Golgi matrix protein GM130 and is required for Golgi fragmentation in mitosis. *Cell.* 94:783-93.

Matuliene, J., R. Essner, J. Ryu, Y. Hamaguchi, P.W. Baas, T. Haraguchi, Y. Hiraoka, and R. Kuriyama. 1999. Function of a minus-end-directed kinesin-like motor protein in mammalian cells. *J Cell Sci.* 112 (Pt 22):4041-50.

Mayer, T.U., T.M. Kapoor, S.J. Haggarty, R.W. King, S.L. Schreiber, and T.J. Mitchison. 1999. Small molecule inhibitor of mitotic spindle bipolarity identified in a phenotype-based screen. *Science*. 286:971-4.

Mayr, M.I., S. Hummer, J. Bormann, T. Gruner, S. Adio, G. Woehlke, and T.U. Mayer. 2007. The human kinesin Kif18A is a motile microtubule depolymerase essential for chromosome congression. *Curr Biol*. 17:488-98.

McCollum, D. 2004. Cytokinesis: the central spindle takes center stage. *Curr Biol*. 14:R953-5.

Miki, H., Y. Okada, and N. Hirokawa. 2005. Analysis of the kinesin superfamily: insights into structure and function. *Trends Cell Biol*. 15:467-76.

Miller, A.L., and W.M. Bement. 2009. Regulation of cytokinesis by Rho GTPase flux. *Nat Cell Biol*. 11:71-7.

Mishima, M., S. Kaitna, and M. Glotzer. 2002. Central spindle assembly and cytokinesis require a kinesin-like protein/RhoGAP complex with microtubule bundling activity. *Dev Cell*. 2:41-54.

Mishima, M., V. Pavicic, U. Gruneberg, E.A. Nigg, and M. Glotzer. 2004. Cell cycle regulation of central spindle assembly. *Nature*. 430:908-13.

Mitchison, T., and M. Kirschner. 1984. Dynamic instability of microtubule growth. *Nature*. 312:237-42.

Mitchison, T.J. 1994. Towards a pharmacological genetics. *Chem Biol*. 1:3-6.

Mollinari, C., J.P. Kleman, W. Jiang, G. Schoehn, T. Hunter, and R.L. Margolis. 2002. PRC1 is a microtubule binding and bundling protein essential to maintain the mitotic spindle midzone. *J Cell Biol*. 157:1175-86.

Morgan, D.O. 1997. Cyclin-dependent kinases: engines, clocks, and microprocessors. *Annu Rev Cell Dev Biol*. 13:261-91.

Murata-Hori, M., M. Tatsuka, and Y.L. Wang. 2002. Probing the dynamics and functions of aurora B kinase in living cells during mitosis and cytokinesis. *Mol Biol Cell*. 13:1099-108.

Murthy, K., and P. Wadsworth. 2008. Dual role for microtubules in regulating cortical contractility during cytokinesis. *J Cell Sci*. 121:2350-9.

Musacchio, A., and E.D. Salmon. 2007. The spindle-assembly checkpoint in space and time. *Nat Rev Mol Cell Biol*. 8:379-93.

Neef, R., U. Gruneberg, R. Kopajtich, X. Li, E.A. Nigg, H. Sillje, and F.A. Barr. 2007. Choice of Plk1 docking partners during mitosis and cytokinesis is controlled by the activation state of Cdk1. *Nat Cell Biol*. 9:436-44.

Neef, R., U.R. Klein, R. Kopajtich, and F.A. Barr. 2006. Cooperation between mitotic kinesins controls the late stages of cytokinesis. *Curr Biol*. 16:301-7.

Neef, R., C. Preisinger, J. Sutcliffe, R. Kopajtich, E.A. Nigg, T.U. Mayer, and F.A. Barr. 2003. Phosphorylation of mitotic kinesin-like protein 2 by polo-like kinase 1 is required for cytokinesis. *J Cell Biol*. 162:863-75.

Nigg, E.A. 1992. Assembly-disassembly of the nuclear lamina. *Curr Opin Cell Biol*. 4:105-9.

Nigg, E.A. 2001. Mitotic kinases as regulators of cell division and its checkpoints. *Nat Rev Mol Cell Biol*. 2:21-32.

Norden, C., M. Mendoza, J. Dobbelaere, C.V. Kotwaliwale, S. Biggins, and Y. Barral. 2006. The NoCut pathway links completion of cytokinesis to spindle midzone function to prevent chromosome breakage. *Cell*. 125:85-98.

Ohi, R., T. Sapra, J. Howard, and T.J. Mitchison. 2004. Differentiation of cytoplasmic and meiotic spindle assembly MCAK functions by Aurora B-dependent phosphorylation. *Mol Biol Cell.* 15:2895-906.

Osborn, M., and K. Weber. 1976. Cytoplasmic microtubules in tissue culture cells appear to grow from an organizing structure towards the plasma membrane. *Proc Natl Acad Sci U S A.* 73:867-71.

Parry, D.A., and P.M. Steinert. 1992. Intermediate filament structure. *Curr Opin Cell Biol.* 4:94-8.

Pereira, G., and E. Schiebel. 2003. Separase regulates INCENP-Aurora B anaphase spindle function through Cdc14. *Science.* 302:2120-4.

Peter, M., J. Nakagawa, M. Doree, J.C. Labbe, and E.A. Nigg. 1990. In vitro disassembly of the nuclear lamina and M phase-specific phosphorylation of lamins by cdc2 kinase. *Cell.* 61:591-602.

Peters, J.M. 2006. The anaphase promoting complex/cyclosome: a machine designed to destroy. *Nat Rev Mol Cell Biol.* 7:644-56.

Petronczki, M., M. Glotzer, N. Kraut, and J.M. Peters. 2007. Polo-like kinase 1 triggers the initiation of cytokinesis in human cells by promoting recruitment of the RhoGEF Ect2 to the central spindle. *Dev Cell.* 12:713-25.

Petronczki, M., P. Lenart, and J.M. Peters. 2008. Polo on the Rise-from Mitotic Entry to Cytokinesis with Plk1. *Dev Cell.* 14:646-59.

Piekny, A., M. Werner, and M. Glotzer. 2005. Cytokinesis: welcome to the Rho zone. *Trends Cell Biol.* 15:651-8.

Pines, J. 2006. Mitosis: a matter of getting rid of the right protein at the right time. *Trends Cell Biol.* 16:55-63.

Pinsky, B.A., and S. Biggins. 2005. The spindle checkpoint: tension versus attachment. *Trends Cell Biol.* 15:486-93.

Queralt, E., and F. Uhlmann. 2008. Cdk-counteracting phosphatases unlock mitotic exit. *Curr Opin Cell Biol.* 20:661-8.

Rice, S., A.W. Lin, D. Safer, C.L. Hart, N. Naber, B.O. Carragher, S.M. Cain, E. Pechatnikova, E.M. Wilson-Kubalek, M. Whittaker, E. Pate, R. Cooke, E.W. Taylor, R.A. Milligan, and R.D. Vale. 1999. A structural change in the kinesin motor protein that drives motility. *Nature.* 402:778-84.

Ridley, A.J., M.A. Schwartz, K. Burridge, R.A. Firtel, M.H. Ginsberg, G. Borisy, J.T. Parsons, and A.R. Horwitz. 2003. Cell migration: integrating signals from front to back. *Science.* 302:1704-9.

Rieder, C.L., R.W. Cole, A. Khodjakov, and G. Sluder. 1995. The checkpoint delaying anaphase in response to chromosome monoorientation is mediated by an inhibitory signal produced by unattached kinetochores. *J Cell Biol.* 130:941-8.

Rieder, C.L., and A. Khodjakov. 2003. Mitosis through the microscope: advances in seeing inside live dividing cells. *Science.* 300:91-6.

Rodriguez, L.G., X. Wu, and J.L. Guan. 2005. Wound-healing assay. *Methods Mol Biol.* 294:23-9.

Ruchaud, S., M. Carmena, and W.C. Earnshaw. 2007. Chromosomal passengers: conducting cell division. *Nat Rev Mol Cell Biol.* 8:798-812.

Salmon, E.D., R.J. Leslie, W.M. Saxton, M.L. Karow, and J.R. McIntosh. 1984. Spindle microtubule dynamics in sea urchin embryos: analysis using a fluorescein-labeled

tubulin and measurements of fluorescence redistribution after laser photobleaching. *J Cell Biol.* 99:2165-74.

Santamaria, A., R. Neef, U. Eberspacher, K. Eis, M. Husemann, D. Mumberg, S. Prechtl, V. Schulze, G. Siemeister, L. Wortmann, F.A. Barr, and E.A. Nigg. 2007. Use of the novel Plk1 inhibitor ZK-thiazolidinone to elucidate functions of Plk1 in early and late stages of mitosis. *Mol Biol Cell.* 18:4024-36.

Sarli, V., S. Huemmer, N. Sunder-Plassmann, T.U. Mayer, and A. Giannis. 2005. Synthesis and biological evaluation of novel EG5 inhibitors. *Chembiochem.* 6:2005-13.

Sarria, A.J., S.K. Nordeen, and R.M. Evans. 1990. Regulated expression of vimentin cDNA in cells in the presence and absence of a preexisting vimentin filament network. *J Cell Biol.* 111:553-65.

Saxton, W.M., and J.R. McIntosh. 1987. Interzone microtubule behavior in late anaphase and telophase spindles. *J Cell Biol.* 105:875-86.

Saxton, W.M., D.L. Stemple, R.J. Leslie, E.D. Salmon, M. Zavortink, and J.R. McIntosh. 1984. Tubulin dynamics in cultured mammalian cells. *J Cell Biol.* 99:2175-86.

Scholey, J.M., M.E. Porter, P.M. Grissom, and J.R. McIntosh. 1985. Identification of kinesin in sea urchin eggs, and evidence for its localization in the mitotic spindle. *Nature.* 318:483-6.

Schreiber, S.L. 1998. Chemical genetics resulting from a passion for synthetic organic chemistry. *Bioorg Med Chem.* 6:1127-52.

Schumacher, J.M., A. Golden, and P.J. Donovan. 1998. AIR-2: An Aurora/Ipl1-related protein kinase associated with chromosomes and midbody microtubules is required for polar body extrusion and cytokinesis in Caenorhabditis elegans embryos. *J Cell Biol.* 143:1635-46.

Severson, A.F., D.R. Hamill, J.C. Carter, J. Schumacher, and B. Bowerman. 2000. The aurora-related kinase AIR-2 recruits ZEN-4/CeMKLP1 to the mitotic spindle at metaphase and is required for cytokinesis. *Curr Biol.* 10:1162-71.

Shannon, K.B., J.C. Canman, C. Ben Moree, J.S. Tirnauer, and E.D. Salmon. 2005. Taxol-stabilized microtubules can position the cytokinetic furrow in mammalian cells. *Mol Biol Cell.* 16:4423-36.

Sihag, R.K., M. Inagaki, T. Yamaguchi, T.B. Shea, and H.C. Pant. 2007. Role of phosphorylation on the structural dynamics and function of types III and IV intermediate filaments. *Exp Cell Res.* 313:2098-109.

Stegmeier, F., and A. Amon. 2004. Closing mitosis: the functions of the Cdc14 phosphatase and its regulation. *Annu Rev Genet.* 38:203-32.

Steigemann, P., C. Wurzenberger, M.H. Schmitz, M. Held, J. Guizetti, S. Maar, and D.W. Gerlich. 2009. Aurora B-mediated abscission checkpoint protects against tetraploidization. *Cell.* 136:473-84.

Stemmann, O., H. Zou, S.A. Gerber, S.P. Gygi, and M.W. Kirschner. 2001. Dual inhibition of sister chromatid separation at metaphase. *Cell.* 107:715-26.

Straight, A.F., A. Cheung, J. Limouze, I. Chen, N.J. Westwood, J.R. Sellers, and T.J. Mitchison. 2003. Dissecting temporal and spatial control of cytokinesis with a myosin II Inhibitor. *Science.* 299:1743-7.

Straight, A.F., and C.M. Field. 2000. Microtubules, membranes and cytokinesis. *Curr Biol.* 10:R760-70.

Sullivan, M., and D.O. Morgan. 2007. Finishing mitosis, one step at a time. *Nat Rev Mol Cell Biol.* 8:894-903.

Sumara, I., M. Quadroni, C. Frei, M.H. Olma, G. Sumara, R. Ricci, and M. Peter. 2007. A Cul3-based E3 ligase removes Aurora B from mitotic chromosomes, regulating mitotic progression and completion of cytokinesis in human cells. *Dev Cell*. 12:887-900.

Sunder-Plassmann, N., V. Sarli, M. Gartner, M. Utz, J. Seiler, S. Huemmer, T.U. Mayer, T. Surrey, and A. Giannis. 2005. Synthesis and biological evaluation of new tetrahydro-beta-carbolines as inhibitors of the mitotic kinesin Eg5. *Bioorg Med Chem*. 13:6094-111.

Tatsuka, M., H. Katayama, T. Ota, T. Tanaka, S. Odashima, F. Suzuki, and Y. Terada. 1998. Multinuclearity and increased ploidy caused by overexpression of the aurora- and Ipl1-like midbody-associated protein mitotic kinase in human cancer cells. *Cancer Res*. 58:4811-6.

Terada, Y., M. Tatsuka, F. Suzuki, Y. Yasuda, S. Fujita, and M. Otsu. 1998. AIM-1: a mammalian midbody-associated protein required for cytokinesis. *Embo J*. 17:667-76.

Vader, G., R.H. Medema, and S.M. Lens. 2006. The chromosomal passenger complex: guiding Aurora-B through mitosis. *J Cell Biol*. 173:833-7.

Vale, R.D., T.S. Reese, and M.P. Sheetz. 1985. Identification of a novel force-generating protein, kinesin, involved in microtubule-based motility. *Cell*. 42:39-50.

Vong, Q.P., K. Cao, H.Y. Li, P.A. Iglesias, and Y. Zheng. 2005. Chromosome alignment and segregation regulated by ubiquitination of survivin. *Science*. 310:1499-504.

Wheatley, S.P., S.E. Kandels-Lewis, R.R. Adams, A.M. Ainsztein, and W.C. Earnshaw. 2001. INCENP binds directly to tubulin and requires dynamic microtubules to target to the cleavage furrow. *Exp Cell Res*. 262:122-7.

Wheatley, S.P., and Y. Wang. 1996. Midzone microtubule bundles are continuously required for cytokinesis in cultured epithelial cells. *J Cell Biol*. 135:981-9.

Woehlke, G., and M. Schliwa. 2000. Walking on two heads: the many talents of kinesin. *Nat Rev Mol Cell Biol*. 1:50-8.

Wolf, F., R. Sigl, and S. Geley. 2007. '... The end of the beginning': cdk1 thresholds and exit from mitosis. *Cell Cycle*. 6:1408-11.

Wordeman, L. 2005. Microtubule-depolymerizing kinesins. *Curr Opin Cell Biol*. 17:82-8.

Wu, J.Q., J.Y. Guo, W. Tang, C.S. Yang, C.D. Freel, C. Chen, A.C. Nairn, and S. Kornbluth. 2009. PP1-mediated dephosphorylation of phosphoproteins at mitotic exit is controlled by inhibitor-1 and PP1 phosphorylation. *Nat Cell Biol*. 11:644-51.

Yamaguchi, T., H. Goto, T. Yokoyama, H. Sillje, A. Hanisch, A. Uldschmid, Y. Takai, T. Oguri, E.A. Nigg, and M. Inagaki. 2005. Phosphorylation by Cdk1 induces Plk1-mediated vimentin phosphorylation during mitosis. *J Cell Biol*. 171:431-6.

Yan, Y., V. Sardana, B. Xu, C. Homnick, W. Halczenko, C.A. Buser, M. Schaber, G.D. Hartman, H.E. Huber, and L.C. Kuo. 2004. Inhibition of a mitotic motor protein: where, how, and conformational consequences. *J Mol Biol*. 335:547-54.

Yasui, Y., H. Goto, S. Matsui, E. Manser, L. Lim, K. Nagata, and M. Inagaki. 2001. Protein kinases required for segregation of vimentin filaments in mitotic process. *Oncogene*. 20:2868-76.

Yasui, Y., T. Urano, A. Kawajiri, K. Nagata, M. Tatsuka, H. Saya, K. Furukawa, T. Takahashi, I. Izawa, and M. Inagaki. 2004. Autophosphorylation of a newly identified site of Aurora-B is indispensable for cytokinesis. *J Biol Chem*. 279:12997-3003.

Yildiz, A., M. Tomishige, R.D. Vale, and P.R. Selvin. 2004. Kinesin walks hand-over-hand. *Science*. 303:676-8.

Yokoyama, T., H. Goto, I. Izawa, H. Mizutani, and M. Inagaki. 2005. Aurora-B and Rho-kinase/ROCK, the two cleavage furrow kinases, independently regulate the progression of cytokinesis: possible existence of a novel cleavage furrow kinase phosphorylates ezrin/radixin/moesin (ERM). *Genes Cells*. 10:127-37.

Yuce, O., A. Piekny, and M. Glotzer. 2005. An ECT2-centralspindlin complex regulates the localization and function of RhoA. *J Cell Biol*. 170:571-82.

Curriculum Vitae

Name   Stefan Hümmer
Place and Date of birth   20th june 1979, Werneck (Germany)
Nationality   German

EDUCATION

2004-2009   **Ph.D.,** Ludwig Maximilian Universität München

2003-2004   **Diploma thesis,** Max Planck Institute for Biochemistry, Munich, First degree
                  with honors

2003   **Diploma,** University of Würzburg, First degree with honors

2002-2003   Study of Biology at University of Würzburg

2002   **Pre-diploma,** University of Regensburg

1999-2002   Study of Biology at University of Regensburg

RESEARCH EXPERIENCE

2004-   **Doctorate Thesis.** University of Konstanz, Department of Genetics and Max
                  Planck Institute for Biochemistry, Department of Cell Biology, Chemical
                  Genetics Group, Munich
                  Supervisor: Prof. Dr. Erich A. Nigg and Prof. Dr. Thomas U. Mayer
                  Thesis: Functional characterization of the mitotic kinesin Mklp2

2003 -2004   **Diploma Thesis.** Max Planck Institute for Biochemistry, Department of Cell
                  Biology, Munich
                  Supervisor: Prof. Dr. Erich A. Nigg and Prof. Dr. Thomas U. Mayer
                  Thesis: Screen for small molecule inhibitors of mitotic kinesins

08-10/2002   **Summer internship.** Max Planck Institute for Biochemistry, Department of
                  Cell Biology, Munich
                  Supervisor: Dr. Anton Gartner

FELLOWSHIPS

2004-2006   Fonds der chemischen Industrie, **Ph.D. fellowship**

Publications

Parts of this work are published in:

Hümmer, S., and Mayer, T.U. (2009). Cdk1 negatively regulates midzone localization of the mitotic kinesin mklp2 and the chromosomal passenger complex. Curr Biol 19, 607-612.

Mayr, M.I., **Hümmer, S**., Bormann, J., Gruner, T., Adio, S., Woehlke, G., and Mayer, T.U. (2007). The human kinesin Kif18A is a motile microtubule depolymerase essential for chromosome congression. Curr Biol 17, 488-498.

Florian, S., **Hümmer, S**., Catarinella, M., and Mayer, T.U. (2007). Chemical genetics: reshaping biology through chemistry. HFSP journal 1, 104-114.

Elowe, S., **Hümmer, S**., Uldschmid, A., Li, X., and Nigg, E.A. (2007). Tension-sensitive Plk1 phosphorylation on BubR1 regulates the stability of kinetochore microtubule interactions. Genes & Development 21, 2205-2219.

Lessmann, T., Leuenberger, M.G., Menninger, S., Lopez-Canet, M., Muller, O., **Hümmer, S**., Bormann, J., Korn, K., Fava, E., Zerial, M., Mayer, T.U., and Waldmann, H. (2007). Natural product-derived modulators of cell cycle progression and viral entry by enantioselective oxa Diels-Alder reactions on the solid phase. Chemistry & biology 14, 443-451.

Chalamalasetty, R.B., **Hümmer, S**., Nigg, E.A., and Sillje, H.H. (2006). Influence of human Ect2 depletion and overexpression on cleavage furrow formation and abscission. Journal of cell science 119, 3008-3019.

Sarli, V.*, **Huemmer, S**. *, Sunder-Plassmann, N., Mayer, T.U., and Giannis, A. (2005). Synthesis and biological evaluation of novel EG5 inhibitors. Chembiochem 6, 2005-2013.
*These authors contribute equally to this work**

Sunder-Plassmann, N., Sarli, V., Gartner, M., Utz, M., Seiler, J., **Huemmer, S**., Mayer, T.U., Surrey, T., and Giannis, A. (2005). Synthesis and biological evaluation of new tetrahydro-beta-carbolines as inhibitors of the mitotic kinesin Eg5. Bioorganic & medicinal chemistry 13, 6094-6111.

PATENTS

Nigg, E.A., Mayer, T.U., **Huemmer, S.**, Barr, F. A., Bormann, J. (2006). 2-Phenylquinoxalines as inhibitors for MPP1. European Patent EP1683523.

Surrey, T., Giannis, A., Vernos, I., Gartner, M., Sarli, V., Mayer, T.U., **Huemmer, S.** (2005). Quinazoline derivatives, process for their preparation, their use as antimitotics and pharmaceutical compositions comprising said derivatives. European Patent EP 2005011836.